TP 8046E

Transport Canada
Development

Transports Canada
Développement

Catenary Deflection Under Wind and Ice Loading

Prepared for
Transportation
Development Centre

Transport Canada

by
Canadian Pacific
Consulting Services Ltd.

and
Morrison Hershfield Ltd.

October 1986

Canada

85038

TP8046E

CATENARY DEFLECTION UNDER WIND AND ICE LOADING

Prepared for

Transportation Development Centre
Transport Canada

by

Canadian Pacific Consulting Services Ltd.

and

Morrison Hershfield Ltd.

October 1986

DISCLAIMER

The contents of this report reflect the view of Canadian Pacific Consulting Services Ltd. and Morrison Hershfield Limited and not necessarily the official view or opinions of the Transportation Development Centre of Transport Canada.

LANGUAGE NOTICE

Un sommaire en français de ce rapport est inclus avant la Table des matières.

FORMULE DE DOCUMENTATION POUR RAPPORT

1. N° du rapport Transports Canada	2. N° de l'étude — CDT	3. N° de catalogue du destinataire
TP8046E	6754	

4. Titre et sous-titre	5. Date du rapport
Catenary Deflection Under Wind and Ice Loading	October 1986
	6. N° du rapport de l'organisme exécutant C85038

7. Auteur(s)	8. N° de dossier Transports Canada
L.C. Tait, P.A. Irwin, S.L. Gamble, D.A.B. Turner	D1465-317-23

9. Nom et adresse de l'organisme exécutant	10. N° de dossier — ASC
Société d'études et de consultation du Canadien Pacifique (Ltée) 740, rue Notre Dame ouest, Suite 760 Montréal (Québec) H3C 3X6	14SD.T8200-4-4571
	11. N° de contrat — ASC ou Transports Canada OSD85-00069

12. Nom et adresse de l'organisme parrain	13. Genre de rapport et période visée
Centre de développement des transports 200, boul. Dorchester ouest Suite 601, Tour ouest Montréal (Québec) H2Z 1X4	Final
	14. Code de l'organisme parrain
15. Remarques additionnelles	16. Agent de projet — CDT C. Alfred Versailles

17. Résumé

Une portion de caténaire spécifique d'une électrification sous 25-50kV, 60 Hz d'une voie ferrée, sur laquelle circule un trafic lourd, a été réalisée en vraie grandeur et installée sur l'île du Prince-Edouard dans un lieu exposé aux vents. Des capteurs aux ultrasons ont servi à mesurer les déflexions verticales et horizontales du fil de contact, les signaux de sortie étant enregistrés automatiquement par un micro-ordinateur in situ sur une période de cinq mois. Des graphiques ont été obtenus montrant les déflexions maximales et moyennes en fonction de la composante, normale au fil, de la vitesse moyenne du vent. Malheureusement, aucune donnée utilisable sur la charge des glaces n'a pu être recueillie.

La déflexion horizontale maximale du fil de contact dans le cas de la portée la plus longue (70 m) à une vitesse moyenne de vent de 12,2 m/s a été de 200 mm, environ, y compris la déflexion du support, celui-ci figurant pour approximativement 10 p. 100 de ce total, compte tenu de la forme de caténaire considérée. La déflexion verticale entre crêtes s'est établie entre 40 et 50 mm, l'amplitude devant être prise en compte dans la conception de la caténaire et du système de captage du courant.

Le rapport présente le logiciel utilisé pour calculer les déflexions dues au vent dans le cas de caténaires simples à flexibilité variable. Il formule également des recommandations concernant les valeurs devant être introduites dans le logiciel en ce qui concerne le coefficient de traînée du fil de contact, la vitesse moyenne du vent et la charge des glaces.

18. Mots-clés	19. Diffusion
Electrification, voies ferrées, caténaire, conducteur aérien, déflexion du fil de contact, charge due au vent.	Le Centre de développement des transports dispose d'un nombre limité d'exemplaires.

20. Classification de sécurité (de ce rapport)	21. Classification de sécurité (de cette page)	22. Nombre de pages	23. Prix
Non classifié	Non classifiée	99	

REPORT DOCUMENTATION FORM

1. Transport Canada Report No.	2. TDC Project No.	3. Recipient's Catalogue No.
TP8046E	6754	

4. Title and Subtitle	5. Report Date
CATENARY DEFLECTION UNDER WIND AND ICE LOADING	October 1986
	6. Performing Organization Report No. C-85038
7. Author(s)	8. Transport Canada File No.
L.C. Tait, P.A. Irwin, S.L. Gamble, D.A.B. Turner	D1465-317-23
9. Performing Organization Name and Address Canadian Pacific Consulting Services Ltd. 740 Notre-Dame Street West, Suite 760 Montreal, Quebec H3C 3X6	10. DSS File No. 14SD.T8200-4-4571
	11. DSS or Transport Canada Contract No. OSD85-00069
12. Sponsoring Agency Name and Address Transportation Development Centre (TDC) 200 Dorchester Blvd. West West Tower, Suite 601 Montreal, Quebec H2Z 1X4	13. Type of Report and Period Covered FINAL
	14. Sponsoring Agency Code
15. Supplementary Notes	16. TDC Project Officer C. Alfred Versailles

17. Abstract

A full-scale catenary test section, typical of a 25-50 kV, 60 Hz main line heavy haul freight railway, was installed on a wind-exposed site in Prince Edward Island. Ultrasonic ranging techniques were used for measuring horizontal and vertical dynamic deflections of the contact wire. Transducer outputs were automatically recorded by an on-site microcomputer over a 5-month period. Results are depicted as graphical plots of mean and peak deflections against the mean wind speed normal to the contact wire. Unfortunately, no usable ice loading data were obtained.

At a mean wind speed of 12.2 m/s, contact wire peak horizontal deflections for the longest span (70 m) were approximately 200 mm, including mast deflections making up approximately 10% of the total for this particular catenary design. Peak-to-peak vertical oscillations of 40 to 50 mm were experienced and should be evaluated with regard to pantograph contact and catenary design.

The report includes a microcomputer software program to predict wind-induced deflections of simple catenary overhead contact systems of the level or sagged contact type. Recommendations are made for values of wire drag coefficient, mean wind speed and ice accretion to be used in the program.

18. Key Words	19. Distribution Statement
Rail Electrification; Catenary; Overhead Contact System; Wire Deflection; Wind Loading; Instrumentation; Ultrasonic; Program; Design; Microcomputer	Limited number of copies available from the Transportation Development Centre on request.

20. Security Classification (of this report)	21. Security Classification (of this page)	22. No. of Pages	23. Price
Unclassified	Unclassified	99	

TDC/CDT 79-005

SUMMARY

For railway electrification in Canada, the establishment of valid design criteria requires more information on catenary deflection under wind and ice loading. This report presents the results of a full-scale catenary test that was conducted under realistic environmental conditions to obtain and evaluate useful data. Field test results were incorporated in the development of a microcomputer software program. The program evaluates and predicts the wind-induced deflection of overhead contact systems used in modern electrified railways.

Prime contractor for the project was Canadian Pacific Consulting Services Ltd. The Guelph wind tunnel laboratories of Morrison Hershfield Ltd. were retained to design and implement special test instrumentation, to record the data in the field and to develop the microcomputer program.

A full-scale, half section of catenary, typical of a 25-50 kV, 60 Hz mainline heavy haul freight railway, was installed on flat pastureland near Borden, Prince Edward Island. It included one span each of 55, 60, 65 and 70 metres with a constant tension of 9.8 kN and a stagger of ±400 mm on alternate masts. The test site was exposed to strong prevailing westerly winds from the Northumberland Strait.

The catenary was instrumented with 27 transducers, which monitored different aspects of the motion of the wire and mast system as well as the ambient wind conditions. The vertical and horizontal dynamic deflections of the catenary contact wire were measured by ultrasonic displacement transducers. Mast motions and ice buildup were measured with strain gauges. Accelerometers were used to estimate the dynamic components of the wire motion. All transducer outputs were correlated to the mean wind speed normal to the contact wire. Transducer signals were reduced and stored by a dedicated on-site microcomputer. These data were acquired between mid-January and the end of May, 1986.

Two black and white video cameras were also installed to provide visual information on the motions of two of the catenary spans. A video tape recording from these cameras forms a part of this report.

During the test period no significant natural ice buildup was noted at the field test installation site, although severe ice storms were experienced in other areas of P.E.I. Late in the winter on a sub-zero day with a significant wind, water was sprayed on one span of the installation to artificially build up an ice coating. Shortly thereafter, the wind died down and, unfortunately, no usable data were acquired prior to the melting of the ice. No further suitable opportunities for water spraying occurred.

Peak horizontal deflections of the contact wire measured for the 70 metre span in a mean wind speed of 12.2 m/s were approximately 200 mm including mast deflection. The component of deflection of the contact wire due to bending of the masts was approximately 10 percent of the total for this particular catenary design.

The field test results showed that the contact wire also experienced peak to peak vertical oscillations in the range of 40 to 50 mm throughout the mean wind speed range measured (0-12.2 m/s). This amount of oscillation could potentially affect the contact of the locomotive pantograph and should be evaluated with regard to overhead contact system design.

The report concludes with recommendations regarding the values for the wire drag coefficient, the mean wind speed, and the ice accretion that should be used in the deflection prediction program.

SOMMAIRE

Au Canada, l'électrification des voies ferrées doit être assujettie à des normes particulières de dimensionnement devant être élaborées sur la base d'informations précises sur les déformations de la caténaire sous l'action du vent et des glaces. Ce rapport présente les résultats des essais faits en vraie grandeur dans des conditions naturelles représentatives et visant à recueillir des données utiles puis à les valider, ces résultats étant ensuite utilisés pour la mise au point d'un logiciel permettant de prédire les déflexions dues au vent des fils conducteurs aériens utilisés dans les réseaux électrifiés modernes.

Le contractant principal, la Société d'études et de consultation du Canadien Pacifique Ltée, a sous-traité à la Morrison Hershfield Ltd. les travaux d'étude en soufflerie des instrument de mesure devant servir aux essais ainsi que ceux de saisie des données in situ et de mise au point du logiciel.

Une portion de caténaire, réplique fidèle de celle utilisée en traction électrique lourde sous 25-50 kV, 60 Hz, a été réalisée en vraie grandeur et installée près de Borden (Île-du-Prince-Édouard) en un lieu de pâturage plat exposé aux vents violents d'ouest soufflant du détroit de Northumberland. Cette portion comprenait quatre portées ayant 55, 60, 65 et 70 m de longueur, tendues à la tension constante de 9,8 kN, le fil étant désaxé périodiquement sur une distance de 400 mm de part et d'autre de l'axe de la voie.

Vingt-sept capteurs avaient été implantés afin de mesurer les divers paramètres de mouvement du fil et de ses supports, ainsi que la direction, la vitesse et la température des vents dominants. Des capteurs de déplacement aux ultrasons ont servi à mesurer les déflexions verticales et horizontales du fil de contact; des capteurs à jauges de contraint ont été utilisés pour les mouvements des supports et la charge de la glace et des accéléromètres pour mesurer les composantes dynamiques du fil de contact. Tous les signaux de sortie des capteurs ont été calés

par rapport à la composante, normale au fil, de la vitesse moyenne du vent, réduits et stockés dans la mémoire d'un micro-ordinateur spécifique. Tous ces travaux de mesurage ont eu lieu de la mi-janvier à la fin de mai 1986.

Deux vidéocaméras noir et blanc ont servi à filmer deux des quatre portées, la bande vidéo correspondante étant annexée au rapport.

Durant la période d'essai, aucune accumulation importante de glace n'a été signalée sur les lieux, malgré les violentes tempêtes et le verglas qui ont sévi ailleurs sur l'île. Un jour d'hiver où la température était tombée au-dessous de 0°C et qu'un vent violent soufflait, une des portées a été arrosée d'eau afin de provoquer la formation de glace. Malheureusement, le vent tomba peu de temps après et la glace se mit à fondre avant qu'une information utile ait pu être recueillie. L'arrosage n'a pu être répété par la suite, faute d'occasion propice.

La déflexion horizontale maximale du fil de contact, mesurée dans le cas de la portée de 70 m de long à une vitesse moyenne de vent de 12,2 m/s, a été de 200 mm, environ, y compris la déflexion du support qui représente, compte tenu du type de suspension caténaire utilisé, environ 10 p. 100 de la déflexion totale mesurée.

Quant à la déflexion verticale entre crtes du fil de contact, elle s'est établie entre 40 et 50 mm dans la gamme des vitesses moyennes du vent considérée, à savoir entre 0 et 12,2 m/s. Avec une telle amplitude, les conditions d'un bon captage du courant risquent de ne pas toujours se réaliser et il faudra en tenir compte dans la conception de la caténaire.

Le rapport formule des recommandations sur les valeurs à introduire dans le logiciel de calcul des déflexions concernant le coefficient de traînée du fil de contact, la vitesse moyenne du vent et la charge des glaces.

TABLE OF CONTENTS

		Page
1.0	INTRODUCTION	1
1.1	Background	1
1.2	TDC Contract	2
2.0	CATENARY DESIGN AND PROJECT IMPLEMENTATION	3
3.0	DESCRIPTION OF INSTRUMENTATION	4
3.1	Layout	4
3.2	Data Acquisition Computer	6
3.3	Video Recording System	8
3.4	Wind Instrument	10
3.5	Contact Wire Deflection Transducers	11
3.6	Icing Load Cells	15
3.7	Tower Deflections	16
3.8	Wire Accelerations	17
3.9	Data Acquisition Software	19
4.0	FIELD TEST RESULTS	20
4.1	General	20
4.2	Wind	20
4.3	Horizontal Displacement of Contact Wire	21
4.4	Vertical Displacement of Contact Wire	29
4.5	Ice Loading	29
4.6	Deflection of Towers	30
4.7	Lateral Acceleration of Messenger and Contact Wires	35
4.8	Videotape Records of Contact Wire Motions	39
5.0	DEFLECTION PREDICTION PROGRAM	40
5.1	General	40
5.2	General Notes on the Use of the OCS Deflection Program (OCS.BAS)	41
5.3	Input Parameters	41

TABLE OF CONTENTS (Cont'd)

		Page
5.4	Outputs	46
5.5	Comparison of Computer Predictions with Field Test Data	47
6.0	CONCLUSIONS	57
6.1	Test Method	57
6.2	Prevailing Winds	58
6.3	Horizontal Deflection	58
6.4	Vertical Deflection	58
6.5	Tower Deflection	58
6.6	Computer Program	58
6.7	Local Wind Climate	59

APPENDICES

A. CATENARY DESIGN AND PROJECT IMPLEMENTATION

B. STATICS AND MECHANICS OF CATENARY SYSTEM

C. RESPONSE OF CATENARY TO WIND ACTION

D. SOURCE CODE LISTING FOR CATENARY DEFLICTION PROGRAM OCS.BAS

FIGURES

1	Layout of Catenary Monitoring Instrumentation System	5
2	Schematic of Computer System Components	7
3	Camera Mounting on Poles 13 and 14	9
4	Schematic of Video Recording System	9
5	Schematic of Wind Monitoring System	10
6	Wind Speed, Direction and Temperature Transducers	11
7	Ultrasonic Displacement Transducer Positioning	13

Page

FIGURES (Cont'd)

8	Schematic of Ultrasonic Displacement Transducer System	14
9	Calibration of Ultrasonic Displacement Transducers	14
10	Schematic Diagram of Icing Load Cell System	15
11	Tower Strain Gauge Installation	16
12	Schematic of Tower Deflection Transducer System	17
13	Accelerometers at Pole 14	18
14	Schematic of Accelerometer Systems	18
15	Results from Channel 5	25
16	Results from Channel 7	26
17	Results from Channel 13	27
18	Results from Channel 15	28
19	Results from Channel 20	31
20	Results from Channel 21	32
21	Results from Channel 22	33
22	Results from Channel 23	34
23	Results from Channel 25	36
24	Results from Channel 26	37
25	Results from Channel 27	38
26	Drag Coefficient of Circular Cylinder Versus Reynold's Number	43

1.0 INTRODUCTION

1.1 Background

In railway electrification, satisfactory current collection from an overhead contact system (OCS) is an essential function that must be achieved under all weather conditions in which trains can operate. The ability of the locomotive pantograph to ensure uninterrupted current collection depends on pantograph characteristics and contact wire position.

Engineering design of overhead contact systems must allow for a number of conditions which result in a displacement of the contact wire relative to the pantograph. These conditions include track cross-level tolerance, track alignment, locomotive side bearing tilt, pantograph sway due to mountings, OCS erection tolerances, static offset, stagger, and 'blow-off'. Static offset is the distance of the contact wire from track centre line on curves. Stagger is a planned horizontal offset of the contact wire in opposite directions at alternate poles which ensures distributed wear on the pantograph collector bar. 'Blow-off' refers to lateral deflection of the contact wire from its static position due to transverse winds.

The worst case displacement due to each of the above conditions can be measured individually and used in design calculations. In practice, these conditions do not all occur simultaneously so that engineering on the basis of the algebraic sum of displacements will result in uneconomic over-design. Some railways design for the contact wire displacement limit as 70 percent of the algebraic sum of individual displacements. Other use a root mean square formula.

A major contribution to contact wire displacement is blow-off. The deflection is greatest at mid-span and is a function of wire tensions, the projected area of the catenary, the aerodynamic drag characteristics of the wires and the wind velocity. Deflection due to wind affects the maximum width of the pantograph collector bar and the maximum acceptable spacing of

poles or support structures. Consequently, estimation of blow-off has a direct bearing on the number of structures required and hence on costs.

The effect of wind is aggravated in northern climates by the formation of ice on exposed surfaces under certain climatic conditions. Ice coatings increase the projected area of the OCS and increase deflections due to wind. Currently-used design calculations assume that the worst case transverse wind loading and maximum ice thickness occur at the same time. The validity of this assumption is questionable because, empirically, it is known that ice coatings on wires tend to break off in high winds due to wire flexure.

For railway electrification in the Canadian context, the establishment of valid design criteria requires more information on catenary deflection under wind and ice loading. The purpose of this study was to undertake a full scale catenary test under realistic environmental conditions to obtain and evaluate data that can be used to define electrification design criteria.

1.2 TDC Contract

In August, 1985 Canadian Pacific Consulting Services Ltd. (CPCS) was awarded contract 14SD.T8200-4-4571 by the Transportation Development Centres (TDC) of Transport Canada to design and install a test section of overhead contact system exposed to wind and ice loading and to monitor its deflection.

CPCS retained under subcontracts, the Guelph wind tunnel laboratories of Morrison Hershfield Limited (MH), F.A. Tucker (Canada) Ltd. and Marenco Engineering Ltd. CPCS managed the project and was responsible for the design and specification of the test catenary. F.A. Tucker installed the catenary. Morrison Hershfield designed and implemented the test instrumentation, recorded test data and developed a micro-computer based software program to predict peak wind induced deflections which incorporated the information on deflections obtained in the field tests. Marenco Engineering provided regular monitoring of catenary and instrumentation at the test site during the test period.

2.0 CATENARY DESIGN AND PROJECT IMPLEMENTATION

Upon receipt of authorization to proceed, work commenced on the project on 1985 07 17 with a planning meeting which involved the principal participants. The result of this meeting was a critical path SPECNET of project activities, their estimated durations and parties responsible for carrying them out. The SPECNET is included in Appendix A as drawing C-85038-01.

CPCS proceeded with preparation of the catenary design and the installation specification. Plan and elevations of the test catenary section are shown in Appendix A, drawing C-85038-02. The design is for a full scale half section of catenary typical of a 25-50 kV, 60 Hz mainline heavy haul freight railway. Included are one span each of 55, 60, 65 and 70 metres with a constant tension of 9.8 kN and a stagger of $\pm$400 mm on alternate masts.

The site selected for installation of the catenary was on the property of Mr. John Reid in Borden, Prince Edward Island. The land is flat, featureless pasture located south of Borden on Amherst Point which extends into the Northumberland Strait in a southeasterly direction. The test site is exposed to strong prevailing westerly winds. Orientation of the catenary was on a line 33 degrees west of true north. Location of the catenary is shown in Appendix A, drawing C-85038-03.

Six catenary masts, six cantilever assemblies and one weight tensioning system were provided by the Transportation Development Centre (TDC) for the project and shipped from NRC Railway laboratories at Uplands, Ontario to the test site. Separate wood poles for the mounting of the test instrumentation, guys for these poles, concrete for the catenary mast foundations, anchors and miscellaneous hardware were supplied by the installation contractor.

70 mm^2 19 strand HD copper messenger wire, 107 mm^2 HD copper grooved contact wire and midspan droppers were purchased from BC Rail.

Installation of the half section of catenary was complete as of 1985 09 30. Following installation of test instrumentation, calibration and verification of computer data logging, test data were collected from January through May of 1986.

In June the test installation was dismantled and the site returned to its original condition.

3.0 DESCRIPTION OF INSTRUMENTATION

3.1 Layout

The instrumentation package developed for the catenary deflection tests consisted of 27 transducers monitoring different aspects of the motion of the wire and tower system as well as the ambient wind conditions. All transducer signals were monitored, reduced and stored by a dedicated on-site microcomputer system. The layout of the system is illustrated in Figure 1. In addition to the 27 transducers, two black and white video cameras were installed to provide visual information on the motions of spans 1 and 2. Figure 1 shows the basic nomenclature of the spans, the steel catenary towers (C1 - C5) and the wooden instrumentation poles (I1 - I6). Data cables from each transducer were run back to a heated trailer which housed all of the power supply, signal conditioning and computer systems. This is also illustrated in Figure 1. A steel pipe mast was erected at the northwest corner of the trailer upon which the wind and temperature instruments were mounted. Electric and telephone services were provided to the trailer.

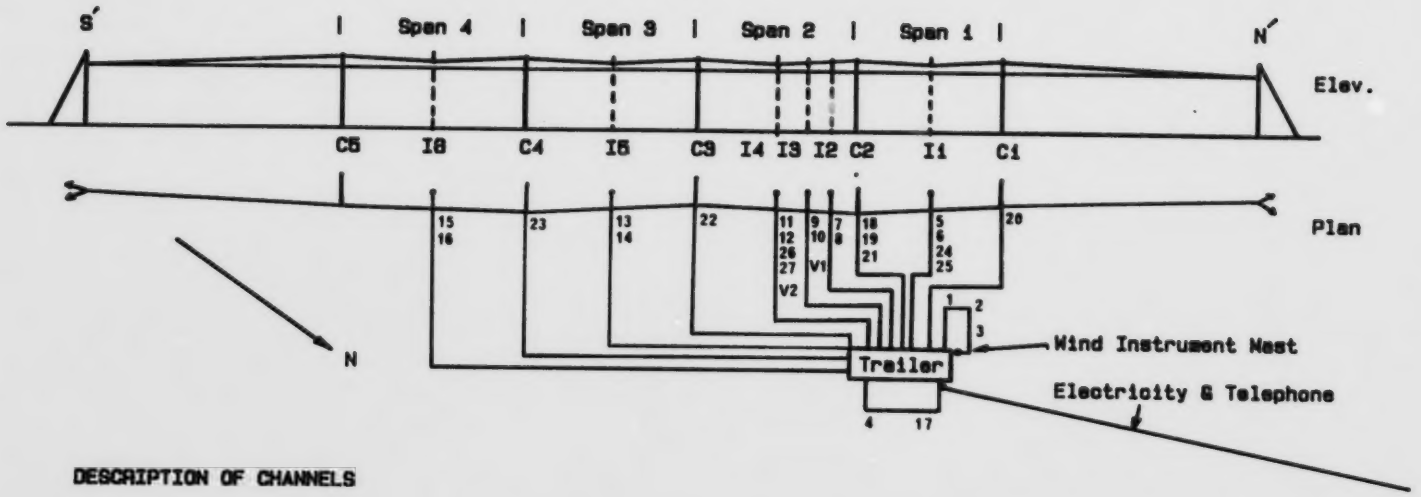

DESCRIPTION OF CHANNELS

1 Wind Speed
2 Wind Direction
3 Dry Bulb Temperature
4 Horizontal Reference UDT
5 Horizontal UDT at I1
6 Vertical UDT at I1
7 Horizontal UDT at I2
8 Vertical UDT at I2
9 Horizontal UDT at I3
10 Vertical UDT at I3
11 Horizontal UDT at I4
12 Vertical UDT at I4
13 Horizontal UDT at I5
14 Vertical UDT at I5
15 Horizontal UDT at I8
16 Vertical UDT at I8
17 Vertical Reference UDT
18 Ice Buildup Load Cell North of C2
19 Ice Buildup Load Cell South of C2
20 Tower Deflection C1
21 Tower Deflection C2
22 Tower Deflection C3
23 Tower Deflection C4
24 Horizontal Acceleration of Catenary Wire at I1
25 Horizontal Acceleration of Contact Wire at I1
26 Horizontal Acceleration of Catenary Wire at I4
27 Horizontal Acceleration of Contact Wire at I4

NOTE: UDT - Ultrasonic Displacement Transducer

FIGURE 1

Layout of Catenary Monitoring Instrumentation System

3.2 Data Acquisition Computer

Figure 2 is a schematic diagram of the computer system and interfaces used for collecting the data from the transducers. The basic computer was a Digital Equipment Corporation LSI 11/23 system equipped with 256 k Bytes of random access memory. The storage device attached to the computer was a dual floppy diskette drive with a combined capacity of one M Byte of operating system, data acquisition software and data storage. On-line control of the computer system was accomplished from within the instrumentation trailer using a video display terminal (VDT). Remote communication with the computer was also accomplished using a modem (modulator/demodulator) which would automatically answer the on-site telephone and establish a communications link with the remote computer or terminal. A fall back switch in the modem/terminal line detected incoming telephone data connections and automatically switched from the on-site VDT to the telephone connection. In this way control of all computer functions except changing of diskettes could be performed remotely.

An analogue to digital (A/D) converter with input multiplexer manufactured by Data Translation was used to sequentially convert the analogue voltage signals from the transducers into digital data for processing by the computer software. This A/D converter had a resolution of 5 mV and a maximum total throughput of 40,000 samples per second. A real time clock (RTC) from the same manufacturer was used to ensure a constant sampling rate of 10 samples per second per channel. With this sampling speed, vibrations of the catenary system of up to 5 Hertz were resolved.

The analogue voltage signals from the transducers were low pass filtered at a 5 Hertz cut-off to eliminate any possible high frequency noise picked up by the long cables connecting the transducers to the instrumentation trailer.

A parallel input/output computer card (Video I/O) was utilized to provide digital signals for use in stopping and starting the record mode of the

video cassette recorder. These digital signals were converted to an appropriate form for connecting to the VCR through a specially constructed interface unit.

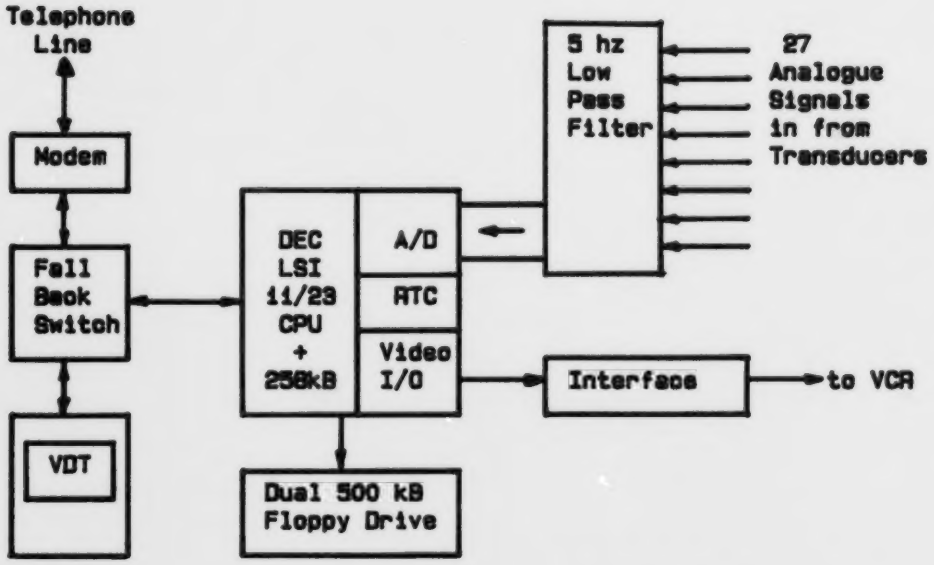

FIGURE 2

Schematic of Computer System Components

3.3 Video Recording System

Two high resolution black and white video surveillance cameras with thermostatically controlled, heated environmental enclosures were installed on instrumentation poles I3 and I4. A photograph of the camera installation is in Figure 3. This photograph shows camera V1 mounted low on pole I3 looking northward along the line at spans 1 and 2. Camera V2 was mounted approximately 60° to the horizontal. The cameras used manual focus lenses with automatic iris control to compensate for varying light conditions.

Figure 4 presents a schematic diagram of the components in the video recording system. Power to the two cameras and the heater units of the environmental enclosures was supplied by a 24 volt power supply in the trailer. Video signals from the cameras were input into a screen splitter which merged the two pictures onto a single video screen format. This allowed simultaneous viewing of both camera angles for comparison of motions in different regions of the catenary system. The merged video signal was passed through a time and date generator to provide permanent identification of the recording. The complete signal was fed into a commercial duty VHS cassette recorder and to a black and white monitor. As mentioned in the previous section, the video cassette recorder was set into record mode and turned off by the computer system. Periodic manual changing of video tape was required.

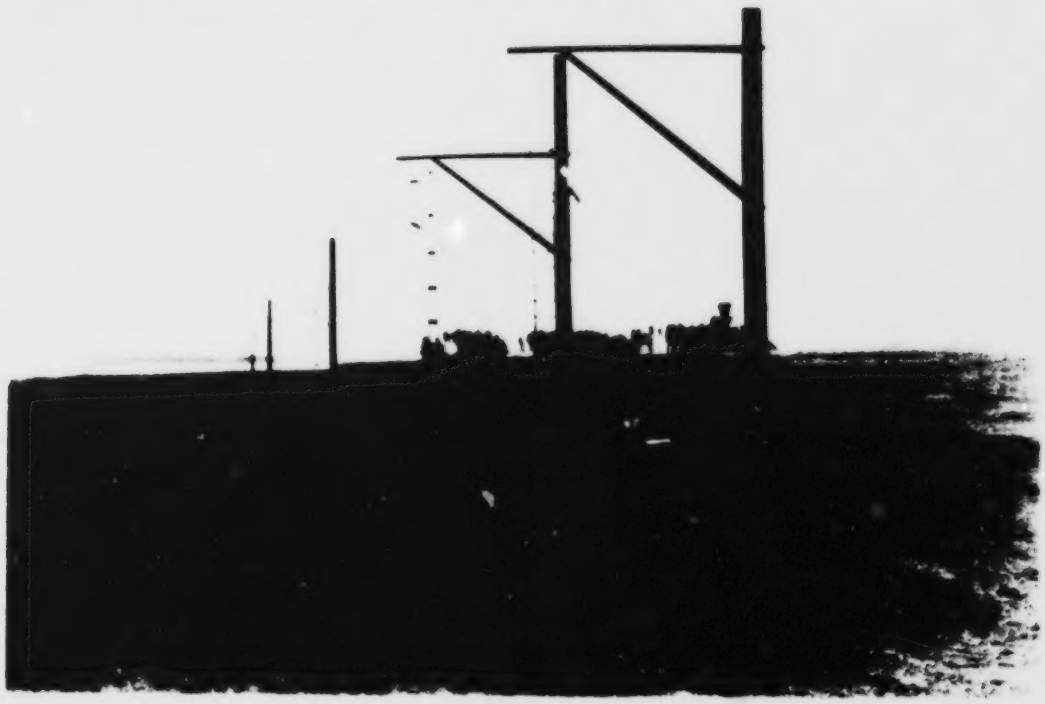

FIGURE 3

Camera Mounting on Poles I3 and I4

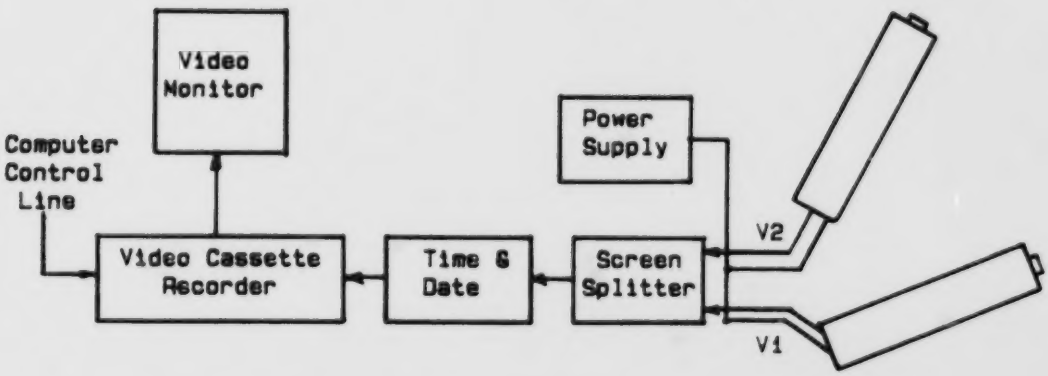

FIGURE 4

Schematic of Video Recording System

3.4 Wind Instrument

A steel pipe pole was erected near the northwest corner of the instrumentation trailer on top of which the propeller/vane type wind anemometer was mounted. The length of this pole was set to hold the anemometer at the same height above ground as the contact wire. Figure 5 is a schematic diagram of the complete wind direction, wind speed and dry bulb temperature monitoring system which was manufactured by R.M. Young Company. Temperature was measured with a radiation shielded system. A photograph of the wind instrument is in Figure 6.

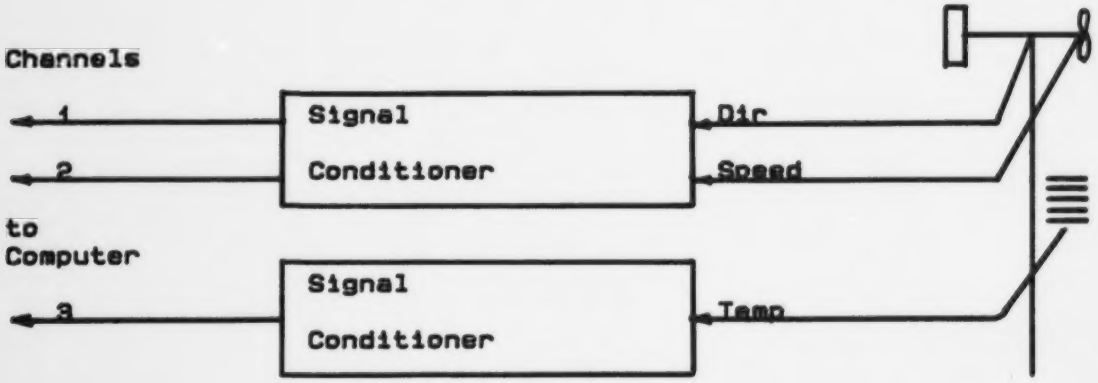

FIGURE 5

Schematic of Wind Monitoring System

FIGURE 6

Wind Speed, Direction and Temperature Transducers

3.5 Contact Wire Deflection Transducers

At the outset of the project an investigation was undertaken to identify a transducer which would be able to resolve fairly small motions of the wires with wire vibration frequencies of up to 5 Hertz. The device had to be available at a low cost and work in such a manner so as to not inhibit the motion of the catenary wire system. To this end, non-contacting optical or ultrasonic transducers were selected as the most likely candidates. Due to the wide range of ambient light conditions and the susceptibility of optical system to dirt and weather, the ultrasonic technique was ultimately chosen.

Since no complete, commercially available system could be found which fit the needs of the present work, Morrison Hershfield Limited, in conjunction with P.S. Technologies, developed a suitable system utilizing several basic components available from Polaroid Inc. and custom built electronics. Figure 7 illustrates the wire displacement transducers and targets. In the system design, two ultrasonic sender/receivers were mounted within a plexiglass weather shielded box at right angles to one another. This box was attached firmly to the contact wire such that the ultrasonic 'beams' would strike the plywood targets at right angles. Since the ultrasonic system measures the distance to the targets, the instantaneous position of the wire would be determined in vertical and horizontal directions at each of the six monitored locations along the wire. In this case, the targets remained in a fixed location mounted on the stiff, guyed poles and the sender/receiver units moved with the contact wire. A single, loosely draped cable from the sender/receiver unit carried transmit pulses and received echo signals to and from the electronics package mounted in a weather resistant enclosure on the instrumentation pole. A schematic diagram of a complete two direction displacement transducer system is in Figure 8. The electronics boxes which were mounted on the instrumentation poles contained the necessary hardware to drive the outgoing sound pulses or 'chirps' and receive, identify and time the echoed chirp. The electronics also produced a voltage output proportional to the time delay or in other words the distance between the sender/receiver and the target. The vertical and horizontal units were chirped alternately so as to eliminate error due to cross reception of echoes between the two directions. The chirp repetition rate of ten per second enabled up to 5 Hertz wire vibrations to be measured. Distance resolution of the ultrasonic transducers was 3.3 mm and their range was 0.3 to 3.0 metres.

To identify changes in the distance measured due to the effect of temperature on the speed of sound in air, two channels of transducers were set up outside the instrumentation trailer measuring fixed distances. Changes noted on these channels could be used to correct values obtained from the

wire displacement channels. A single power supply provided all power required for the 14 ultrasonic measurement channels.

The ultrasonic transducer channels were individually calibrated in place by inserting a temporary target between the sender/receiver and the fixed target at a known distance from the fixed target. The change in output signal allowed a linear calibration coefficient to be calculated. Figure 9 contains a photograph of this procedure with the calibration target in place.

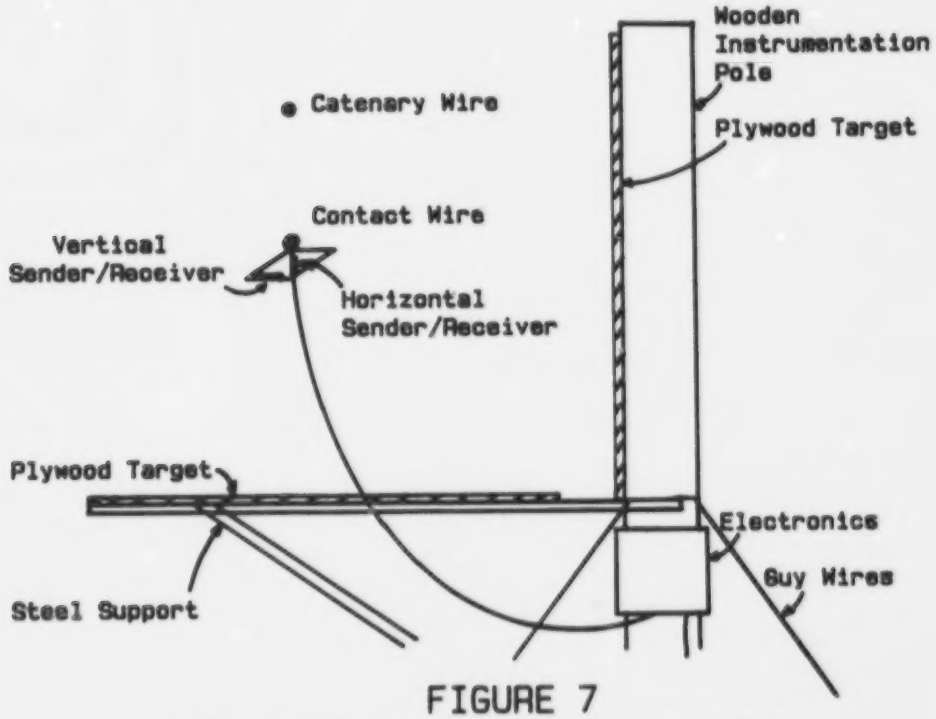

FIGURE 7

Ultrasonic Displacement Transducer Positioning

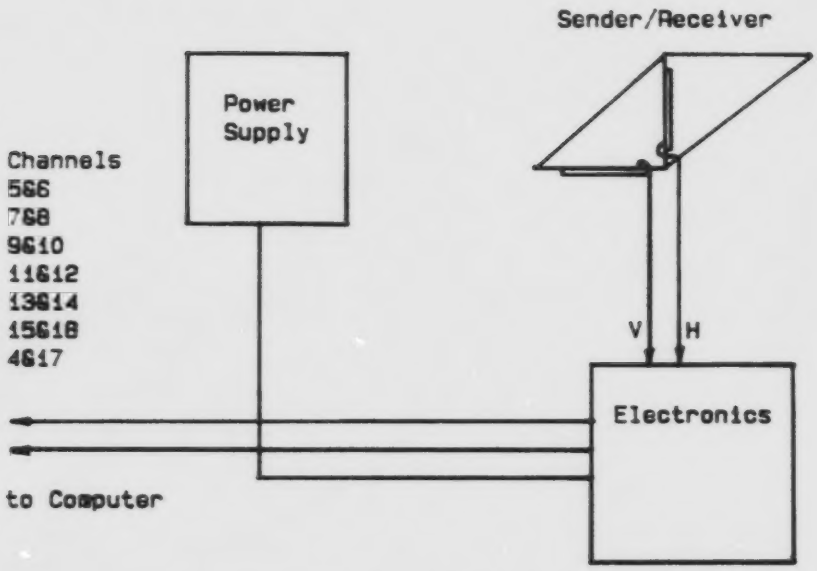

FIGURE 8

Schematic of Ultrasonic Displacement Transducer System

FIGURE 9

Calibration of Ultrasonic Displacement Transducers

3.6 Icing Load Cells

To determine whether or not the catenary wire system carried a significant amount of ice, two of the droppers between the catenary and the contact wire were replaced with specially made droppers incorporating tension load cells. These load cells were essentially strain gauged aluminum turnbuckles and were placed at the first dropper north of tower C2 and at the first dropper south of tower C2. A schematic diagram of the load cell system is in Figure 10. Vishay strain gauge signal conditioners were used to convert strain gauge readings into voltages suitable for input to the computer.

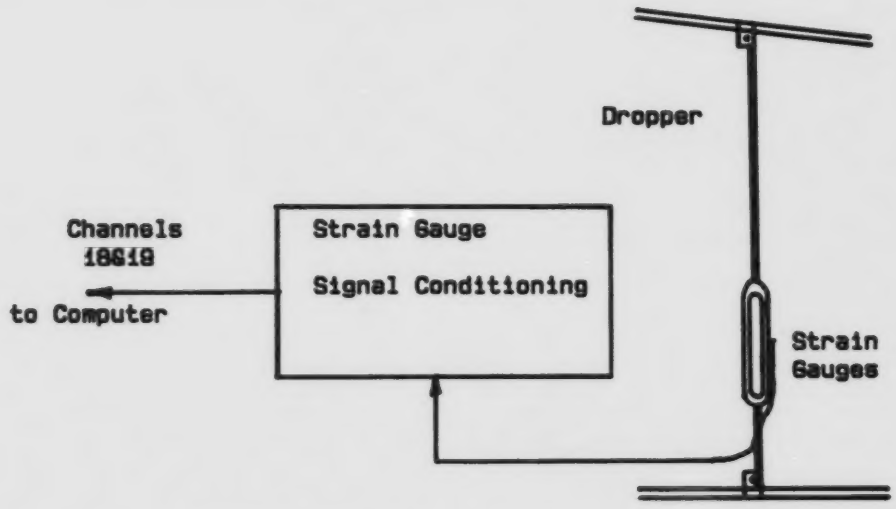

FIGURE 10

Schematic Diagram of Icing Load Cell System

3.7 Tower Deflections

Spot weldable pre-bonded strain gauges were installed near the base of each of towers C1 through C4. These were arranged in a half bridge with one active gauge and one gauge oriented such that it only measured thermal expansion effects. This approach was taken to minimize thermal drifting of the zero deflection strain reading. Figure 11 contains a photograph of a strain gauge installation with its water tight outer covering. Figure 12 is a schematic diagram of the tower deflection measurement system. Signal conditioning similar to that used for the icing load cells was used to provide a voltage signal output for the computer.

This system was calibrated at each tower by applying known deflections to the tower and measuring the corresponding outputs.

FIGURE 11
Tower Strain Gauge Installation

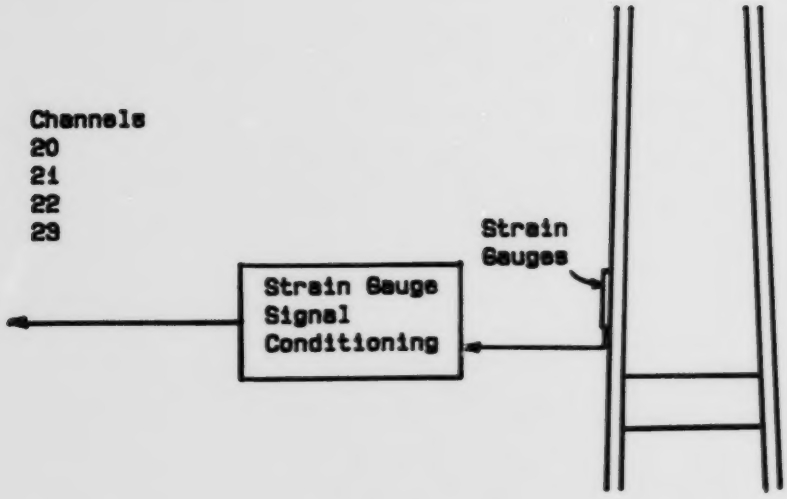

FIGURE 12

Schematic of Tower Deflection Transducer System

3.8 Wire Accelerations

As a second method of determining the oscillating portion of the wire deflection as well as a comparison of the horizontal modes of vibration of the catenary and contact wires, Sunstrand QA-800 servo accelerometers were installed on both of these wires at instrumentation poles I1 and I4. These accelerometers were encased in plexiglass boxes for weather resistance and clamped on the wires. Figure 13 contains a photograph showing the mounting of these accelerometers at I4. Also visible in this photograph is the I4 ultrasonic sender/receiver and camera number V2. In this photograph however, the plywood horizontal and vertical targets had not as yet been installed. Figure 14 is a schematic diagram of the accelerometer system. These devices have a current output therefore a ranging resistor was used to provide a voltage input for the computer. Calibration was achieved through tilting the accelerometer to produce various accelerations between zero and one g.

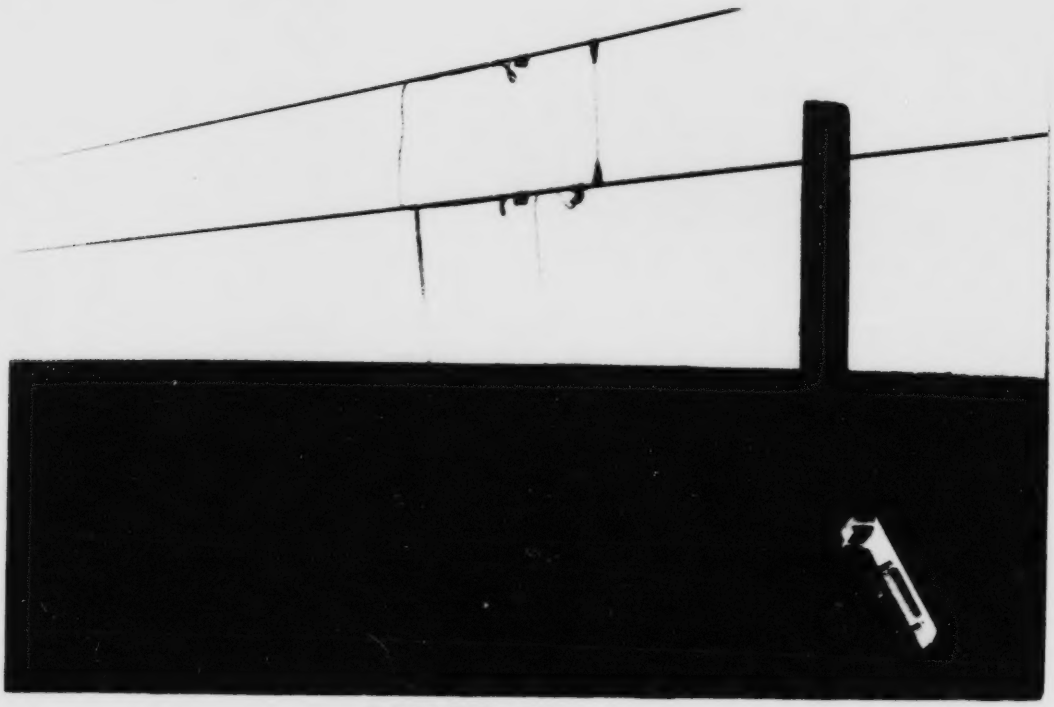

FIGURE 13

Accelerometers at Pole I4

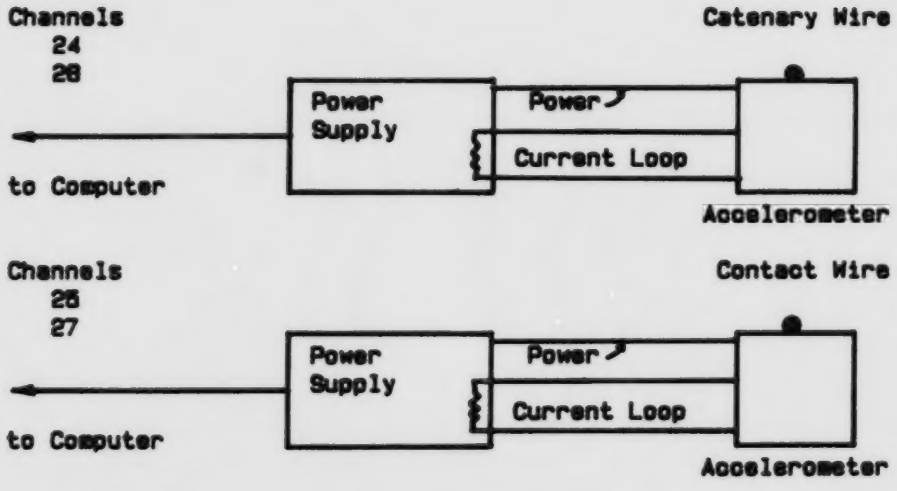

FIGURE 14

Schematic of Accelerometer Systems

3.9 Data Acquisition Software

Software for collecting, reducing and storing the 27 channels of data was written by Morrison Hershfield Limited expressly for the particular needs of the catenary deflection tests. Due to the long time period over which the data collection was to be performed and the high rate of sampling to collect information on wire vibrations (10/sec x 27 channels = 270 data points per second), the data could be stored only during significant wind events. In this way, the calm wind situations which were of little interest would be screened out. To create this screening algorithm, two resettable threshold wind speeds were established within the program. When the hourly average wind speed was below the lower threshold only hourly wind speed, direction and temperature summaries would be written to floppy diskette. This small amount of data occupied minimal space on the diskette.

Hourly average wind speeds which exceeded the lower threshold speed but remained lower than the upper threshold caused the next stage of data storage to be performed. In this speed range all 27 channels were sampled for a six minute time interval which was long enough to obtain a representative amount of gusting and wire motions. At the end of each of these time periods a summary including the minimum value, the maximum value, the mean value and root mean square for each channel were written to the diskette.

When the hourly average value exceeded the upper threshold speed, time histories were written to the diskette. This meant that all sampled data points on all channels were written directly to the diskette to allow further analysis of the correlation of the motions of various portions of the catenary system. Also during these high wind periods, the video recorder was set into record mode by the computer program.

4.0 FIELD TEST RESULTS

4.1 General

The field installation began collecting data from the 27 channels of instrumentation in mid-January, 1986 and data collection was discontinued on the last day of May 1986. During this time period several significant wind events took place. However there was an unusual lack of ice storms at the site. This was as observed by local residents comparing this winter's conditions with those of the recent past. One storm caused wide spread commercial power outages. Power failed at the test site and the data recorded by the computer was lost. A large amount of data totalling approximately 100 floppy diskettes full of information was retrieved. These diskettes were sent to Morrison Hershfield Limited's laboratory where the information was removed for analysis and the diskettes returned for reuse. During the test period the modem telephone link between the in-house computer and the on-site computer was used extensively for system performance monitoring and for a small amount of data transfer.

4.2 Wind

The wind instrument system described in Section 2.4 was pre-calibrated by the manufacturer prior to delivery and installation. These calibrations were checked while at Morrison Hershfield Limited's laboratory using the in-house wind tunnel for wind speed calibration, angle measurements for the wind direction check and various internal and external temperatures for checking the calibration of the RTD (resistive temperature device) transducer.

During installation the wind direction vane was oriented so that it produced an output proportional to the wind direction measured clockwise from the catenary centre-line with zero degrees being toward the northern end. The catenary line as installed was actually oriented with its northern end towards a direction of 327 degrees measured clockwise from true north.

As previously stated in Section 3.9 the data acquisition software used the hourly average wind speed to determine whether or not to store data on floppy diskette for further analysis. These hourly values of minimum and maximum, mean and root-mean-square values for each of the three wind related channels were stored on floppy diskette as hourly summaries even if the wind speed was not enough to exceed the threshold values.

The data gathered from the wind instruments was not analyzed in detail by itself but is inherently incorporated in the results presented for the other quantities of interest. For the analyses of these other channels, the prime quantity of interest was the component of wind speed normal to the catenary line. The measured wind direction was used to determine this component. The temperature was also used in the correction of the ultrasonic displacement transducer outputs for the change in the speed of sound due to temperature.

The highest six minute mean wind speed component normal to the catenary line was found to be 44 km/h (12.2 m/s). During this time period, the wind was gusting to peak values of approximately 61 km/h (17 m/s). During this particular wind event, the wind came from a direction which was, on average, normal to the catenary line.

Examination of the six minute average data showed that the most frequent strong winds occurred from directions between southwest and north (57% of strong wind events) and east through southeast (30% of strong wind events). Strong winds approached the catenary system within 10 degrees of normal to the centreline 20.3% of the time.

4.3 Horizontal Displacement of Contact Wire

The horizontal displacement of the contact wire was measured using ultrasonic displacement transducers described in Section 3.5. Since these transducers utilize a time delay measurement between emitting and receiving a sound pulse, their calibration was linearly dependent on the speed of

sound. It was the intent at the outset of the study to use the outputs from two displacement transducers which were positioned to read a fixed distance as correction for temperature. Analysis of the data recorded from these, however, showed that simple drifting of the zero point of these two channels (4 and 17) was greater than the change of calibration due to temperature. Therefore this approach for correction was abandoned and the temperature measured from channel 3 was used to calculate a new speed of sound which then allowed correction of the calibration to the displacement transducers.

The nature of unattended field instrumentation studies such as this one is that problems with some of the equipment are bound to occur over a period of a few months especially when the equipment is exposed to the elements. For this reason at the design stage the approach was taken to provide many independent channels of each type of measurement system in order to obtain the redundancy of information required to ensure that usable data were collected. To this end six ultrasonic displacement transducers were installed to measure horizontal deflections of the contact wire at locations illustrated in Figure 1.

Channels 5, 7, 9, 11, 13 and 15 recorded by the computer were the signals from these transducers. During the months of data collection, approximately 250 hours of six minute average data were collected for each channel of input. This represented a very large amount of data to be manipulated and presented. These data were screened by computer to remove the points which were not reliable. The remaining data were then plotted on a linear scale against the normal component of measured mean wind speed as discussed in the previous section. These plots are in figures 15 through 18. It can be seen by examining the data that a fair amount of vertical scatter is present in all plots. This scatter is better on some channels of ultrasonic displacement transducer than on others. It was attributed to drifting of the zero deflection output voltage of the transducers.

To handle the resetting of zero points in the best possible way, the data were examined to determine when the normal component of wind speed was very

near zero. This occurred when the actual wind was calm or when the wind was aligned close to the catenary centre-line (a reading between 350 and 10 degrees). At these points in the data, zero values were reset for each of the displacement measuring channels (including the tower measurements which will be discussed later). These zero values were then subtracted from all subsequent data collected until another suitable zero reading situation occurred. The plots presented contain the zero corrected data. Although this technique reduced the scatter in the data, much remains. Unfortunately on some channels the scatter was felt to be too large to allow useful conclusions to be drawn so their information has not been included. Also on these plots is a line representing the predicted deflection which will be discussed in a later section.

a) 70 Metre Span

Figure 15 contains two plots of the data recorded from channel 5 which was the displacement of the contact wire horizontally from the no wind position at instrumentation pole I1 which was situated at the midpoint of the 70 metre span. The results presented for this location as well as for all other locations include the deflection of the towers as the transducers measured the total deflection of the contact wire relative to the heavily guyed instrumentation poles. The two plots in the figure present data for the mean deflection of the wire and the maximum excursion during the six minute averaging period. The horizontal axis of each of the plots is the normal component of mean wind speed in metres per second (m/s) and covers a range of zero to 25, the range of greatest interest in determining the horizontal deflection of overhead contact systems in Canada. These plots show that this channel produced good results with fairly low scatter. The curvature of the collection of points exhibits visually a dependency of displacement on the square of wind speed, as expected from theoretical considerations.

The scatter produced by the zero drift problem causes the data grouping not to go through zero at under conditions of zero wind. Shifting of the results to compensate for this vertical axis intercept would produce the best estimate of deflection obtained from the field tests and would bring

the data into better agreement with the theoretical curve. The majority of the data obtained occurred at mean wind speeds normal to the wire of up to 9 m/s with the highest speed data taken under mean wind speeds of 12.2 m/s.

b) 65 Metre Span

Figure 16 presents plots of the mean and peak deflections measured at instrumentation pole I2 which was located 10.8 metres from tower C2 in the 65 metre span. This was channel 7 recorded by the data acquisition computer. Two other locations in this span (channels 9 and 11) which were on poles I3 at 21.6 metres from tower C2 and on pole I4 at midspan produced data sets with too much scatter to be considered useful. These results have therefore not been presented.

The data presented in the figure, although exhibiting more scatter than the results in Figure 15, do show some distinct trends. These trends show slopes and curvatures that are much shallower than those seen previously. This is due to the fact that this was a shorter span and also the point of measurement was not at the mid-point of the span. Both of these effects should produce smaller deflections at a given wind speed than the previous 70 metre span data.

c) 60 Metre Span

Figure 17 contains plots of mean and peak results for channel 13 which measured the midspan deflection of the 60 metre span at instrumentation pole I5. Comparisons with the theory are similar to those for the 70 metre span.

d) 55 Metre Span

Mean and peak horizontal deflections at the mid point of the 55 metre span (instrumentation pole I6 recorded on channel 15) are presented in Figure 18. Greater scatter is present in these data but again significant trends can be identified. Also the reduction in deflection at a given mean speed due to shorter span length can be seen.

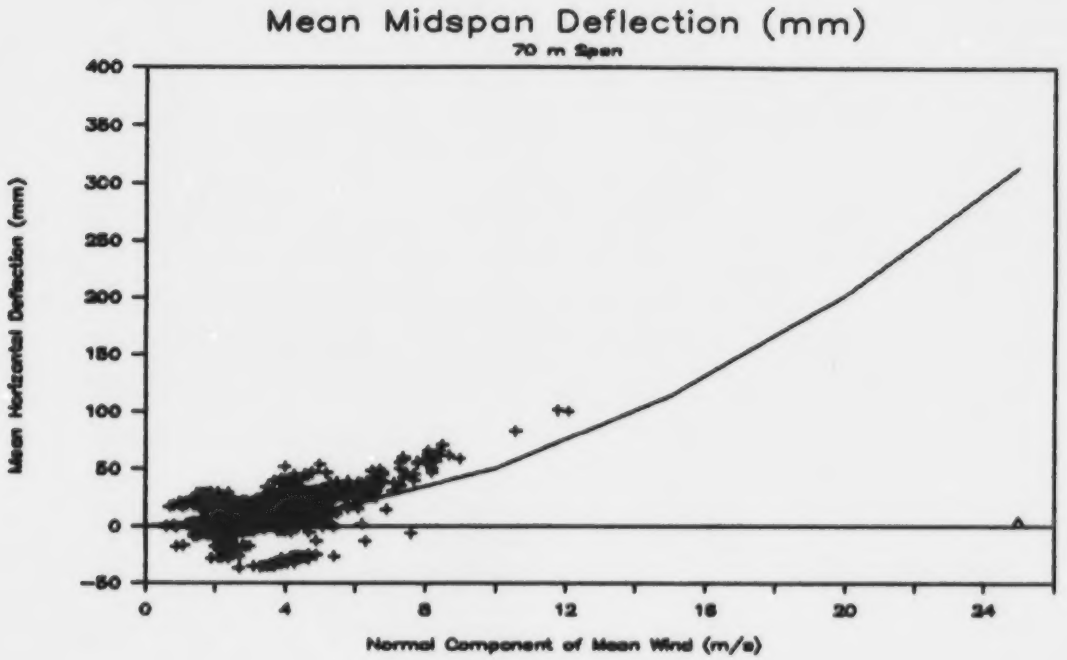

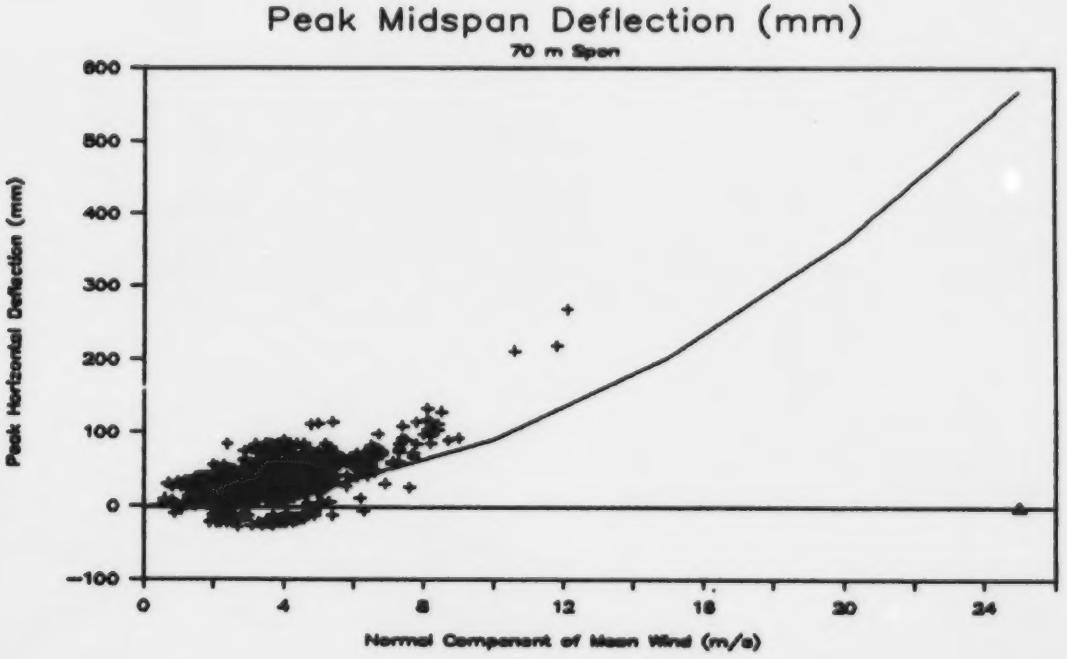

Figure 15
Results from Channel 5

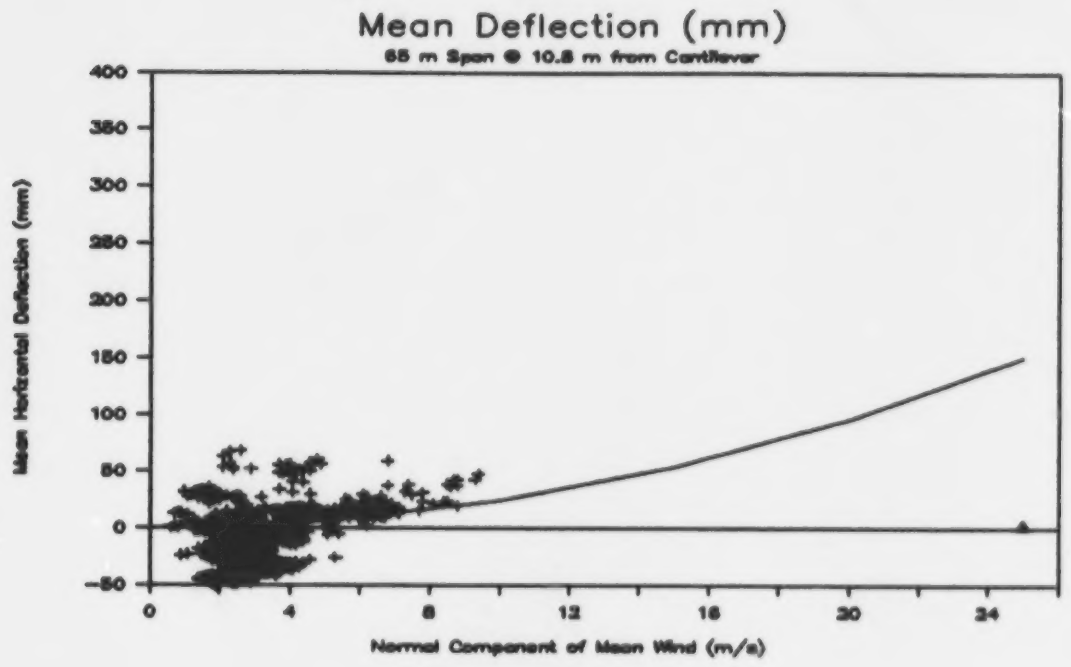

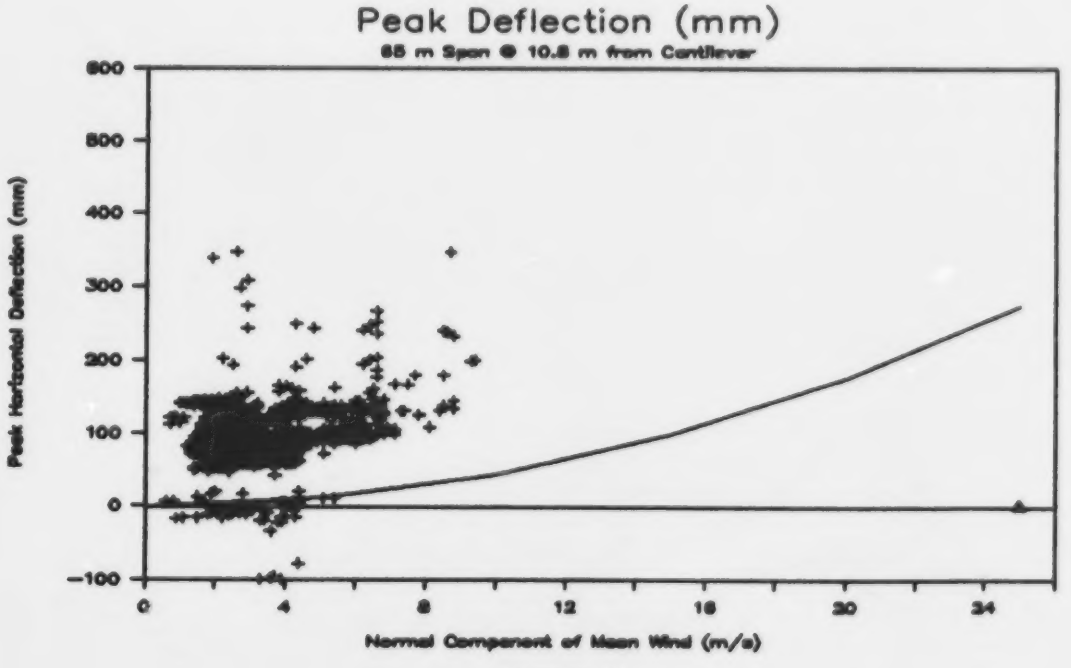

Figure 16
Results from Channel 7

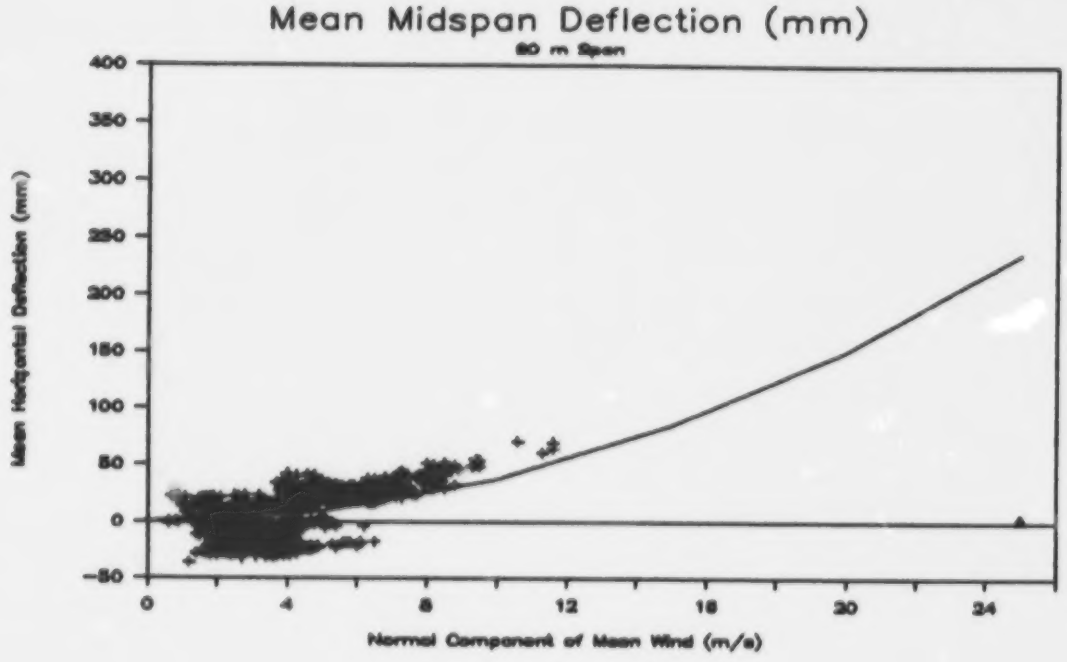

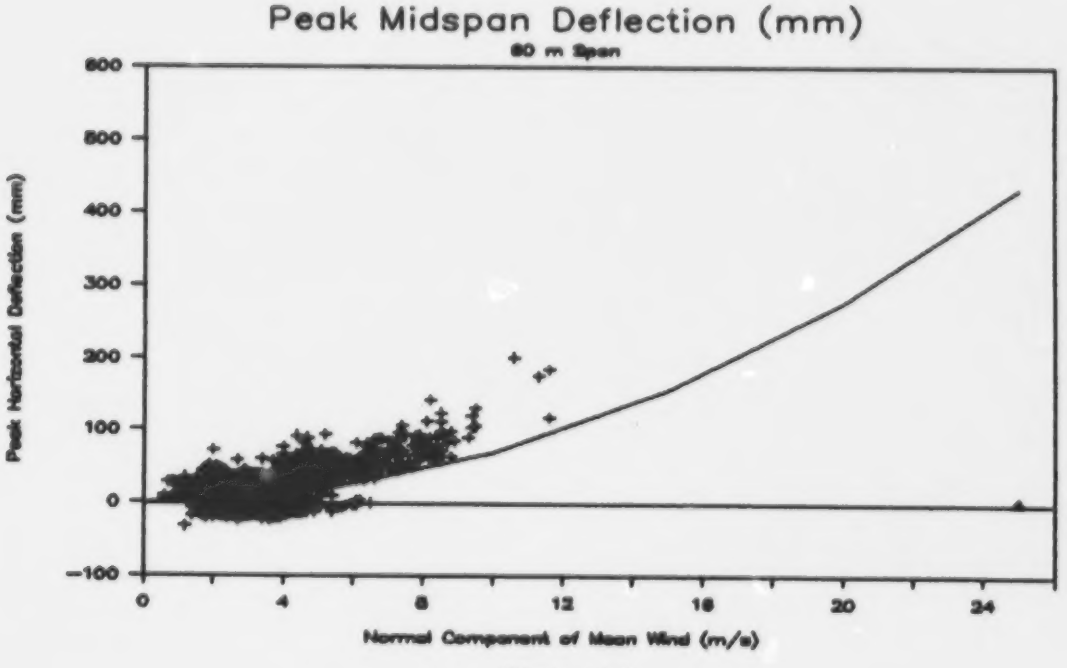

Figure 17
Results from Channel 13

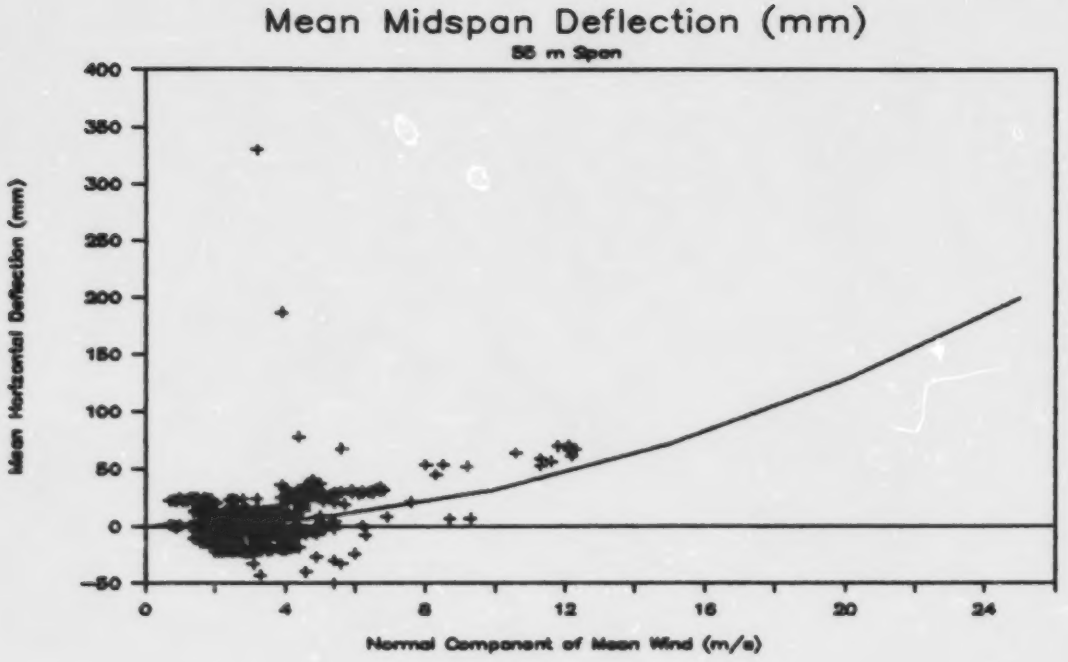

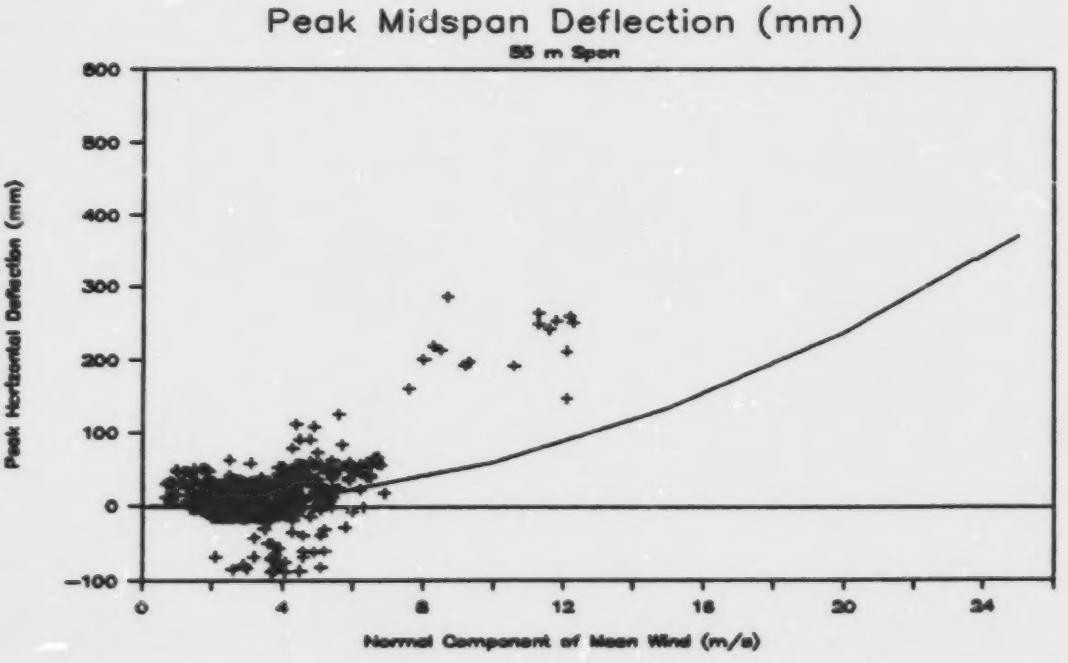

Figure 18
Results from Channel 15

4.4 Vertical Displacement of Contact Wire

Ultrasonic displacement transducers similar to those used for measuring the horizontal deflection of the contact wire were used to measure vertical deflection of the contact wire at each of the instrumentation poles. Since the cross-sectional shapes of the wires used for both the contact and messenger wires were symmetrical, there is no lift component and the mean vertical deflection is expected to be very near zero. The only vertical mean deflection would arise due to the unequal horizontal deflections of the contact and messenger wires. This effect is expected to be very small in relation to vertical oscillation caused by wind turbulence. A heavily worn contact wire with its asymmetrical cross-sectional shape could produce a lift force thus producing some vertical mean deflection.

The vertical contact wire displacements were measured on channels 6, 8, 10, 12, 14 and 16. Inspection of these results illustrated that typical peak to peak motions of the contact wire were of the order of 40 to 50 mm. This vertical motion did not appear to have a large dependence on wind speed as seen in the horizontal motion results.

4.5 Ice Loading

During the test period no significant natural ice buildup was noted at the field test installation site. Severe ice storms were experienced in Charlottetown but these unfortunately did not affect the Borden site region. As a result the icing load cells installed in the two droppers on the north and south sides of tower C2 (channels 18 and 19) did not register any ice loads. This situation was evaluated at a point late in the winter and it was decided that it would be necessary to artificially build up ice on the catenary system. To do this, on a sub-zero day with a significant wind, water was sprayed on one span of the installation and a reasonable accretion of ice was obtained. Shortly thereafter the wind which had been significant died out and no usable data was acquired prior to the melting of the ice. This was done toward the end of the unusually mild winter and no further suitable opportunities for water spraying occurred.

4.6 Deflection of Towers

The tower deflections as the height of the contact wire were monitored by strain gauges mounted near the ground on towers C1 through C4 (channels 20 through 23 respectively). These were calibrated to produce deflections directly by applying several known deflections to the tower and noting the output. This technique assumes that the anchorage of the towers was solid throughout the monitoring period.

The results obtained from these channels are presented as plots of mean and peak tower deflections at contact wire height in Figures 19 through 22. These plots show a fairly large amount of scatter on all channels tested. These data also cover only the very low end of the wind speed range of approximately zero to 5 m/s. Although interpretation is difficult, it does appear that at 5 m/s there is about 1 mm of tower deflection at the height of the contact wire. This is based on the assumptions that the roughly horizontal line groupings of points that can be discerned are in fact data from a particular wind event and that during the shorter time period of one event the drift of the zero is not significant. It appears that the 5 m/s end of a number of these groupings is about 1 mm greater deflection than the estimated zero wind deflection. In comparison with the mean deflections measured at the mid-points of the various spans under 5 m/s wind speed, this value represents on the order of 10 percent of the total deflection. Note that the midspan deflections presented in this study contain the tower deflections also.

The ratio of peak to mean tower motions seems to be of about the same magnitude as that for the contact wire deflections, i.e. around 2:1.

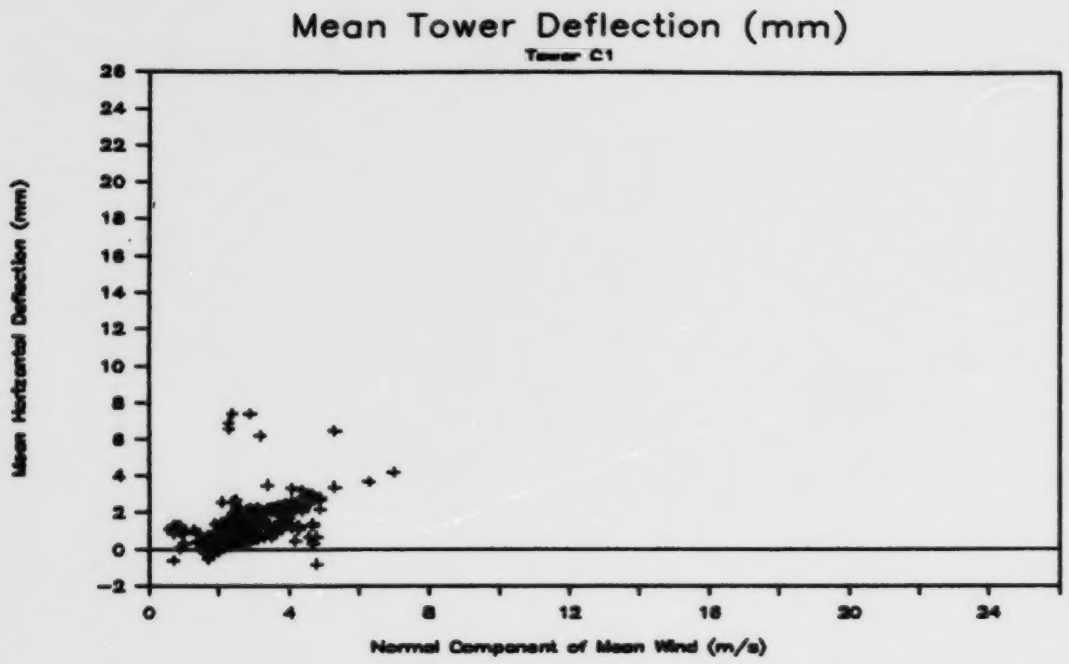

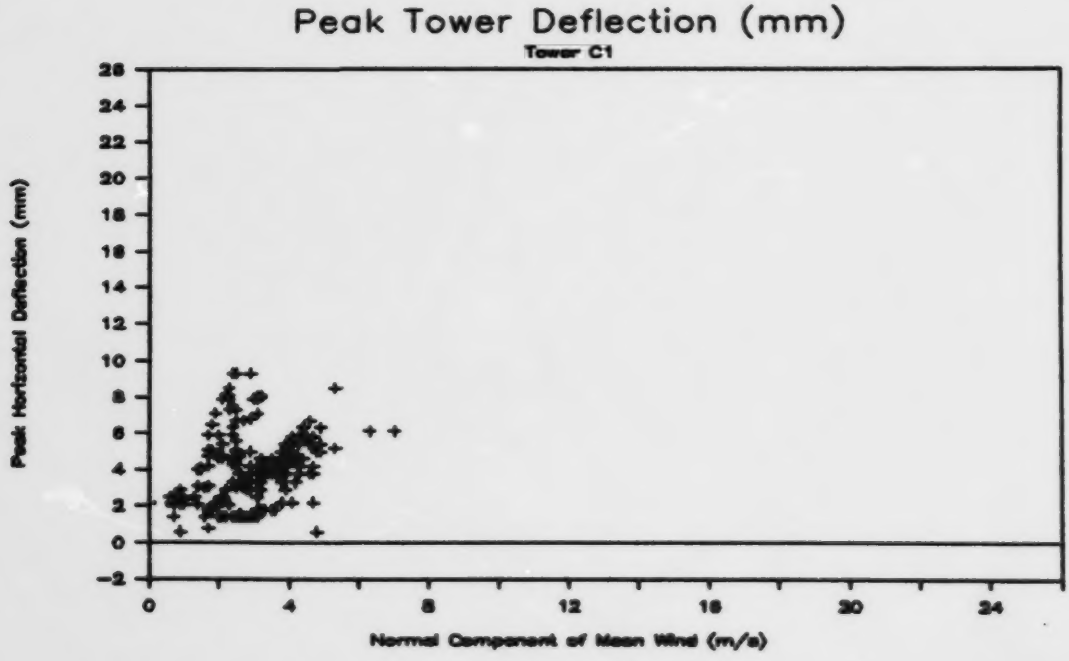

Figure 19
Results from Channel 20

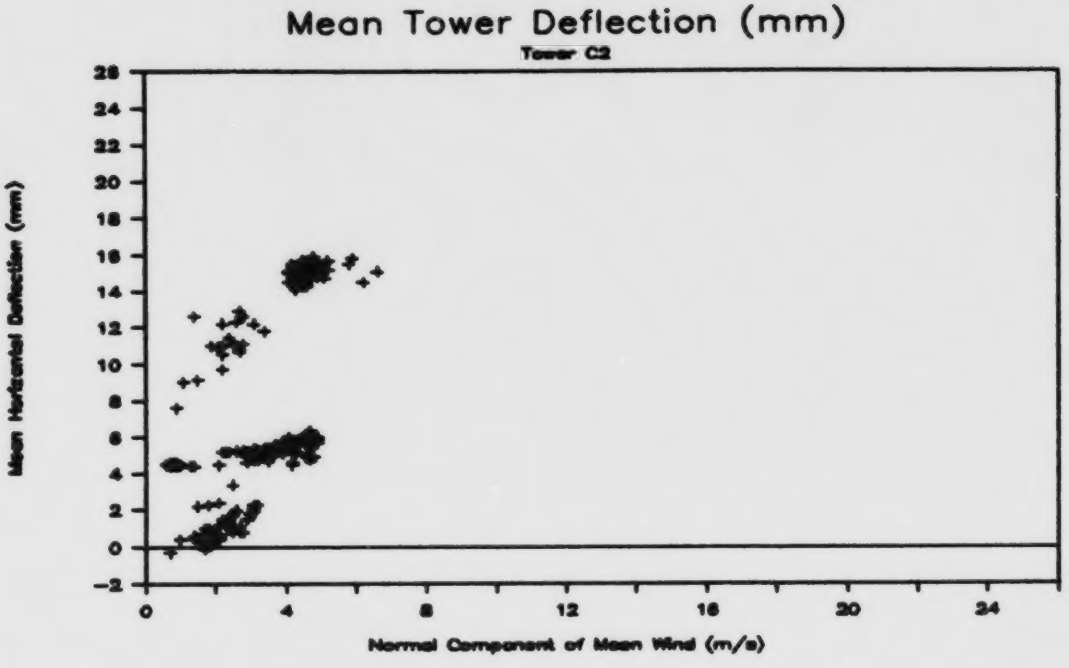

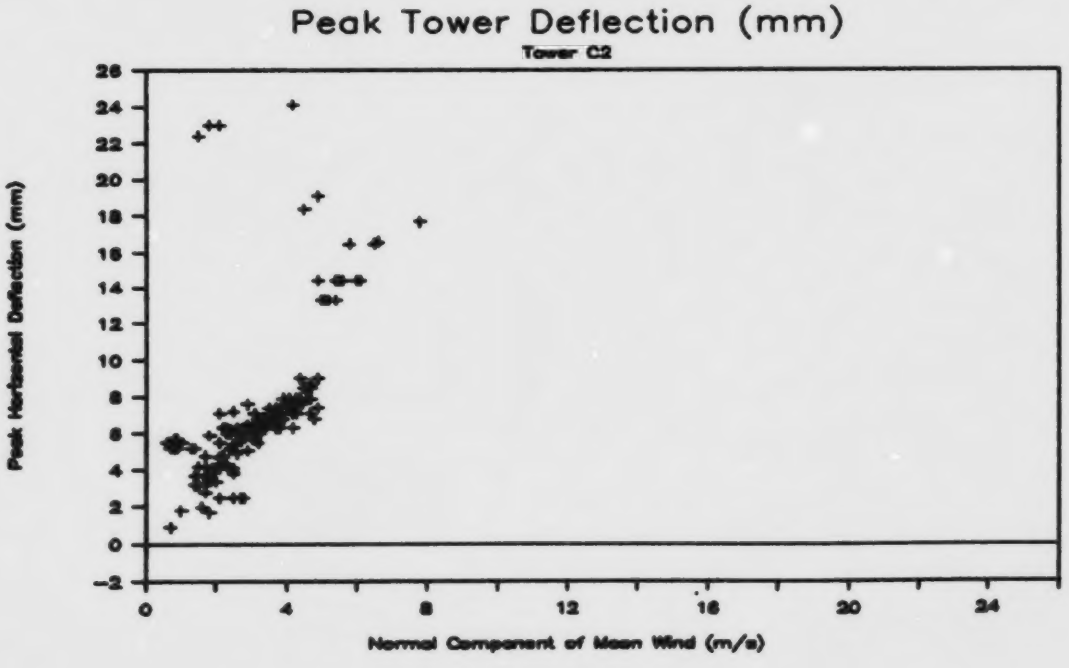

Figure 20
Results from Channel 21

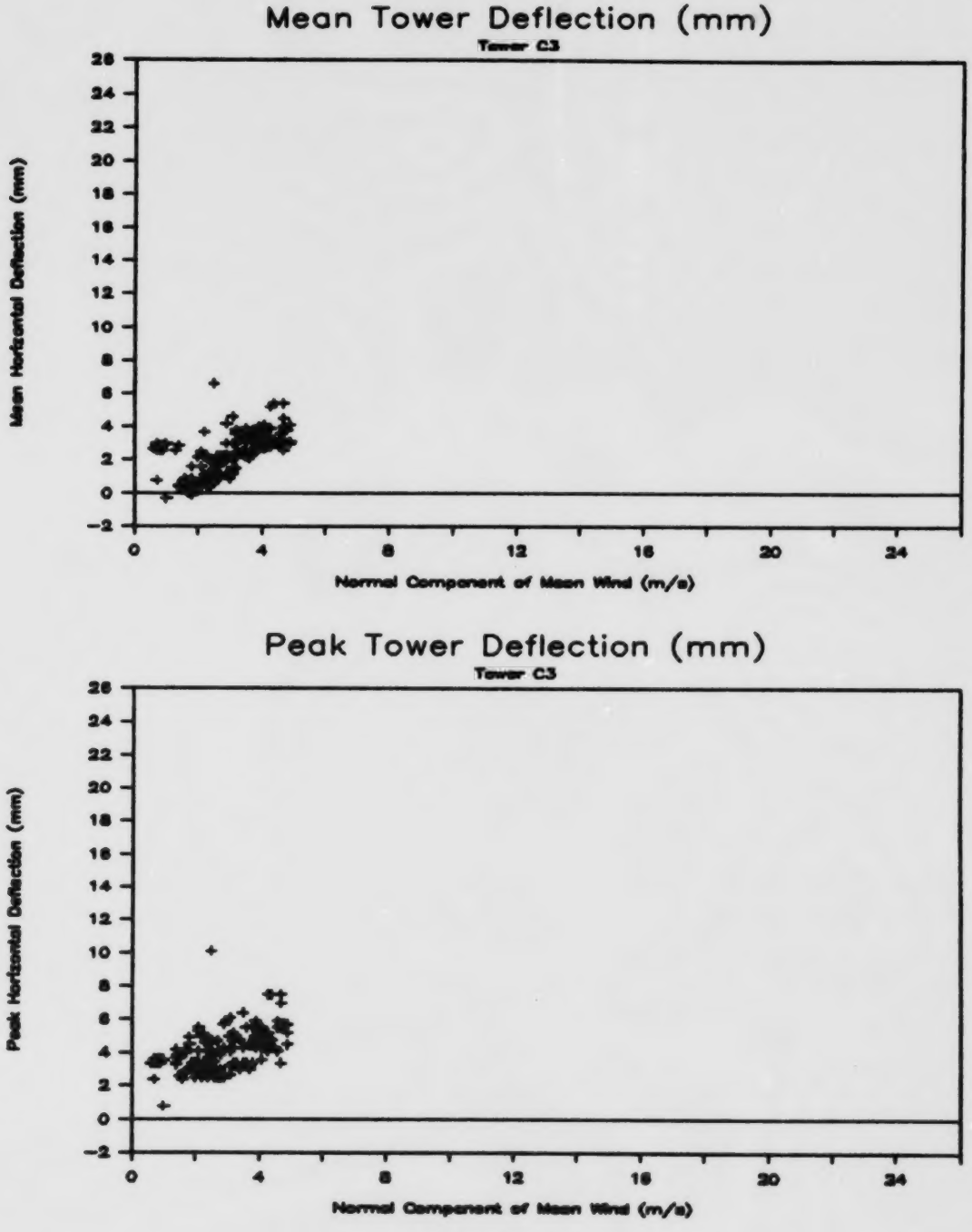
Mean Tower Deflection (mm)
Tower C3
Mean Horizontal Deflection (mm)
Normal Component of Mean Wind (m/s)
Peak Tower Deflection (mm)
Tower C3
Peak Horizontal Deflection (mm)
Normal Component of Mean Wind (m/s)

Figure 21
Results from Channel 22

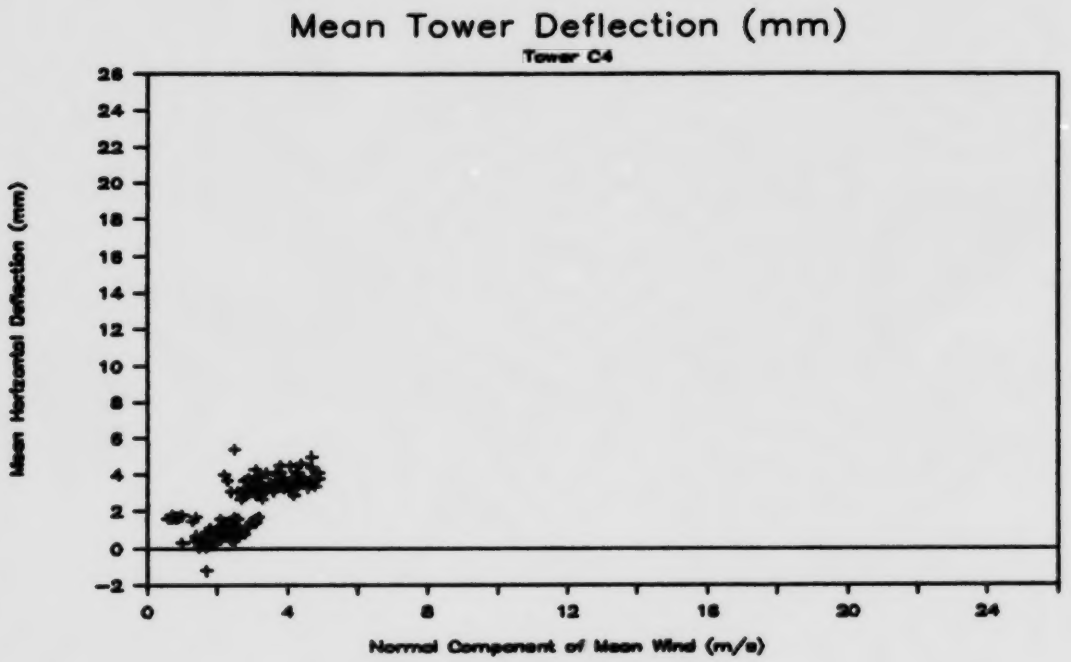

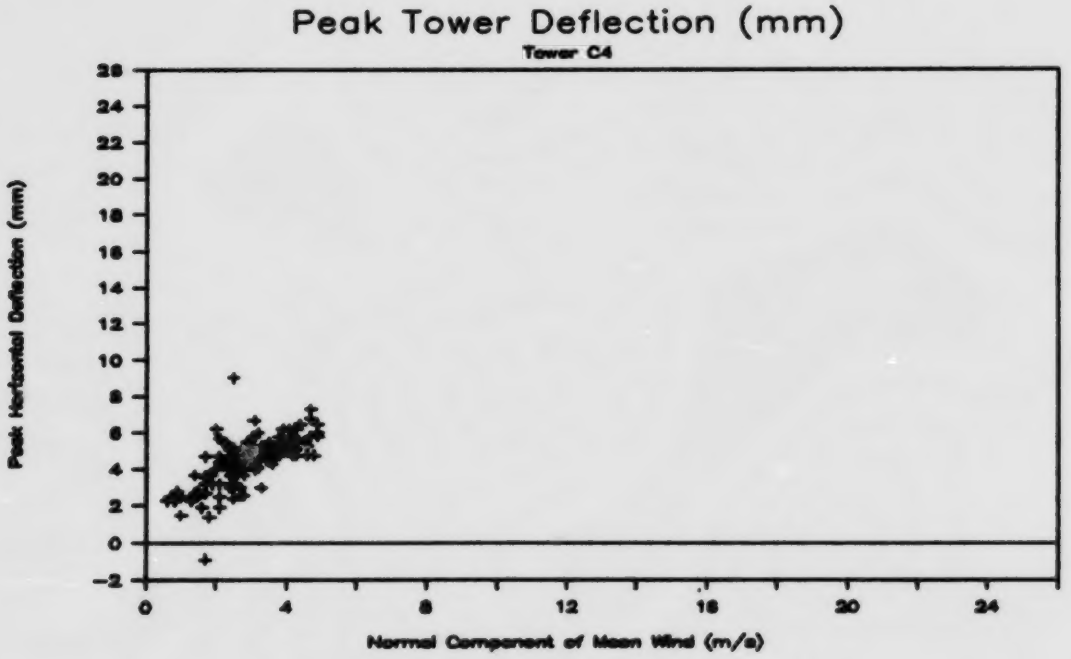

Figure 22
Results from Channel 23

4.7 Lateral Acceleration of Messenger and Contact Wires

Accelerometers were installed at the mid-points of the 70 and 65 metre spans on the messenger and contact wires and measured accelerations in the horizontal direction. Channels 24 and 26 measured motions of the messenger wire and channels 25 and 27 measured motions of the contact wire.

Since the mean acceleration of any sinusoidal vibration is zero and the zeroes on these channels were adjusted to remove any gravitational component, the quantities of interest from these channels are the peak acceleration and the RMS acceleration. Figures 23 through 25 contain plots of the peak and RMS accelerations measured on these channels (channel 24 omitted due to instrument problems). Due to the inherently greater stability of the accelerometer the scatter in the data is less than on the displacement channels. These accelerometers were installed primarily as a backup approach to determining the dynamic components of the horizontal motions. The results show peak accelerations after correction for zero shift of approximately 130 and 110 milli-g for the contact wires of the 70 and 65 metre spans respectively at a mean normal wind speed of 10 m/s. As a point of reference, if the oscillation of the wire were sinusoidal at the natural frequency of the system, these peak displacements would correspond to peak displacements of 49 and 45 mm. Measured peak factors can be obtained from these curves by taking the ratio of peak/RMS. The data show that a value of 4.0 to 4.5 is representative in general.

The accelerometer outputs were also used at the setup stage to determine the natural frequencies of the 70 and 65 metre spans. These were found to be 0.80 and 0.85 Hertz. Also at this stage, the catenary was manually excited in low wind conditions and then allowed to decay naturally. Using a chart recorder trace of this decay and employing a logarithmic decrement method of estimating the mechanical damping, a value of 0.8% was found. This falls within the expected range of 0.5 to 1.0%.

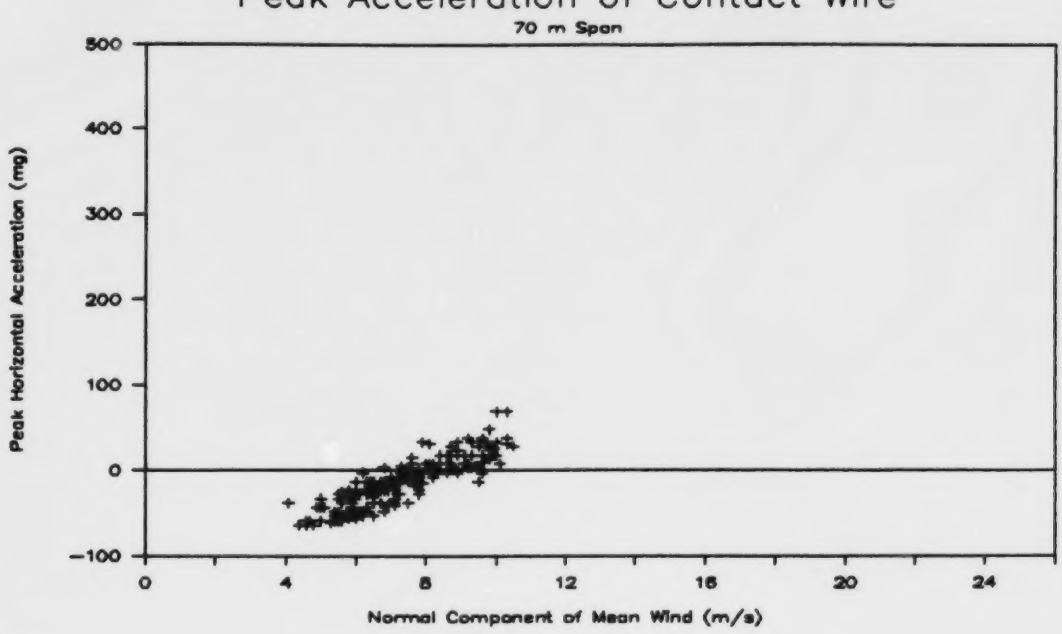

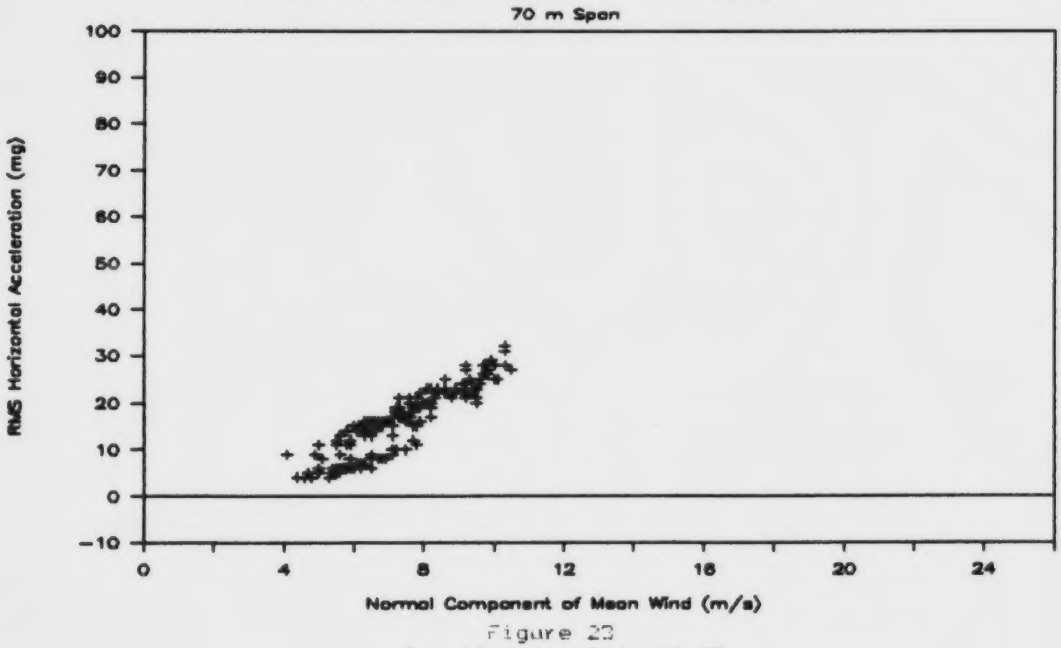

Figure 23
Results from Channel 25

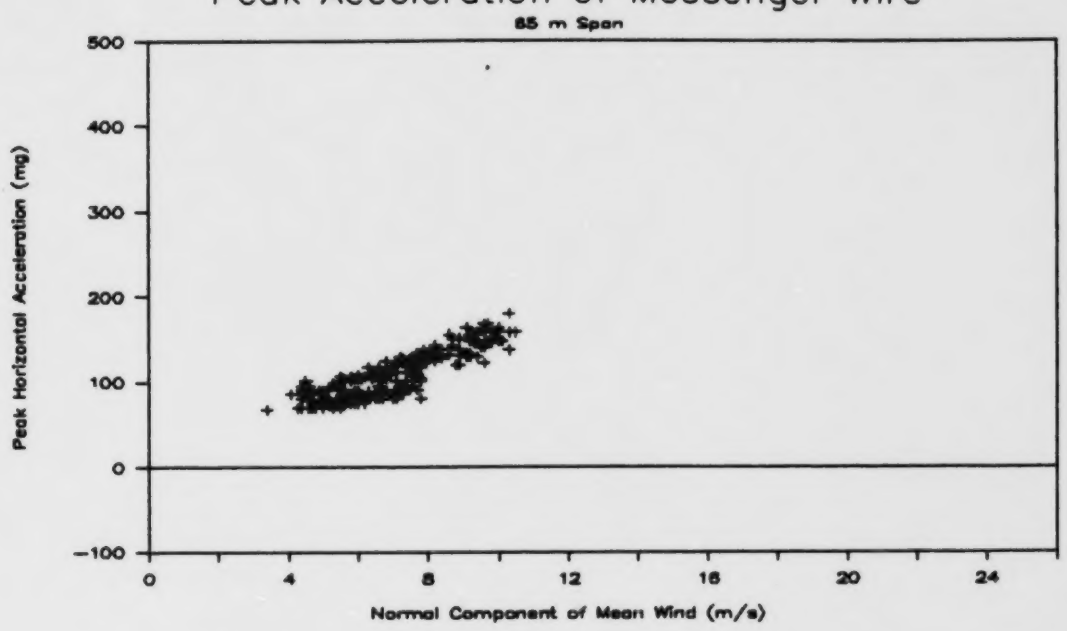

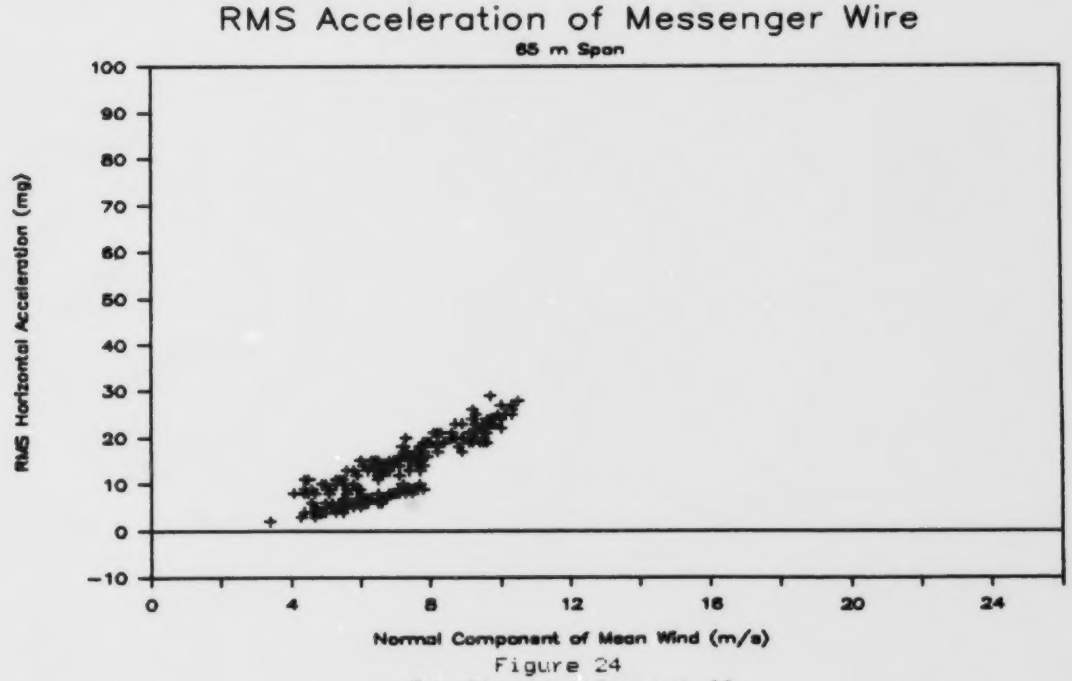

Figure 24
Results from Channel 26

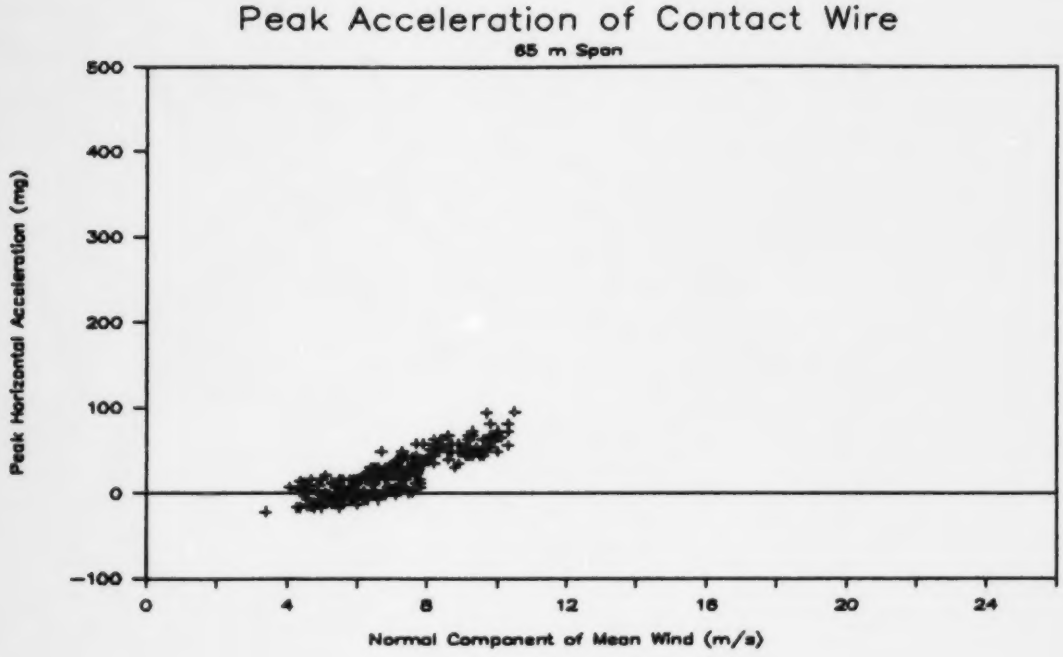

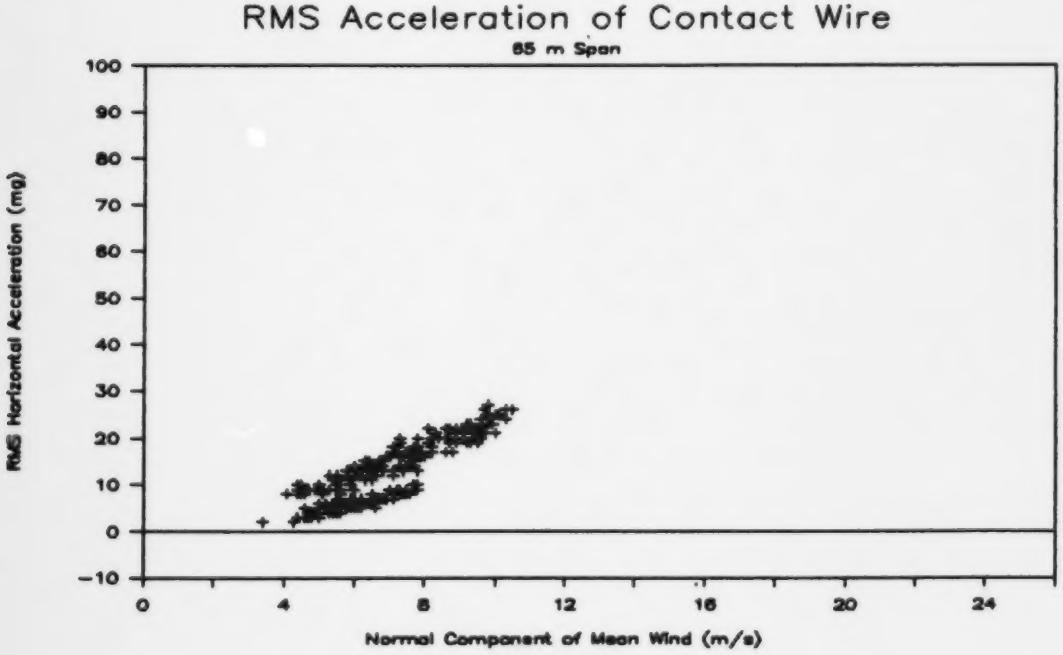

Figure 25
Results from Channel 27

4.8 Videotape Records of Contact Wire Motions

The computer was capable of turning on the videotape recorder during periods of high winds. It was hoped at the outset that the two cameras installed would be able to record visually the manner in which ice was shed from the wires and also to capture any large oscillatory motions of the system due to the combined action of wind and ice. The unusually ice free conditions during the test period made it impossible to record the desired icing events. A large number of hours of video tape records were retrieved containing normal wind events. Although in the camera views it is difficult to discern mean wire displacements, the oscillations can be seen. Under the conditions recorded however, these motions are not large. A sample video tape record of a few minutes has been included with this report. Since the rest of the video tape records are very similar to this one, and in general uneventful, they have not been included. They will be archived for further analysis if required in the future.

5.0 DEFLECTION PREDICTION PROGRAM

5.1 General

As stated in the introduction, it was the intent of the present work to develop a detailed method for evaluating the wind induced deflection of the overhead contact systems used in modern rail systems. It was decided at the outset that the most appropriate form for deflection prediction would be a computer program which would run on IBM PC or compatible computers. These would include all microcomputers operating under the MS-DOS operating system.

The program developed by Morrison Hershfield Limited was written in the BASIC language and is designed to operate without any special hardware requirements. The important results are written to a simple text screen and the option is given for the user to have hardcopy produced on a standard printer device if one is available. Being written in standard BASIC code, the program could be easily ported to virtually any computer capable of interpreting or compiling BASIC. Source code for the program is contained in Appendix D.

The theoretical background for the deflection prediction program lies in the turbulent buffeting theory for line like structures used extensively for prediction of wind induced motions of flexible structures such as long span bridges. The theory, as it pertains to the motions of the catenary system, is described in detail in Appendices B and C. Appendix B describes the statics and mechanics of the catenary system and Appendix C describes the response of the catenary system to the turbulent action of the wind.

5.2 General Notes on the Use of the OCS Deflection Program (OCS.BAS)

The program has been written with the aim of being as self contained and self explanatory as possible. With these objectives in mind, input parameters are typed in at the appropriate prompt with the option of entering an 'H' at any prompt to obtain a 'Help' text describing the prompt and the details of its input. Where applicable, values are suggested to cover the more usual conditions. The program does not allow an input value of zero at any prompt as a zero indicates to the program that the existing value is correct and no change will take place in the value. Should a value of zero be desired for an input parameter, a very small non-zero value should be entered (i.e. .00001). The program steps sequentially through all the required input parameters allowing the operator to either type in a new value or to simply press the 'ENTER' key if he chooses to retain the existing value. After all prompts have been acted upon, the program rewrites the screen and asks the operator to check that all quantities are correctly entered. If the values are all correct, the calculations are performed and the results are presented on the screen. At this point, the operator is given the choice of hardcopy printout of the screen, a detailed printout of the input and calculated values or no hardcopy. The operator then may choose to return for additional calculations or to quit the program.

The program makes the assumption that the overhead contact system is a simple catenary of the level or sagged contact type. It should be noted that the deflections produced by the program do not include any tower deflections. These must be calculated separately and summed with the program output.

5.3 Input Parameters

The input section of the program is a table of values on the screen that the operator must fill in or alter to suit his particular catenary system. The following is a brief description of the required inputs:

a) Wire Diameter

This value must be entered for both the contact and the messenger wire. It is the vertical dimension of the wire and as such, is the thickness of the wire as viewed in elevation. It must be entered in millimeters.

b) Wire Mass

This value is the mass per metre of wire and must be entered for both wires. It can easily be calculated from the cross-sectional area of the wire and the density of the wire material. It is specified in units of kilograms per metre.

c) Drag Coefficient

Both the contact and the messenger wires have their own particular drag coefficient. These drag coefficients must be obtained from the literature or through special wind tunnel tests. Most wire shapes have been tested extensively in previous work and have generally accepted values for their drag coefficients. One complicating feature of the drag coefficient of rounded section cylinders is that the drag coefficient does not remain constant for all sizes of cylinder and wind speeds. Figure 26 contains a plot of the accepted drag coefficient for smooth circular cylinders in smooth wind flow versus Reynold's Number (equal to the diameter of the cylinder times the wind speed divided by the kinematic viscosity of air). The range for typical catenary wires is indicated in the plot. It can be seen that the drag coefficient for circular contact wires could be in the range of 1.0 to 1.2. We suggest that the conservative value of 1.2 be used in this instance. For stranded wires, a value of 1.0 is generally accepted.

A heavily worn contact wire could also exhibit a drag coefficient as low as 0.6 as it would become more streamlined. In addition, the frontal area would be much reduced. Icing can also introduce shape changes and, therefore, drag coefficient changes.

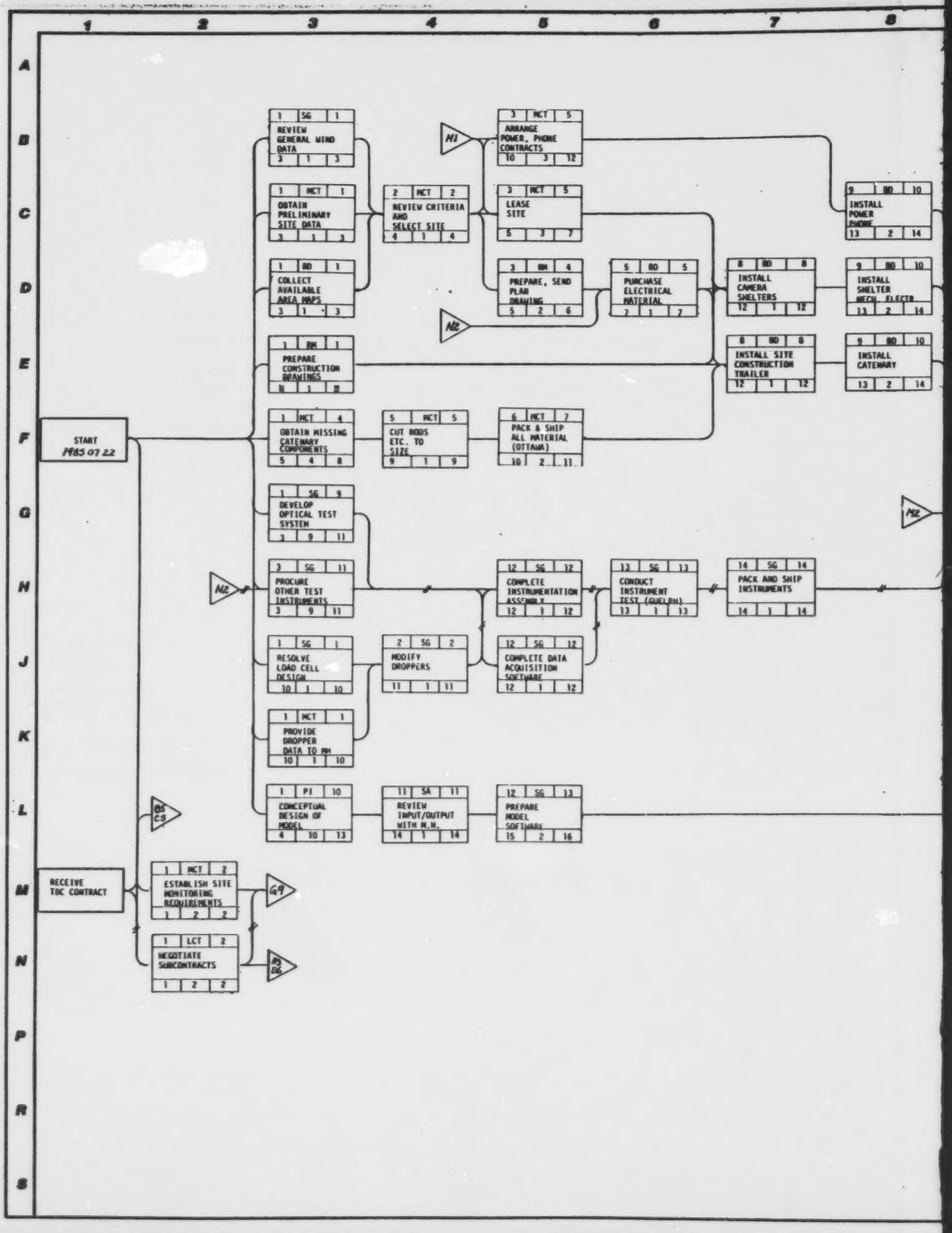
START M85 07 22
RECEIVE TBC CONTRACT
1 SG 1 REVIEW GENERAL WIND DATA 3 1 3
1 MCT 1 OBTAIN PRELIMINARY SITE DATA 3 1 3
1 BD 1 COLLECT AVAILABLE AREA MAPS 3 1 3
1 RM 1 PREPARE CONSTRUCTION DRAWINGS 11 1 11
1 MCT 4 OBTAIN MISSING CATENARY COMPONENTS 5 4 8
1 SG 9 DEVELOP OPTICAL TEST SYSTEM 3 9 11
3 SG 11 PROCURE OTHER TEST INSTRUMENTS 3 9 11
1 SG 1 RESOLVE LOAD CELL DESIGN 10 1 10
1 MCT 1 PROVIDE DROPPER DATA TO RM 10 1 10
1 PI 10 CONCEPTUAL DESIGN OF MODEL 4 10 13
2 MCT 2 REVIEW CRITERIA AND SELECT SITE 4 1 4
5 MCT 5 CUT RODS ETC. TO SIZE 9 1 9
2 SG 2 MODIFY DROPPERS 11 1 11
11 SA 11 REVIEW INPUT/OUTPUT WITH N.H. 14 1 14
3 MCT 5 ARRANGE POWER, PHONE CONTRACTS 10 3 12
3 MCT 5 LEASE SITE 5 3 7
3 RM 4 PREPARE, SEND PLAN DRAWING 5 2 6
6 MCT 7 PACK & SHIP ALL MATERIAL (OTTAWA) 10 2 11
5 BD 5 PURCHASE ELECTRICAL MATERIAL 7 1 7
12 SG 12 COMPLETE INSTRUMENTATION ASSEMBLY 12 1 12
12 SG 12 COMPLETE DATA ACQUISITION SOFTWARE 12 1 12
13 SG 13 CONDUCT INSTRUMENT TEST (GUELPH) 13 1 13
13 SG 13 PREPARE MODEL SOFTWARE 15 2 16
14 SG 14 PACK AND SHIP INSTRUMENTS 14 1 14
8 BD 8 INSTALL CAMERA SHELTERS 12 1 12
8 BD 8 INSTALL SITE CONSTRUCTION TRAILER 12 1 12
9 BD 10 INSTALL POWER PHONE 13 2 14
9 BD 10 INSTALL SHELTER MECH. ELECTR 13 2 14
9 BD 10 INSTALL CATENARY 13 2 14
1 MCT 2 ESTABLISH SITE MONITORING REQUIREMENTS 1 2 2
1 LCT 2 NEGOTIATE SUBCONTRACTS 1 2 2
M1
M2
M2
M2
G9
A5 D6
B5 C9

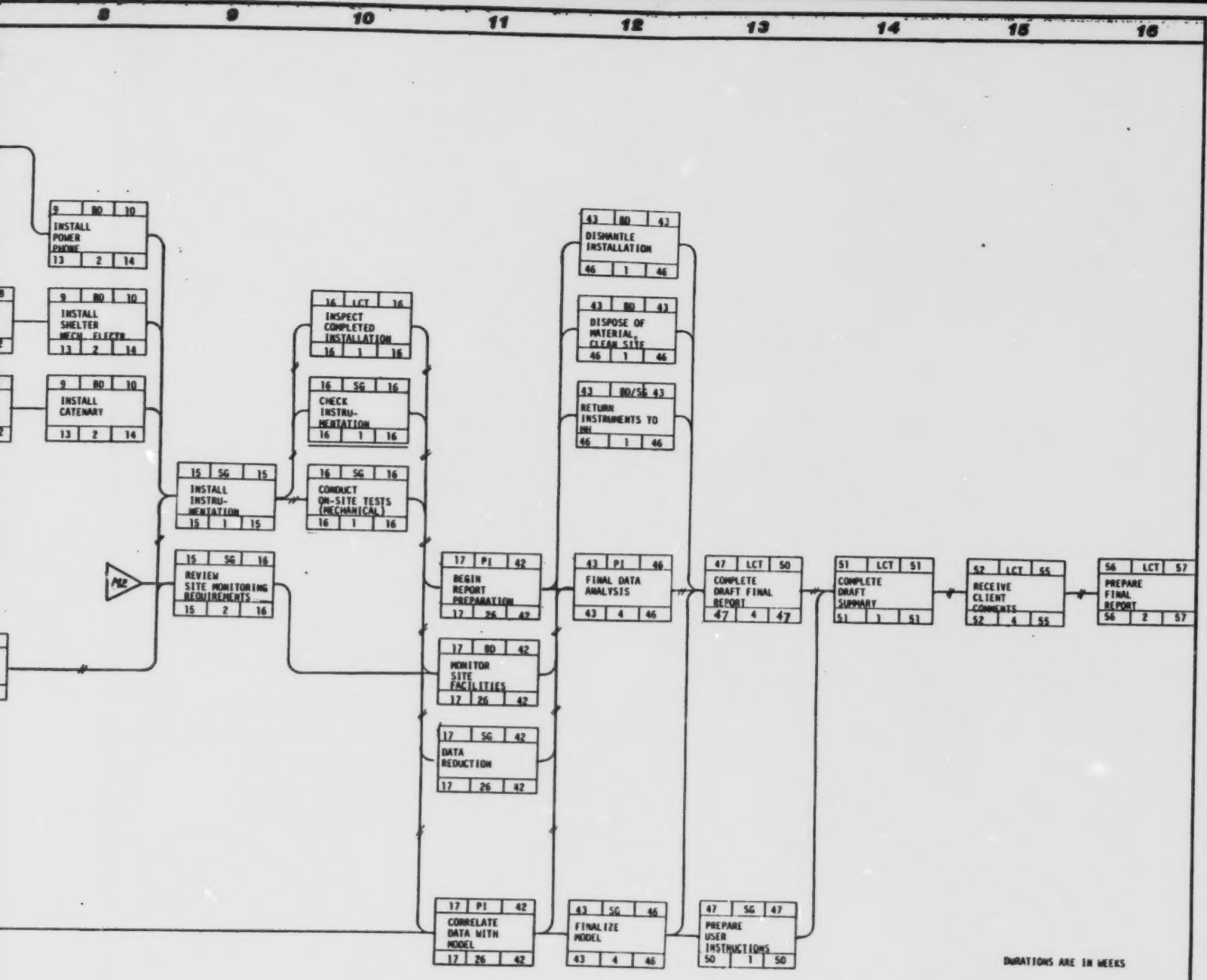

DURATIONS ARE IN WEEKS

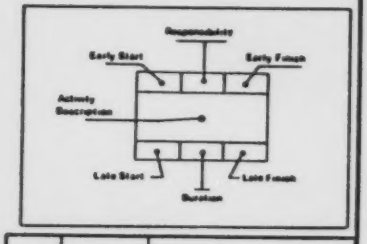

LEGEND:

S.A.	STEVEN ASHMORE
B.D.	BILL DAWSON
S.G.	SCOTT GAMBLE
P.I.	PETER IRWIN
R.M.	REAL MESSIER
L.C.T.	LORNE TAIT
M.C.T.	MIKE TURCOT

CRITICAL PATH ——//——

DATE	BY	REVISION
850722	DABT	

SPEC

NETWORK FOR
T3C CATENARY DEFLECTION TEST

N° C-85038-01

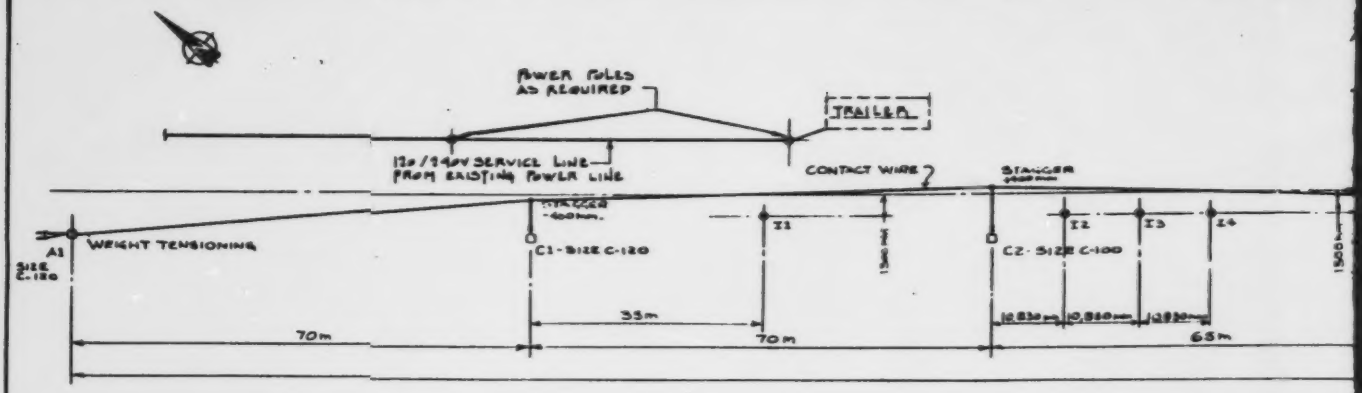

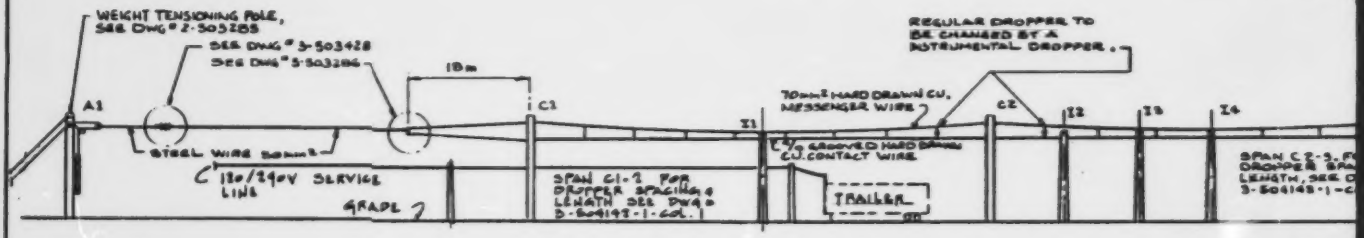

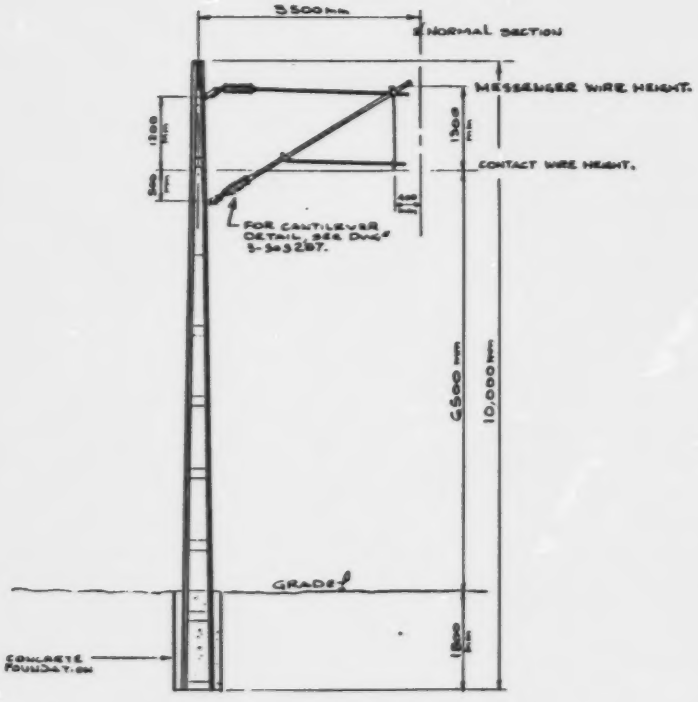

TYPICAL ELEVATION OF CANTILEVER POLE

Scale = 1:50

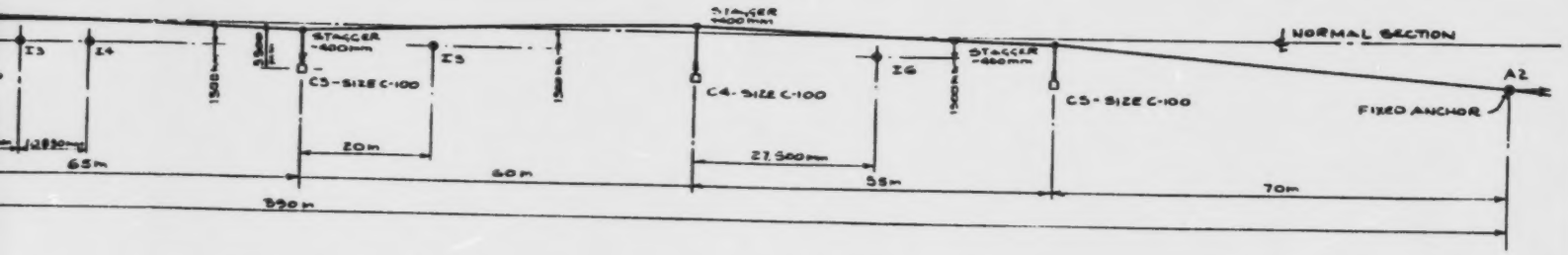

PLAN

SCALE - HORIZONTAL 1:600
VERTICAL 1:250

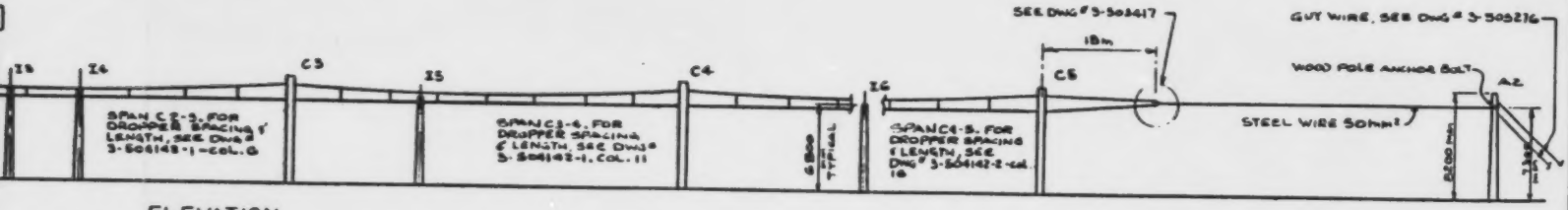

ELEVATION

SCALE - HORIZONTAL 1:600
VERTICAL 1:250

LEGEND:

- □ CATENARY STEEL POLE
- ● CATENARY & INSTRUMENTAL WOOD POLE
- ○ POWER WOOD POLE
- → GUY WIRE ANCHOR

REFERENCE DRAWINGS:

- 1-503274 - DROPPER
- 3-503276 GUY FOR WEIGHT & FIXED TENSIONING
- 2-503285 WEIGHT TENSIONING
- 7-503286 ADJUSTEMENT OF BALANCE ARM
- 3-503287 SINGLE CANTILEVER
- 3-503417 FIXED TENSIONING ASSEMBLY
- 3-503428 TENSIONING INSULATOR
- 3-503430 ADJUSTEMENT OF CANTILEVERS
- 3-505142/1 TABLE OF DROPPERS,
- 3-503 142/2 TABLE OF DROPPERS

NO	DATE	REVISIONS

A DETAIL NO
B DETAIL NO WHERE DETAIL INDICATED
C SHEET NO WHERE DETAIL SHOWN

SEAL

Canadian Pacific
Consulting Services Ltd.

740 Notre-Dame Street West, suite 700
Montreal, H3C 3X6

PROJECT
TDC CATENARY DEFLECTION TEST

DRAWING
PLAN & ELEVATIONS

DRAWN BY R.M.E. 85.8.2.	DATE AUG. 9/85
CHECKED	FILE NO 85038
SCALE AS NOTED	SHEET NO. C-85038-02 REV

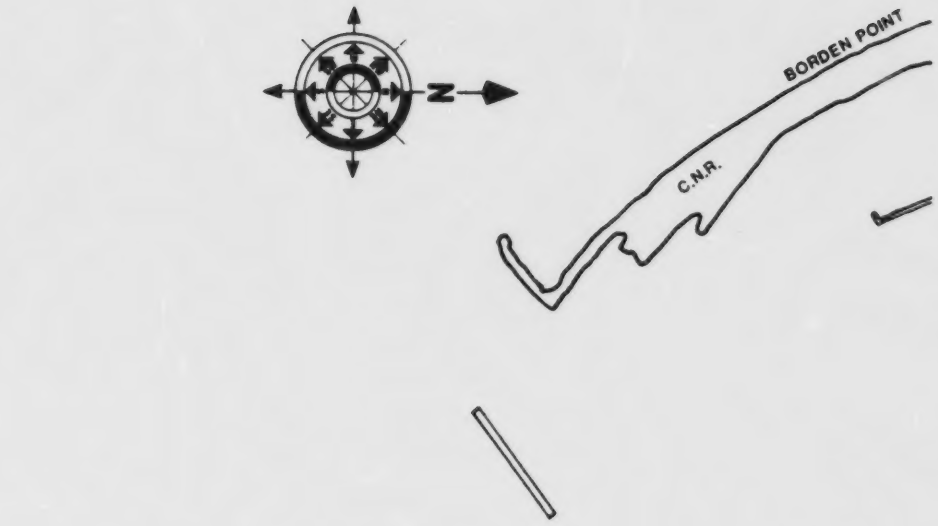

CATENARY DEFLECTION TEST SITE
C85038-03

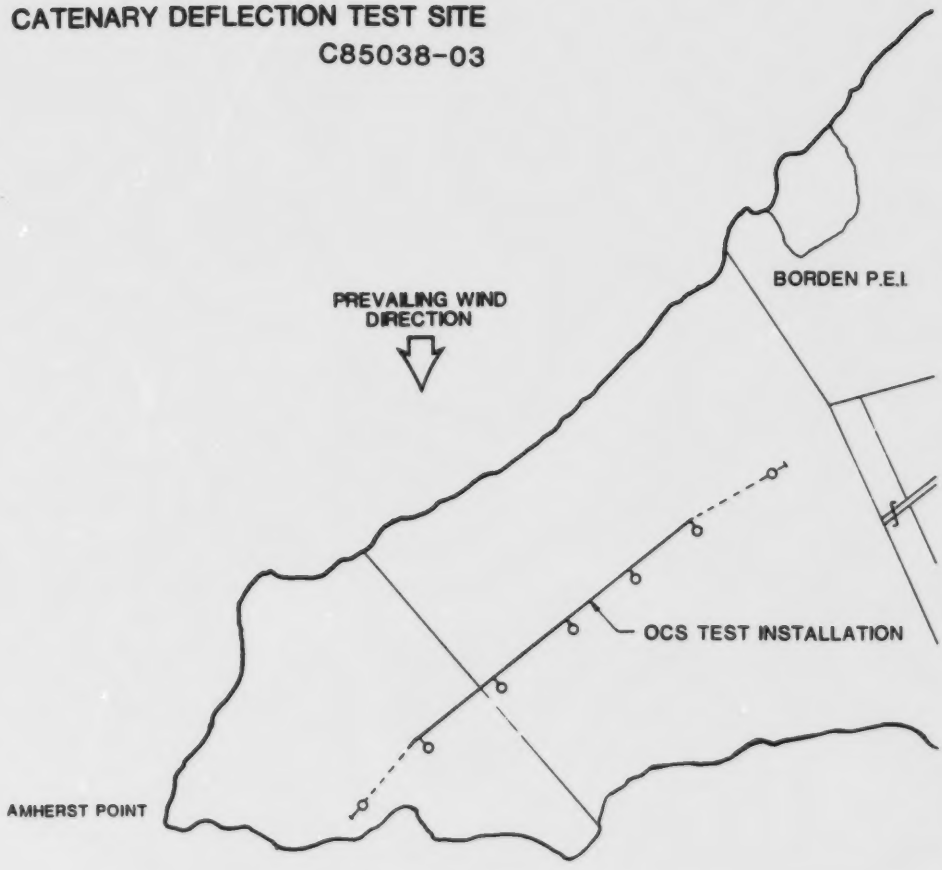

APPENDIX B

STATICS AND MECHANICS OF CATENARY SYSTEM

APPENDIX B

STATICS AND MECHANICS OF CATENARY SYSTEM

1. Static Deflection Shape

A span of length L of the catenary system is shown in Figures 1 (a) and 1 (b) in plan view. The local horizontal deflections of the contact and messenger wires are denoted respectively by x_c and x_m in Figure 1 (b). Figure 1 (a) is for the case where there is no messenger wire while Figure 1 (b) is for the case where there is a messenger wire. For a uniform wind load it can be easily shown as follows that for the case where there is only one wire the horizontal deflection shape is that of a parabola. Consider an elemental length, δy, of the wire. The horizontal wind force on it is $f\,\delta y$ where f is the force per unit length. The restraining force is

$$-\frac{d}{dy}\left(Te\,\frac{dx}{dy}\right)\delta y$$

where Te is the wire tension which can be taken as a constant along the span for the catenary wires because they have very small sag. Since the wind force is balanced by the restraining force, we have

$$Te\,\frac{d_2\,x}{dy^2} = -f \qquad (1)$$

thus

$$\frac{dx}{dy} = \frac{-f}{Te}\,y + C_1 \qquad (2)$$

and

$$x = \frac{-f}{Te}\,\frac{y^2}{2} + C_1\,y + C_2 \qquad (3)$$

Since $x = 0$ when $y = 0$, $C_2 = 0$.

Also, since $x = 0$ when $y = L$

$$C_1 = \frac{f}{Te} \frac{L}{2} \tag{4}$$

Thus the expression for the deflection shape is

$$x = \frac{f L^2}{2 Te} \left(1 - \frac{y}{L}\right) \frac{y}{L} \tag{5}$$

At the midspan position y/L = 1/2, and so the midspan deflection is

$$x = \frac{f L^2}{8 Te} \tag{6}$$

For the case of Figure 1 (b) the analysis is more complex because of the presence of the messenger wire and the forces in the dropper wires joining the contact wire to it. Therefore, the solution for the deflection shape is no longer strictly the simple parabolic curve of the form of equation 5. However, it is not expected to differ very much from it. In fact, for the special case where the wind force on the messenger wire is exactly the same as on the contact wire, the horizontal shapes of both wires revert to the parabola exactly. In the present study the simplifying assumption will be adopted that the static and dynamic deflection shapes of both wires are parabolic and it is not expected that this will lead to any significant inaccuracy in the predicted deflections.

2. Modes of Vibration of Catenary System (Equal Tensions)

We consider at this stage the case where the tensions in the messenger and contact wires are equal. Section 4 details with the unequal tension case. The modes of vibration of the catenary system can be derived from the equations of motion for the case of zero wind and by ignoring small dissipative terms, i.e. treating it as a conservative system. To simplify analysis, modes of vibration involving more than a single half wave on each span are ignored and the forms of the deflection shapes of the contact and messenger wires are both assumed to be parabolic but not necessarily equal in magnitude or even of the same sign. These approximations are not expected to give rise to significant inaccuracy since higher modes involving more than one half wave have roughly double the natural frequency and so experience little wind excitation and for the fundamental mode

the parabolic shape is quite close to the real shape. Also, the tower deflections are ignored. Thus the deflections of the contact and the messenger wires are taken to be respectively

$$x_c = \phi(y)\, q_c\,(t) \tag{7}$$

and $x_m = \phi(y)\, q_m\,(t)$

where $\phi\,(y)$ is the deflection shape and $q_c\,(t)$ and $q_m\,(t)$ are sinusoidal functions of time. In accordance with the assumption of parabolic deflection shape

$$\phi(y) = 4\left(1 - \frac{Y}{L}\right)\frac{Y}{L} \tag{8}$$

Now for a conservative system described by the two independent coordinates, q_c and q_m, classical mechanics shows that the equations of motion are

$$\frac{d}{dt}\left(\frac{\partial KE}{\partial \dot{q}_c}\right) + \frac{\partial PE}{\partial q_c} = 0 \tag{9}$$

$$\frac{d}{dt}\left(\frac{\partial KE}{\partial \dot{q}_m}\right) + \frac{\partial PE}{\partial q_m} = 0$$

where KE and PE are respectively the total kinetic and potential energies of the system.

The expression for the total kinetic energy of the catenary system can be shown to be

$$KE = \frac{1}{2}\left(\dot{q}_c^2\, m_c + \dot{q}_m^2\, m_m\right)\int_0^L \phi^2\,(y)\, dy \tag{10}$$

where m_c and m_m are the mass per unit length of the contact and messenger wires respectively.

The potential energy comes from three sources (we are ignoring a small fourth source, i.e. the towers). The first is from the contact wire for which the potential energy contribution is

$$(PE)_c = -\frac{Te}{4} q_c^2 \int_0^L \phi \frac{d^2\phi}{dy^2} dy \tag{11}$$

The second source is the messenger wire for which the contribution is

$$(PE)_m = -\frac{Te}{4} q_m^2 \int_0^L \phi \frac{d^2\phi}{dy^2} dy \tag{12}$$

The third source is from the dropper wires for which the contribution is

$$(PE)_d = \frac{1}{2} m_c g (q_c - q_m)^2 \int_0^L \frac{1}{l_d} \phi^2 dy \tag{13}$$

where g is the acceleration due to gravity and l_d is the length of the dropper.

Upon substituting equations (10) through (13) into equation (9) the following equations of motion are derived

$$\ddot{q}_c m_c L I + q_c \left(\frac{Te\ J}{2L} + m_c g K\right) - q_m m_c g K = 0 \tag{14}$$

$$\ddot{q}_m m_m L I + q_m \left(\frac{Te\ J}{2L} + m_c g K\right) - q_c m_c g K = 0$$

in which

$$I = \frac{1}{L} \int_0^L \phi^2 dy$$

$$J = -L \int_0^L \phi \frac{d^2\phi}{dy^2} dy \tag{15}$$

and

$$K = \int_0^L \frac{1}{l_d} \phi^2 dy$$

For the assumed parabolic form of Φ (equation 8), the above integrals I, J and K can be shown to be I = 8/15, J = 16/3 and

$$K = \frac{8\,\bar{T}e}{\bar{m}_m + 1} \left[\frac{1}{\sqrt{a}} \; (1 + a)^2 \; \text{ARCTAN}\left(\frac{1}{\sqrt{a}}\right) - \frac{5}{3} - a \right] \tag{16}$$

In the expression for K

$$\bar{T}e = \frac{Te}{2\,L\,m_c\,g} \;,\; \bar{m}_m = \frac{m_m}{m_c} \;,\; a = \frac{8\,l_{do}}{L} \; \frac{\bar{T}e}{\bar{m}_m + 1} \tag{17}$$

and l_{d_o} = dropper length at mid span

Writing the ratio q_m/q_c as R and substituting q_c = constant x sin $\omega_o t$ in equation (14) the following relations are derived

$$\begin{aligned} &- \omega_o^2 \; L\,m_c\,I + \frac{Te\,J}{2\,L} + m_c\,g\,K\,(1 - R) = 0 \\ &- \omega_o^2\,R\,L\,m_m\,I + R\,\frac{T_e}{2L}\,J - m_c\,g\,K\,(1 - R) = 0 \end{aligned} \tag{18}$$

After eliminating ω_o and with some further manipulation the following quadratic equation for the ratio R is derived

$$\bar{m}_m\,R^2 + R\left(\frac{\bar{T}e\,J}{K} + 1\right) \; (1 - \bar{m}_m) - 1 = 0 \tag{19}$$

where $\bar{m}_m$, $\bar{T}_e$, J and K are given in equations (16) and (17). The solutions to equation (19) are

$$R = \frac{-\left(\frac{\bar{T}e\,J}{K} + 1\right) \; (1 - \bar{m}_m) \pm \sqrt{\left(\frac{\bar{T}e\,J}{K} + 1\right)^2 \; (1 - \bar{m}_m)^2 + 4\,\bar{m}_m}}{2\,\bar{m}_m} \tag{20}$$

Typically there is one positive solution for R which is for the fundamental mode, and one negative solution which signifies the messenger wire's deflection is in the opposite direction to that of the contact wire. This last mode is generally at substantially higher frequency than the fundamental mode, being roughly in the range of the other higher modes already ignored, and as a result is not nearly as susceptible to wind excitation as the fundamental mode. Thus only the fundamental mode solution, i.e. R positive, is likely to be important. With R known from equation (20) the value of the modal frequency, n_o, in Hz can be deduced to be

$$n_o = \frac{\omega_o}{2\pi} = \frac{1}{2\pi}\sqrt{\frac{q\ K}{L\ I}} \cdot \sqrt{\frac{\bar{T}e\ J}{K} + 1 - R} \qquad (21)$$

It is worth noting that in the special case where the two wires are identical (i.e. $m_c = m_m$ and R = 1) equation (21) reduces to

$$n_o = \frac{1}{2L}\sqrt{\frac{Te}{2\ m_c}} \cdot \sqrt{\frac{10}{\pi}} \qquad (22)$$

The factor $\sqrt{10/\pi}$ has the value 1.0066 so we recover to a close approximation the expression for the fundamental natural frequency of a single wire of mass 2 m_c (remember that the two wires together have mass 2 m_c in this case) at tension T_e, which is

$$n_o = \frac{1}{2L}\sqrt{\frac{Te}{2\ m_c}} \qquad (23)$$

3. Static Equations with Wind Forces (Equal Tensions)

Considering the case where only a steady wind force acts and therefore there is no motion, the static equations can be derived from equations (9) by deleting the kinetic energy term (which is now zero) and adding to the right hand side the generalized aerodynamic force. Again, at this stage we assume equal tensions in the messenger and contact wires, leaving the unequal tension case to the next section.

$$\frac{\partial PE}{\partial q_c} = F_{GC} \qquad (24)$$

$$\frac{\partial PE}{\partial q_m} = F_{GM}$$

where

$$F_{GC} = \int_0^L F_c \, \phi \, dy$$

$$F_{GM} = \int_0^L F_m \, \phi \, dy \qquad (25)$$

and F_c and F_m are respectively the mean wind forces per unit length on the contact and messenger wires. Since F_c and F_m are both independent of y they can be taken outside the integral in equation (25). Substituting the potential energy expressions, equations (11) through (13) and using the parabolic expression for (equation 8), it is found after some manipulation that the midspan deflection is

$$\bar{x}_c = q_c = \frac{L^2}{4\,Te} \; F_c \left(\frac{1 + \left(\frac{F_m}{F_c}\right) \frac{3}{16} \frac{K}{Te}}{1 + \frac{3}{8} \frac{K}{Te}} \right) \qquad (26)$$

It can be noted that if the messenger wire were identical to the contact wire ($F_m = F_c$) this relation would reduce to

$$q_c = \frac{L^2 \, F_c}{4\,Te} = \frac{L^2 \, F_c}{\frac{8}{2}\,Te} \qquad (27)$$

This recovers the conventional expression for the deflection of a single wire under lateral load when it has tension 1/2 Te (remembering here that the tension T_e is half in the contact and half in the messenger wire).

The midspan static deflection of the messenger wire is given by

$$q_m = \frac{\left(\frac{2}{3} \frac{F_m \, L}{m_c \, g \, K} + q_c\right)}{\left(\frac{Te}{K} + 1\right)} \qquad (28)$$

4. Effect of Unequal Tensions in Messenger and Contact Wires

Dynamic Results:-

The analysis is not greatly altered when the tensions in the two wires are unequal. In the equations of motions, Equation 14 of Section 2, Te/2 must be

replaced in the first equation by T_{ec}, the contact wire tension and in the second equal by T_{em}, the messenger wire tension. Then following through the same analysis steps as before it is found that the solution for the ratio, R, of messenger to contact wire deflection is the same as before, Equation 20, except that Te is replaced by $\overline{Te}^*$ where

$$\overline{T}_e^* = \frac{T_{ec}}{L\, m_c\, g} \left[\frac{(T_{em}/T_{ec}) - \bar{m}_m}{1 - \bar{m}_m} \right] \tag{29}$$

Also in the expression for K, Equation 16, $\overline{Te}$ must be replaced by $\overline{T}_{ec} = T_{ec}/(Lm_cg)$.

Static Results:-

In a somewhat similar fashion to the dynamic analysis, Te/2 is replaced by T_{ec} in Equation 11 and by T_{em} in Equation 12 of Section 3. This then leads to the following modified expressions for the contact and messenger wire deflections

$$\overline{x}_c = q_c = \frac{F_c\, L^2}{8\, T_{ec}} \left[\frac{1 + \left(1 + \frac{F_m}{F_c}\right)\frac{3}{16}\, \frac{K}{T_{em}}}{1 + \frac{3}{16}\, K \left(\frac{1}{T_{em}} + \frac{1}{T_{ec}}\right)} \right] \tag{30}$$

and

$$q_m = \frac{\frac{2}{3}\, F_m\, L + q_c\, g\, K}{\left(\frac{T_{em}}{L}\, J + m_c\, g\, K\right)} \tag{31}$$

where $\overline{T}_{em} = T_{em}/Lm_cg$.

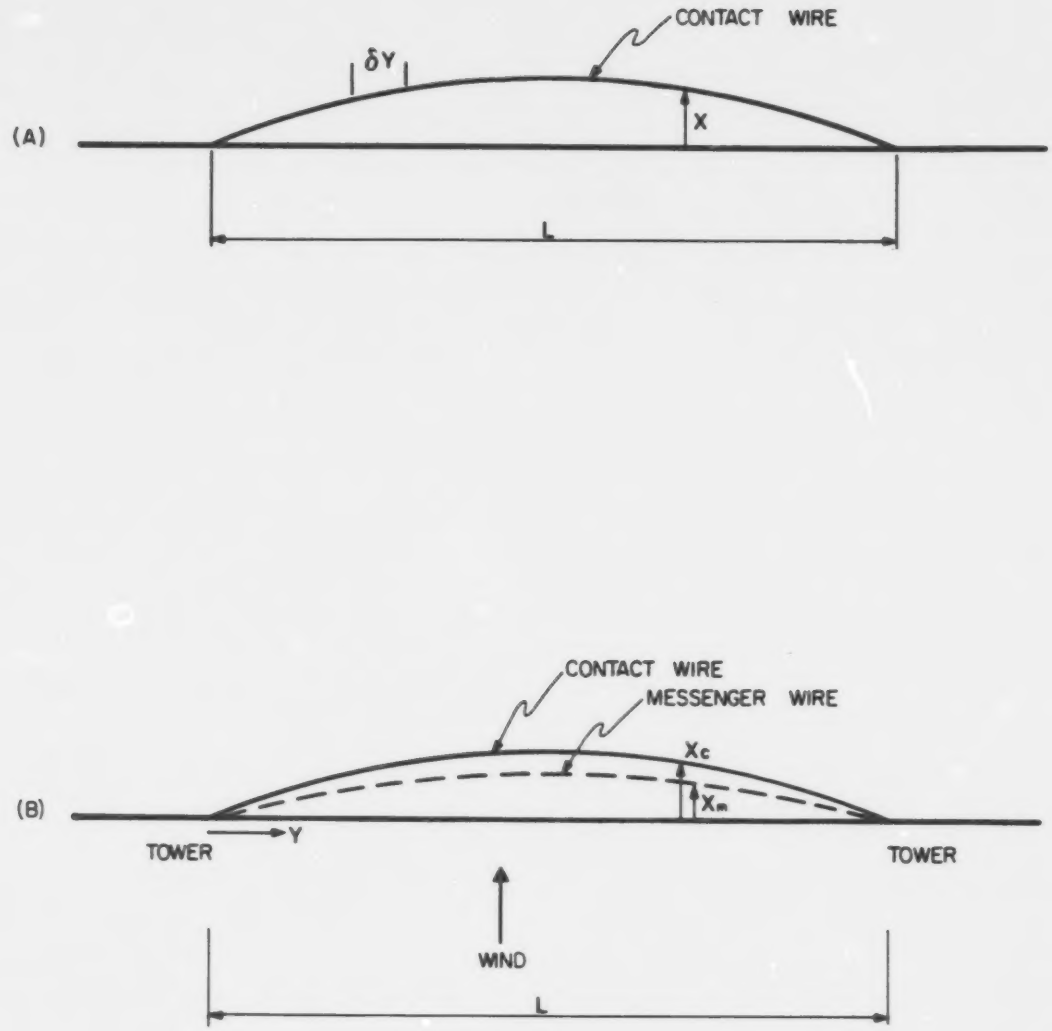

FIGURE 1

PLAN VIEW OF ONE CATENARY SPAN

APPENDIX C

RESPONSE OF CATENARY TO WIND ACTION

APPENDIX C

RESPONSE OF CATENARY TO WIND ACTION

1. Introduction

In a wind storm the catenary and tower system experiences fluctuating wind forces superimposed upon a mean force, the force fluctuations being due to the turbulence or gustiness of the wind. The turbulence results not only in fluctuations of wind force with time but also generates force fluctuations that are not perfectly correlated over the length of even one span; for example, when the peak gust force per unit length of span is reached at the span centre it may not be anywhere close to the peak value at the span ends. Theories have been developed for predicting the response of 'line-like' structures to this type of wind action, as in References 1 and 2 for example. This appendix describes the application of these theories to the catenary problem. The following analysis is for the case where the wind is normal to the span.

2. Equations of Horizontal Motion of the Catenary

Since the wind force is unsteady the catenary deflection varies with time. The inertia of the catenary must therefore be considered in determining the catenary motions caused by wind action. Therefore, the best starting for analyzing the problem is the equation of motion of the catenary. For a particular mode of vibration the deflection shape, x_c, of the contact wire can be written

$$x_c = \Phi_c (y)\, q\, (t) \qquad (1)$$

where

$\Phi_c (y)$ = mode shape

y = spanwise coordinate with origin at one end of the span

q = the normal coordinate for the mode of vibration

t = time

Similarly the deflection shape, x_m, of the messenger wire is

$$x_m = \phi_m (y)\ q\ (t) \tag{2}$$

where $\phi_m(y)$ = the mode shape of the messenger wire. Using energy methods similar to those described in Appendix B, the equation of motion of the catenary system can then be shown to be

$$M_G\ (\ddot{q} + 2\zeta\ \omega_o\ \dot{q} + \omega_o^2\ q) = F_G\ (t) \tag{3}$$

where M_G is the generalized mass and F_G the generalized aerodynamic force.

The quantity ζ is the damping ratio and ω_o is the natural frequency in radians per second. The value of ω_o is determined by the methods in Appendix B. The expression for M_G is

$$M_G = \int_0^L m_c\ \phi_c^2\ d\ y + \int_0^L m_m\ \phi_m^2\ dy \tag{4}$$

+ possible additional term for the tower

where m_c and m_m are the mass per unit span for the contact and messenger wires respectively. The tower term will be neglected.

The generalized aerodynamic force, F_G, is given by

$$F_G = \int_0^L f_c\ (y,t)\ \ \phi_c\ (y)\ dy + \int_0^L f_m\ (y,t)\ \ \phi_m\ (y)\ dy \tag{5}$$

+ possible additional term for the tower

where f_c (y, t) and F_m (y, t) and the aerodynamic drag forces per unit span on the contact and messenger wires respectively. Again the tower term will be neglected.

The dropper wires joining the contact wire to the messenger wire strictly result in further terms in the generalized mass and force but they are expected to be small and therefore have been ignored.

3. Simplification of Generalized Mass

Now the form of the deflection shape of the messenger wire is expected to be very similar to that of the contact wire. Therefore, the assumption that the ratio $\phi_m : \phi_c$ is constant along the span is made and the value of the constant is called R, i.e.

$$\frac{\phi_m}{\phi_c} = R \tag{6}$$

The above assumptions are in line with those in Appendix B and the constant R has the same meaning as in that appendix. Thus, using the fact that m_c and m_m are both constants along the span also, we may write Equation (4) as

$$M_G = m_c \int_0^L \phi_c^2 \, d y \, \left(1 + \frac{m_m}{m_c} R^2\right) \tag{7}$$

For a parabolic mode shape of the form

$$\phi_c = 1 - \left(\frac{2y}{L} - 1\right)^2 \tag{8}$$

the integral in Equation (7) becomes

$$\int_0^L \phi_c^2 \, dy = \frac{8}{15} \, L \tag{9}$$

so the generalized mass becomes

$$M_G = \frac{8}{15} m_c L \left(1 + \frac{m_m}{m_c} R^2\right) \tag{10}$$

4. Relation for Wind Force

The horizontal wind force on the contact wire per unit length may be expressed as the sum of the mean force, F_C, and fluctuating component f_c. By definition the mean of f_c is zero. Assuming that the horizontal force is insensitive to small deviations of the wind velocity vector from the normal to the plane of the messenger and contact wires, the expression for the horizontal force on the contact wire may be written

$$F_c + f_c = \tfrac{1}{2} \rho (U + u - \dot{x}_c)^2 c_c d_c \qquad (11)$$

where

U = mean wind velocity

u = fluctuating component of wind velocity in the direction of the mean

and

ρ = air density

Typically u is substantially smaller than U so a reasonable approximation is

$$F_c + f_c = \tfrac{1}{2} \rho (U^2 + 2 (u - \dot{x}_c) U) c_c d_c \qquad (12)$$

Since the time averages (i.e. the means) of f_c and u are zero by definition, by taking the time average of both sides of Equation (12) it is found that the mean force is given by

$$F_c = \tfrac{1}{2} \rho U^2 c_c d_c \qquad (13)$$

By subtracting Equation (13) from Equation (12) the expression for the fluctuating force is therefore

$$f_c = \rho U c_c d_c (u - \dot{x}_c) \qquad (14)$$

Similarly the unsteady force on the messenger wire is

$$f_m = \rho U C_m d_m (u - \dot{x}_m) \tag{15}$$

Here we have assumed that, because the vertical separation of the contact and messenger wires is small, especially at midspan where it matters most, the two wires experience identical wind velocities at a given spanwise station.

The generalized wind force is thus

$$F_G = \rho U C_c d_c \left(1 + \frac{C_m d_m}{C_c d_c} R\right) \int_0^L U(y, t) \phi_c(y)\, dy$$
$$- \rho U C_c d_c \left(1 + \frac{C_m d_m}{C_c d_c} R^2\right) \dot{q}(t) \int_0^L \phi_c^2(y)\, dy \tag{16}$$

5. Static Deflection of Contact Wire (Equal Tensions)

Equation 26 of Appendix B gives the expression for the midspan contact wire deflection under horizontal wind load for the case of equal messenger and contact wire tensions. Substituting into that equation the appropriate expressions for the mean wind forces F_c and F_m on the contact and messenger wires the mean midspan deflection of the contact wire is found to be

$$\bar{x}_c = \frac{\rho U^2 C_c d_c}{8 T_e} \left(\frac{1 + \left(1 + \frac{C_m d_m}{C_c d_c}\right) \frac{3}{16} \frac{K}{\bar{T}_e}}{1 + \frac{3}{8} \frac{K}{\bar{T}_e}} \right) \tag{17}$$

6. Solution of Equation of Motion

To solve for the unsteady deflections requires that we solve the equation of motion, Equation (3). Since the deflection fluctuates in the manner of a random variable (because the forces f_c and f_m are random) the form of solution we require is a statistical one, i.e. the root-mean-square deflection or the most probable peak value.

We rewrite the equation of motion, substituting for the unsteady aerodynamic forces using the results of Section 4.

$$M_G (\ddot{q} + 2 \zeta_T \omega_o \dot{q} + \omega_o^2 q) = \rho U C_c d_c \left[1 + \frac{C_m d_m}{C_c d_c} R\right] \int_0^L u (y, t) \phi (y) dy \qquad (18)$$

where the damping ratio, ζ, has had the subscript T added to indicate that it is now the total damping, including aerodynamic damping. The aerodynamic damping comes from taking the $\dot{q}$ term in Equation 16 to the left hand side of the equation of motion and merging it with the existing $\dot{q}$ term It can thereby be shown that the total damping, ζ_T, is

$$\zeta_T = \zeta + \frac{\rho U C_c d_c \left(1 + \frac{C_m d_m}{C_c d_c} R^2\right)}{2 \omega_o m_c \left(1 + \frac{m_m}{m_c} R^2\right)} \qquad (19)$$

where ζ is the structural damping ratio.

With a view to determining eventually the root-mean-square deflection due to wind force fluctuations we express the wind velocity u (y,t) as a Fourier series

$$u (y, t) = \sum_{i=1}^{\infty} (a_i (y) \cos \omega_i t + b_i (y) \sin \omega_i t) \qquad (20)$$

where ω_i is the circular frequency and a_i and b_i are the Fourer coefficients which are functions of the spanwise coordinate y. The solution for q can also be expressed as a Fourier series

$$q = \sum_{i=1}^{\infty} (A_i \cos \omega_i t + B_i \sin \omega_i t) \qquad (21)$$

Substituting Equations 20 and 21 into Equation 18 and then squaring and time averaging the resulting equation gives the following expression.

$$M_G^2 \sum_i ((\omega_o^2 - \omega_i^2)^2 + 4 \zeta_T^2 \omega_o^2 \omega_i^2) \tfrac{1}{2} (A_i^2 + B_i^2)$$

$$= \left[\rho U C_c d_c \left(1 + \frac{C_m d_m}{C_c d_c} R\right)\right]^2 \qquad (22)$$

$$\left(\int_0^L \phi_c (y) \sum_i (a_i (y) \cos \omega_i t + b_i (\bar{y}) \sin \omega_i t) dy\right)^2$$

The overbar on the squared integral on the right hand side indicates the time average. Now it is noted that the squared integral can be represented as the product of two integrals with respect to independent dummy variables y and y' representing different positions along the span, i.e. the integral squared can be written

$$\int_0^L \phi(y) \sum_i (a_i (y) \cos \omega_i t + b_i (y) \sin \omega_i t) dy \qquad (23)$$

$$\times \int_0^L \phi(y') \sum_i (a_i (y') \cos \omega_i t + b_i (y') \sin \omega_i t) dy'$$

Because the variables y and y' are independant, one integral can be taken inside the other so the squared integral of equation 22 becomes

$$\int_0^L \int_0^L \phi(y) \phi(y') \sum_i (a_i (y) \cos \omega_i t + b_i (y) \sin \omega_i t) \qquad (24)$$

$$\times \sum_i (a_i (y') \cos \omega_i t + b_i (y') \sin \omega_i t) dy dy'$$

Taking the time average of this expression it becomes

$$\int_0^L \int_0^L \phi(y) \phi(y') \sum_i \tfrac{1}{2} (a_i (y) a_i (y') + b_i (y) b_i (y')) dy dy' \qquad (25)$$

Returning to the left hand side of equation 22 the factor $1/2 (A_i^2 + B_i^2)$ is by defintion the product of the power spectrum, $S_q (\omega_i)$ of the generalized deflection, q, with the frequency interval used in the summation, $\delta\omega$ say. Also in expression 25 the quantity $1/2 (a_i (y) a_i (y') + b_i (y) b_i (y'))$ is, by definition, the product of the real part of the cross-spectrum, $S_{uu} (\omega_i, y, y')$ of the turbulence velocity, u, at two spanwise locations y and y' with the frequency interval. The symbol S_{uu} is taken in the present context as being the real part of the cross spectrum only, the imaginary part playing no role in the response of the catenary. Thus, equation 22 can be written

$$\omega_o^4 M_G^2 \sum_i ((1 - (\frac{\omega_i}{\omega_o})^2)^2 + 4 \zeta_T^2 (\frac{\omega_i}{\omega_o})^2 S_q (\omega_i) \delta_\omega$$

$$= \left[\rho U C_c d_c \left(1 + \frac{C_m d_m}{C_c d_c} R\right)\right]^2 \tag{26}$$

$$\sum_i \int_0^L \int_0^L (\phi(y) \phi(y') S_{uu} (\omega_i, y, y') \delta_\omega) \delta_y dy'$$

Now if the variations of u were a pure sine wave at a particular frequency there would be the same single frequency present in the response spectrum, S_q. Add another superimposed sine wave of a different frequency to u and another frequency is added to the response. In other words, equation 26 is satisfied not only by the summed series on the left and right hand sides but also on a term by term basis. Thus, we may write

$$S_q (\omega) = \frac{(\rho U C_c d_c L)^2 \left(1 + \frac{C_m d_m}{C_c d_c}\right)^2 \times S_u (\omega) \int_0^1 \int_0^1 \phi(y) \phi(y') S_{uu} (\omega, y, y') d (\frac{y}{L}) d (\frac{y'}{L})}{\omega_o^4 M_G^2 ((1 - (\frac{\omega}{\omega_o})^2)^2 + 4 \zeta_T^2 (\frac{\omega}{\omega_o})^2)} \tag{27}$$

It is usual to normalize the cross specturm $S_{uu} (\omega, y, y')$ by dividing it by the power spectrum, $S_u (\omega)$, of u. Thus we have defined the normalized cross spectrum

$$\bar{S}_{uu} = \frac{S_{uu}}{S_u} \tag{28}$$

and used this form in the above equation. Also the symbol χ will be introduced as short-hand for the reciprocal of the mechanical admittance, i.e.

$$|\chi|^2 = (1 - (\frac{\omega}{\omega_o})^2)^2 + 4 \zeta_T^2 (\frac{\omega}{\omega_o})^2 \tag{29}$$

The double integral factor in equation 27 is of a type often termed the aerodynamic admittance. For shorthand the symbol $|J|^2$ is used to denote

$$|J|^2 = \int_0^L \int_0^L \phi(y) \phi(y') \bar{S}_{uu} (\omega, y, y') d (\frac{y}{L}) d (\frac{y'}{L}) \tag{30}$$

With these notations, equation 27 becomes

$$S_q (\omega) = \frac{(\rho U C_c d_c L)^2 (1 + \frac{C_m d_m}{C_c d_c} R)^2 S_u (\omega) \left|J (\omega)\right|^2}{\omega_o^4 M_G^2 \left|\chi(\omega)\right|^2} \tag{31}$$

Finally to obtain the variance, σ_q^2, of the deflection the power spectrum is integrated over all frequencies

$$\sigma_q^2 = (\rho U C_c d_c L)^2 \left(1 + \frac{C_m d_m}{C_c d_c} R\right)^2 \int_0^\infty \frac{S_u |J|^2}{|\chi|^2} \, d\omega \qquad (32)$$

To obtain the variance of deflection we need now to consider the power spectrum, S_u, of wind velocity and the aerodynamic admittance $|J|^2$.

7. Power Spectrum and Cross Spectrum of Wind Velocity

The power spectrum, S_u, of wind velocity has been measured by numerous researchers. At high wind speeds it is found to conform quite well to von Karman's expression, the origin of which is in the theory of isotropic turbulence[3]. Von Karman's expression is

$$S_u(n) = u'^2 \, 4 \, \frac{L_1}{U} \left(1 + 70.78 \left(\frac{n L_1}{U}\right)^2\right)^{-5/6} \qquad (33)$$

where

n = frequency $\frac{\omega}{2\pi}$

and

u' = root-mean square of turbulence fluctuations in the direction of the mean wind velocity

and L_1 = the integral scale of the turbulence. Data exist which enable L_1 to be specified. Typically at the catenary height it is expected to be 30 metres.

The normalized cross-spectrum, $S_{uu}(n, \Delta y)$, of the wind velocity at two poins spaced at horizontal distance $\Delta y = /y - y'/$ apart at right angles to the wind direction can also be represented by an expression derived from the theory of isotropic turbulence[3] but the expression is quite complex. However, for the typical range of natural frequencies of the contact wire/messenger wire system a simpler and reasonably accurate expression is of the form

$$S_{uu}(n, \Delta y) = e^{-k \frac{n \Delta y}{U}} \qquad (34)$$

where the decay constant K is approximately 7

These expressions for the wind velocity spectrum and cross spectrum can now be used to evaluate the aerodynamimc admittance function $|J|^2$ and hence the integral in equation 32.

8. Aerodynamic Admittance Function

This function $|J|^2$ is given by equation 30. Substituting in this expression the parabolic mode shape, equation 8, and the normalized cross spectrum, equation 34, the aerodynamic admittance $|J|^2$ can be written as

$$|J|^2 = \frac{1}{L^2} \int_{-\frac{L}{2}}^{\frac{L}{2}} \int_{-\frac{L}{2}}^{\frac{L}{2}} e^{-k \frac{n|y' - y|}{U}} \left(1 - \left(\frac{2y}{L}\right)^2\right) \left(1 - \left(\frac{2y'}{L}\right)^2\right) dy\, dy' \qquad (35)$$

where the origin for the span wise variables y and y' has been shifted for convenience in the integral such that it is at the centre of the span.

Evaluating the above integral it is found, after some manipulation, that

$$|J|^2 = \frac{16}{15a} - \frac{32}{3a^3} + \frac{32}{a^4} - \frac{128}{a^6} + 32 \left(\frac{1}{a^2} + \frac{2}{a^3}\right)^2 e^{-a} \qquad (36)$$

where $a = k\, n\, L/U$. Note that as n tends to zero as a goes to zero. By expanding the exponetial in equation 36 in series it can be shown that as a tend to zero $|J|^2$ tends to 4/9.

9. Expression for RMS Deflection

The variance of deflection has been shown to be given by equation 32. Now the integral can be evaluated numerically after substituting for $S_u |J|^2$ and using

respectively equations 33, 35 and 29. In $|\chi|^2$ the total damping ratio ζ_T is given by equation 19. While there is no obstacle to simply evaluating the integral numerically, it is worthwhile exploring whether it can be approximated by analytical expressions.

The function under the integral consists of a broad band or background response with a resonant spike at the natural frequency of the catenary. This suggests the possibility of dividing the integral into two parts; part i) representing the broad band response and part ii) representing the reasonant response. Since the natural frequency of the catenary is quite high in relation to the range of frequencies of the most energetic wind turbulence and since over the narrow frequency band where $|\chi|^2$ becomes very small S_u and J are virtually constant, a reasonable assumption is to express the integral as

$$\int_0^\infty \frac{S_u(n)\ |J(n)|^2}{|\chi(n)|^2}\,dn \cong \int_0^\infty S_u(n)\ J(n)\,dn + S_u(n_o)\ |J(n_o)|^2 \int_0^\infty \frac{1}{|\chi|^2}\,dn \qquad (37)$$

$$= \int_0^\infty S_u(n)\ J(n)\,dn + S_u(n_o)\ |J(n_o)|^2\ \frac{\pi n_o}{4\zeta_T}$$

The integral on the right hand side of the second line of equation 37 can be well fitted by the simple expression

$$\int_0^\infty S_u(n)\ |J(n)|\,dn = \frac{4}{9}\ U'^2\ \left(1 + 0.244\ \left(\frac{L}{L_1}\right)^{0.593}\right)^{-2} \qquad (38)$$

Therefore combining equations 32, 33, 37, 38 and 10 we may write the root-mean-square contact wire deflection at mid-span as

$$\sigma_x = \sigma_q = \frac{\rho U^2\ C_c\ d_c\ \left(1 + \frac{C_m\ d_m}{C_c\ d_c}\ R\right)}{\omega_o^2\ m_c\ \left(1 + \frac{m_m}{m_c}\ R^2\right)}\ \left(\frac{U'}{U}\right)\ \left(\frac{5}{4}\right)\ (B + A)^{\frac{1}{2}} \qquad (39)$$

where

$$B = \frac{1}{1 + 0.244\left(\frac{L}{L_1}\right)^{0.593}}^2 \qquad (40)$$

and

$$A = \frac{9\pi \frac{n_o L_1}{U} \left| J \frac{n_o L}{U} \right|^2}{4\left(1 + 70.78\left(\frac{n_o L_1}{U}\right)^2\right)^{5/6} \zeta_T} \qquad (41)$$

In the expression for A the relation for $|J|^2$ is given by equation 26 (in which n is set to n_o) and the relation for ζ_T is given by equation 19 (in which $\omega_0 = 2\pi n_0$).

10. Total Deflection at Midspan

The total deflection at mid-span is the sum of the mean and dynamic deflections and may be expressed as

$$\hat{x} = \bar{x} + g_p \sigma_x \qquad (42)$$

where g_p = a peak factor with a typical value of 4.0. The peak factor may be approximated by

$$g_p = \sqrt{2 \ln (n_o T)} + \frac{0.577}{\sqrt{2 \ln (n_o T)}} \qquad (43)$$

where T = the duration of the storm event.

In equation 42 $\bar{x}$ is given by equation and σ_x comes from equation 39.

References

1. Davenport, A.G., 'The response of Slender, Line-Like Structures to a Gusty Wind', Proc. Instn. Civ. Engrs. 23, 389 - 408, 1962.

2. Irwin, P.A., 'Wind Tunnel and Analytical Investigations of the Response of Lions Gate Bridge to a Turbulent Wind, National Research Council of Canada, LTR-LA-210, June 1977.

3. Von Karman, T., 'Progress in the Statistical Theory of Turbulence', Nat. Acad. Sci, 34, 530 - 539, 1945.

NOTATION FOR APPENDIX C

a - dimensionless natural frequency based on span length in Appendix C (n_o L/U)

A - see equation 42

B - see equation 41

C_c, C_m - drag coefficients of contact wire and messenger wire respectively

g_p - peak factor, see equation 44

$|J|^2$ - aerodynamic admittance function, see equation 37

L - span length

L_1 - longitudinal turbulence integral scale

m_c, m_m - mass per unit length of contact and messenger wires respectively

n_o - natural frequency

R - ratio of messenger wire deflection to contact wire deflection in the fundamental mode

T - storm event duration

Te - total tension in the two wires

U - wind speed at the height of the contact wire

$\hat{x}$, $\bar{x}$ - peak and mean horizontal deflections respectively of the contact wire

ρ - air density

ρ_T - total of structural and aerodynamic damping ratios

APPENDIX D

SOURCE CODE LISTING FOR CATENARY
DEFLECTION PROGRAM OCS.BAS

APPENDIX D
Listing of Program OCS.BAS

```
1 REM
2 REM
3 REM
4 REM
10 REM DATA SETUP SECTION
15 KEY OFF
20 LET RHO=1.205:REM RHO IN kg\m^3
30 LET G=9.809999:REM m\s^2
40 LET T=3600!
50 GOSUB 1230 :REM CALL SCREEN REFRESH SUBROUTINE
60 REM ******   GET DIAMETER OF CONTACT WIRE
70 LOCATE 8,14
80 INPUT DUM$
90 IF DUM$="H" OR DUM$="h" THEN GOSUB 1450
100 DUM=VAL(DUM$)
110 IF DUM<>0 THEN DC=DUM
120 REM GET MASS PER UNIT LENGTH OF CONTACT WIRE
130 LOCATE 8,28
140 INPUT DUM$
150 IF DUM$="H" OR DUM$="h" THEN GOSUB 1590
160 DUM=VAL(DUM$)
170 IF DUM<>0 THEN MC=DUM
180 REM GET DRAG COEFFICIENT OF CONTACT WIRE
190 LOCATE 8,42
200 INPUT DUM$
210 IF DUM$="H" OR DUM$="h" THEN GOSUB 1730
220 DUM=VAL(DUM$)
230 IF DUM<>0 THEN CC=DUM
231 REM GET TENSION IN CONTACT WIRE
232 LOCATE 8,56
233 INPUT DUM$
234 IF DUM$="H" OR DUM$="h" THEN GOSUB 2000
235 DUM=VAL(DUM$)
236 IF DUM<>0 THEN TEC=DUM
240 REM GET DIAMETER OF MESSSENGER WIRE
250 LOCATE 9,14
260 INPUT DUM$
263 IF DUM$="h" OR DUM$="H" THEN GOSUB 3000
266 DUM=VAL(DUM$)
270 IF DUM<>0 THEN DM=DUM
280 REM GET MASS PER UNIT LENGTH OF MESSENGER WIRE
290 LOCATE 9,28
300 INPUT DUM$
302 IF DUM$="H" OR DUM$="h" THEN GOSUB 4000
304 DUM=VAL(DUM$)
310 IF DUM<>0 THEN MM=DUM
320 REM GET DRAG COEFFICIENT OF MESSENGER WIRE
330 LOCATE 9,42
340 INPUT DUM$
342 IF DUM$="H" OR DUM$="h" THEN GOSUB 5000
344 DUM=VAL(DUM$)
350 IF DUM<>0 THEN CM=DUM
351 REM GET TENSION IN MESSENGER WIRE
352 LOCATE 9,56
353 INPUT DUM$
354 IF DUM$="h" OR DUM$="H" THEN GOSUB 6000
355 DUM=VAL(DUM$)
356 IF DUM<>0 THEN TEM=DUM
360 REM GET NUMBER OF DROPPERS PER SPAN
361 LOCATE 11,42
```

```
362 INPUT DUM$
364 IF DUM$="H" OR DUM$="h" THEN GOSUB 7000
365 DUM=VAL(DUM$)
366 IF DUM<>0 THEN NDROP=DUM
369 REM GET LENGTH OF MIDSPAN DROPPER
370 LOCATE 12,42
380 INPUT DUM$
382 IF DUM$="h" OR DUM$="H" THEN GOSUB 8000
384 DUM=VAL(DUM$)
390 IF DUM<>0 THEN LD0=DUM
400 REM GET LENGTH OF SPAN BETWEEN TOWERS
410 LOCATE 13,42
420 INPUT DUM$
422 IF DUM$="H" OR DUM$="h" THEN GOSUB 9000
424 DUM=VAL(DUM$)
425 IF DUM<>0 THEN L=DUM
430 REM GET RADIUS OF CURVE IN TRACK TANGENT TRACK INDICATOR
431 LOCATE 14,42
432 INPUT DUM$
433 IF DUM$="H" OR DUM$="h" THEN GOSUB 16000
434 IF DUM$="t" OR DUM$="T" THEN RAD$="T"
435 IF VAL(DUM$)<>0 THEN RAD=VAL(DUM$)
436 IF VAL(DUM$)<>0 THEN RAD$="0"
440 REM GET STAGGER
450 LOCATE 15,42
460 INPUT DUM$
462 IF DUM$="H" OR DUM$="h" THEN GOSUB 10000
464 DUM=VAL(DUM$)
470 IF DUM<>0 THEN STAG=DUM
520 REM GET MECHANICAL DAMPING
530 LOCATE 16,42
540 INPUT DUM$
542 IF DUM$="H" OR DUM$="h" THEN GOSUB 11000
544 DUM=VAL(DUM$)
550 IF DUM<>0 THEN ZETA=DUM
560 REM GET MEAN WIND SPEED
570 LOCATE 18,56
580 INPUT DUM$
582 IF DUM$="H" OR DUM$="h" THEN GOSUB 12000
584 DUM=VAL(DUM$)
590 IF DUM<>0 THEN U=DUM
600 REM GET LONGITUDINAL TURBULENCE INTENSITY
610 LOCATE 19,56
620 INPUT DUM$
622 IF DUM$="H" OR DUM$="h" THEN GOSUB 13000
624 DUM=VAL(DUM$)
630 IF DUM<>0 THEN INTENS=DUM
640 REM GET INTEGRAL LENGTH SCALE
650 LOCATE 20,56
660 INPUT DUM$
662 IF DUM$="H" OR DUM$="h" THEN GOSUB 14000
664 DUM=VAL(DUM$)
670 IF DUM<>0 THEN L1=DUM
680 GOSUB 1230 :REM SCREEN REFRESH
690 PRINT
700 INPUT "CHECK INPUT PARAMETERS - OK  Y/N  ",ANS$
710 IF ANS$="N" OR ANS$="n" THEN GOTO 50
711 REM CORRECT VALUES FOR ADDITIONAL MASS AND DRAG OF DROPPERS
712 REM ADDITIONAL .17KG PER DROPPER
713 MCC=MC+.17*NDROP/2!/L :REM 1/2 MASS ON CONTACT
```

```
714 MMC=MM+.17*NDROP/2!/L :REM 1/2 MASS ON MESSENGER
715 REM ADDITIONAL FRONTAL AREA .0075 M^2 PER DROPPER
716 DCC=DC+1000!*.0075*NDROP/2!/L :REM 1/2 AREA ON CONTACT
717 DMC=DM+1000!*.0075*NDROP/2!/L :REM 1/2 AREA ON MESSENGER
720 TECBAR=TEC/L/MCC/G
725 TEMBAR=TEM/L/MCC/G
730 IF MMC<>MCC THEN MMBAR=MMC/MCC ELSE MMBAR=1.0001
735 P=(TEM/TEC-MMBAR)/(1!-MMBAR)
740 ADOT=8!*LDO/L*TEMBAR/(MMBAR+1!)
745 K=8!*TEMBAR/(MMBAR+1!)*(1!/ADOT^.5*(1!+ADOT)^2*ATN(1!/ADOT^.5)-5!/3!-ADOT)
750 J=16!/3!
755 R1=(TECBAR*J*P/K+1!)*(1!-MMBAR)
760 R2=((TECBAR*J*P/K+1!)^2*(1!-MMBAR)^2+4!*MMBAR)^.5
765 R=-R1+R2/2!/MMBAR
770 I=8!/15!
775 NO=1!/2!/3.1415*(G*K/L/I)^.5*(TECBAR*J/K+1!-R)^.5
780 BOBAR1=RHO*U^2*CC*DCC/1000!*L^2/16!/TEC
785 BOBAR2=1!+(1!+CM*DMC/CC/DCC)*3!/16!*K/TEMBAR
790 BOBAR3=1!+3!/16!*K*(1!/TEMBAR+1!/TECBAR)
795 BOBAR=BOBAR1*BOBAR2/BOBAR3
800 GP=(2!*LOG(NO*T))^.5+.577/(2!*LOG(NO*T))^.5
805 UPB=1!/(1!+.244*(L/L1)^.5930001)^2
810 A=7!*NO*L/U
815 MJSQ1=16!/15!/A
820 MJSQ2=32!/3!/A^3
825 MJSQ3=32!/A^4
830 MJSQ4=128!/A^6
835 MJSQ5=32!*(1!/A^2+2!/A^3)^2*EXP(-A)
840 MJSQ=MJSQ1-MJSQ2+MJSQ3-MJSQ4+MJSQ5
845 ZETAT1=RHO*U*CC*DCC/1000!
850 ZETAT2=1!+CM*DMC/CC/DCC*R^2
855 ZETAT3=4!*3.1415*NO*MCC
860 ZETAT4=1!+MMC/MCC*R^2
865 ZETAT=ZETA/100!+ZETAT1*ZETAT2/ZETAT3/ZETAT4
870 UPA1=9!/3.1415/4!*NO*L1/U*MJSQ
875 UPA2=4!*(1!+70.78*(NO*L1/U)^2)^(5!/6!)*ZETAT
880 UPA=UPA1/UPA2
885 SIGMAX1=5!/16!/3.1415^2
890 SIGMAX2=RHO*U^2*CC*DCC/1000!*(1!+CM*DMC/CC/DCC*R)
895 SIGMAX3=NO^2*MCC*(1!+MMC/MCC*R^2)
900 SIGMAX4=INTENS*(UPA+UPB)^.5
905 SIGMAX=SIGMAX1*SIGMAX2/SIGMAX3*SIGMAX4
910 BOMAX=BOBAR+GP*SIGMAX
915 IF RAD$="T" OR RAD$="t" THEN GOSUB 1000 ELSE GOSUB 1100
920  CLS
921  PRINT "                              OCS DEFLECTION PREDICTION"
922  PRINT "                              -------------------------"
923  PRINT " WIRE          DIA.(mm)       MASS (kg/m)   DRAG COEFF.   TENSION (N)"
924  PRINT "               --------       -----------   ----------    -----------"
925  PRINT "CONTACT  ",DC,MC,CC,TEC
926  PRINT "MESSENGER",DM,MM,CM,TEM
928  PRINT "NUMBER OF DROPPERS PER SPAN     ",NDROP
929  PRINT "LENGTH OF DROPPER AT MIDSPAN (m)",LDO
930  PRINT "LENGTH OF SPAN BETWEEN TOWERS (m)",L
931  IF RAD$="T" OR RAD$="t" THEN PRINT "RADIUS OR TANGENT TRACK (m or T)",RADSELSE PRINT "RADIUS OR TANGENT TRACK (m or
932  PRINT "STAGGER (m)                     ",STAG
933  PRINT "MECHANICAL DAMPING OF SYSTEM (%)",ZETA
935  PRINT "MEAN WIND SPEED AT HEIGHT OF CONTACT WIRE (m/s)",U
936  PRINT "LONGITUDINAL TURBULENCE INTENSITY               ",INTENS
937  PRINT "LONGITUDINAL TURBULENCE LENGTH INTEGRAL SCALE (m)",L1
```

```
938 PRINT "--------------------------------------------------------------------------"
940 PRINT "PEAK BLOW-OFF OF CONTACT WIRE FROM NO WIND POSITION (m)",BOMAX
941 IF RAD$<>"T" THEN GOTO 950
942 PRINT "STAGGER EFFECT                                        (m)",STAGEFF
944 PRINT "PEAK DISPLACEMENT INCLUDING STAGGER EFFECT            (m)",PEAK
945 PRINT "DISTANCE FROM MIDSPAN TO SPANWISE LOCATION OF PEAK    (m)",YMAX
946 PRINT "NATURAL FREQUENCY OF CATENARY SYSTEM          (CYCLES/SEC)",N0
947 GOTO 990
950 PRINT "OFFSET AT MIDSPAN DUE TO CURVE RADIUS AND STAGGER",CLOFFS
952 PRINT "PEAK DISPLACEMENT INCLUDING BLOW OFF AND OFFSET  ",CLOFF
990 LOCATE 23,1
992 INPUT "SHIFT PRTSC ->hardcopy  D RETURN ->detailed printout  RETURN -> continue",ANS$
993 IF ANS$="d" OR ANS$="D" THEN GOSUB 19000
996  INPUT "RETURN TO PARAMETER MENU OR QUIT - R or Q:",ANS$
997 IF ANS$<>"Q" AND ANS$<>"q" THEN GOTO 50
998 KEY ON
999 END
1000 REM STRAIGHT TRACK CALCULATIONS
1005 YMAX=ABS(STAG*L/4!/BOMAX)
1010 PEAK=ABS(-STAG^2/4!/BOMAX-BOMAX)
1015 IF YMAX>(L/2!) THEN PEAK=STAG
1017 IF YMAX>(L/2!) THEN YMAX=L/2!
1020 STAGEFF=PEAK-BOMAX
1025 RETURN
1100 REM CURVED TRACK CALCULATIONS
1105 H=RAD-.5*(4!*RAD^2-L^2)^.5
1110 CLOFFS=ABS(H-STAG)
1115 CLOFF=CLOFFS+BOMAX
1120 RETURN
1200 LOCATE 23,1
1210 INPUT "RETURN TO PARAMETER MENU OR QUIT - R or Q:",ANS$
1220 IF ANS$<>"Q" AND ANS$<>"q" THEN GOTO 50 ELSE END
1230 REM INPUT SCREEN SETUP PORTION
1240 CLS
1250 PRINT "                          OCS DEFLECTION PREDICTION"
1260 PRINT "                          -------------------------"
1270 PRINT "Please enter required quantities in the following list.",                    "Do not enter zeroes."
1280 PRINT "If the one on the screen is ok just press return."
1290 PRINT "Enter H when at the appropriate prompt for description of parameter."
1300 PRINT " WIRE          DIA.(mm)      MASS (kg/m)   DRAG COEFF.   TENSION (N)"
1310 PRINT "               --------      -----------   ----------    -----------"
1320 PRINT "CONTACT  ",DC,MC,CC,TEC
1330 PRINT "MESSENGER",DM,MM,CM,TEM
1340 PRINT
1345 PRINT "NUMBER OF DROPPERS PER SPAN     ",NDROP
1350 PRINT "LENGTH OF DROPPER AT MIDSPAN (m)",LDO
1360 PRINT "LENGTH OF SPAN BETWEEN TOWERS (m)",L
1366 IF RAD$="T" OR RAD$="t" THEN PRINT "RADIUS OR TANGENT TRACK (m or T)",RAD$ELSE PRINT "RADIUS OR TANGENT TRACK (m or
1370 PRINT "STAGGER (m)                      ",STAG
1390 PRINT "MECHANICAL DAMPING OF SYSTEM (%)",ZETA
1400 PRINT
1410 PRINT "MEAN WIND SPEED AT HEIGHT OF CONTACT WIRE (m/s)",U
1420 PRINT "LONGITUDINAL TURBULENCE INTENSITY                ",INTENS
1430 PRINT "LONGITUDINAL TURBULENCE LENGTH INTEGRAL SCALE (m)",LI
1440 RETURN
1450 CLS
1460 PRINT "                       HELP FOR CONTACT WIRE DIAMETER"
1470 PRINT "                       ------------------------------"
1480 PRINT
1490 PRINT "     For a circular section wire this value is simply the diameter in mm."
```

```
1500 PRINT "If the contact wire is not circular in section then this value would be the "
1510 PRINT "vertical dimension of the wire. That is the dimension which would be used to"
1520 PRINT "calculate the projected frontal area of the contact wire as seen by the wind."
1530 PRINT "     To account for ice buildup on the wire simply increase the value by an"
1540 PRINT "amount equal to two thicknesses of ice."
1550 PRINT
1560 PRINT
1570 INPUT "RETURN to go back to diameter prompt",ANS
1580 RETURN 50
1590 CLS
1600 PRINT "                          HELP FOR CONTACT WIRE MASS"
1610 PRINT "                          --------------------------"
1620 PRINT
1630 PRINT"     This mass is the mass per unit length of the contact wire given in units"
1640 PRINT "of kg/m. It can be obtained from the cross-sectional area of the wire and"
1650 PRINT "the density of the contact wire material."
1660 PRINT "    If icing conditions are being accounted for this value would be increased"
1670 PRINT "by an amount appropriate for the amount of ice accumulated on the wire."
1680 PRINT
1690 PRINT
1700 INPUT "RETURN to go back to mass prompt",ANS
1710 GOSUB 1230
1720 RETURN 130
1730 CLS
1740 PRINT "                    HELP FOR CONTACT WIRE DRAG COEFFICIENT"
1750 PRINT "                    --------------------------------------"
1760 PRINT
1770 PRINT "     This is the drag coefficient of the contact wire for horizontal"
1780 PRINT "winds as used in standard drag force calculations. These values can be "
1790 PRINT "obtained from engineering handbooks for various cross-sectional shapes."
1800 PRINT "This coefficient is in most cases dependent on the actual diameter of the"
1810 PRINT "wire and the wind speed under consideration. For the typical diameters of"
1811 PRINT "contact and messenger wires used in overhead conduction lines and typical"
1812 PRINT "wind speeds encountered at the heights of contact wires, the following drag"
1813 PRINT "coefficients are suggested:"
1814 PRINT
1815 PRINT "Smooth circular sections                                    1.2"
1816 PRINT "Stranded wire                                               1.0"
1817 PRINT "Ellipse - long vertical axis - aspect ratio 2:1            1.6"
1818 PRINT "Ellipse - long horizontal axis - aspect ratio 1:2          0.6"
1819 PRINT "Square                                                     1.6-2.0"
1820 PRINT
1830 PRINT
1840 INPUT "RETURN to go back to drag coefficient prompt",ANS
1850 GOSUB 1230
1999 RETURN 190
2000 REM WIRE TENSION HELP TEXT
2010 CLS
2020 PRINT "                        HELP FOR CONTACT WIRE TENSION"
2030 PRINT "                        -----------------------------"
2040 PRINT
2050 PRINT "     This value is the tension in Newtons applied to the contact wire."
2060 PRINT "It can be calculated by multiplying the dead weight in kilograms by 9.81"
2070 PRINT "and adding any factor for the pulley system if applicable."
2075 PRINT
2080 PRINT
2090 INPUT "RETURN to go back to tension prompt",ANS
2100 GOSUB 1230
2999 RETURN 231
3000 REM MESSENGER DIAMETER HELP TEXT
```

```
3005 CLS
3010 PRINT "                          HELP FOR MESSENGER WIRE DIAMETER"
3020 PRINT "                          --------------------------------"
3030 PRINT
3040 PRINT "     For a circular section wire this value is simply the diameter in mm."
3050 PRINT "If the messenger wire is not circular in section then this value would be the "
3060 PRINT "vertical dimension of the wire. That is the dimension which would be used to"
3070 PRINT "calculate the projected frontal area of the messenger wire as seen by the wind."
3080 PRINT "     To account for ice buildup on the wire simply increase the value by an"
3090 PRINT "amount equal to two thicknesses of ice."
3100 PRINT
3200 PRINT
3300 INPUT "RETURN to go back to diameter prompt",ANS
3400 GOSUB 1230
3999 RETURN 240
4000 REM HELP FOR MASS OF MESSENGER
4005 CLS
4010 PRINT "                            HELP FOR MESSENGER WIRE MASS"
4020 PRINT "                            ----------------------------"
4030 PRINT
4040 PRINT"     This mass is the mass per unit length of the messenger wire given in units"
4050 PRINT "of kg/m. It can be obtained from the cross-sectional area of the wire and"
4060 PRINT "the density of the messenger wire material."
4070 PRINT "    If icing conditions are being accounted for this value would be increased"
4080 PRINT "by an amount appropriate for the amount of ice accumulated on the wire."
4090 PRINT
4100 PRINT
4110 INPUT "RETURN to go back to mass prompt",ANS
4120 GOSUB 1230
4999 RETURN 280
5000 REM HELP FOR DRAG COEFF OF MESSENGER
5010 CLS
5020 PRINT "                    HELP FOR MESSENGER WIRE DRAG COEFFICIENT"
5030 PRINT "                    ---------------------------------------"
5040 PRINT
5050 PRINT "     This is the drag coefficient of the messenger wire for horizontal"
5060 PRINT "winds as used in standard drag force calculations. These values can be "
5070 PRINT "obtained from engineering handbooks for various cross-sectional shapes."
5080 PRINT "This coefficient is in most cases dependent on the actual diameter of the"
5090 PRINT "wire and the wind speed under consideration. For the typical diameters of"
5100 PRINT "contact and messenger wires used in overhead conduction lines and typical"
5110 PRINT "wind speeds encountered at the heights of contact wires, the following drag"
5120 PRINT "coefficients are suggested:"
5130 PRINT
5140 PRINT "Smooth circular sections                                1.2"
5150 PRINT "Stranded wire                                           1.0"
5160 PRINT "Ellipse - long vertical axis - aspect ratio 2:1         1.6"
5170 PRINT "Ellipse - long horizontal axis - aspect ratio 1:2       0.6"
5180 PRINT "Square                                                  1.6-2.0"
5190 PRINT
5200 PRINT
5210 INPUT "RETURN to go back to drag coefficient prompt",ANS
5220 GOSUB 1230
5999 RETURN 320
6000 REM HELP FOR TENSION IN MESSENGER
6010 CLS
6020 PRINT "                        HELP FOR MESSENGER WIRE TENSION"
6030 PRINT "                        -------------------------------"
6040 PRINT
6050 PRINT "     This value is the tension in Newtons applied to the messenger wire."
```

```
6060 PRINT "It can be calculated by multiplying the dead weight in kilograms by 9.81"
6065 PRINT "and adding any factor for the pulley system if applicable."
6070 PRINT
6080 PRINT
6090 INPUT "RETURN to go back to tension prompt",ANS
6100 GOSUB 1230
6999 RETURN 351
7000 REM HELP FOR NUMBER OF DROPPERS PER SPAN
7010 CLS
7020 PRINT "                        HELP FOR NUMBER OF DROPPERS"
7030 PRINT "                        --------------------------"
7040 PRINT
7050 PRINT"     This parameter is the number of droppers per span not including any"
7060 PRINT "possible ones at the cantilever arms. The program assumes that these are"
7070 PRINT "uniformly distributed along the span and uses the value to add additional"
7080 PRINT "frontal area to the contact and messenger wires in order to correct for"
7090 PRINT "the additional drag caused by these droppers. A constant compensating  area"
7100 PRINT "is added for each dropper regardless of actual length since"
7110 PRINT "the majority of the drag would occur as a result of the clamping devices"
7120 PRINT "alone and that the wire is of small enough diameter to eliminate the "
7130 PRINT "necessity of accounting for various lengths."
7140 PRINT "     If an input of no droppers is desired for determining their effect"
7150 PRINT "on the overall motion of the catenary system simply enter a value of.001"
7160 PRINT "at this prompt as the program will not accept zeroes."
7170 PRINT
7180 PRINT
7190 INPUT "RETURN to go back to the dropper prompt",ANS
7200 GOSUB 1230
7999 RETURN 360
8000 REM HELP FOR LENGTH OF MIDSPAN DROPPER
8010 CLS
8020 PRINT "                    HELP FOR LENGTH OF MIDSPAN DROPPER"
8030 PRINT "                    ----------------------------------"
8040 PRINT
8050 PRINT "     The length of the midspan dropper is required in order to calculate"
8060 PRINT "the coupling of motions of the messenger wire with those of the contact"
8070 PRINT "wire. The motions of the messenger and contact wires will quite often"
8080 PRINT "be different since in general they would have different diameters, drag"
8090 PRINT "coefficients, masses and tensions."
8100 PRINT
8110 PRINT
8120 INPUT "RETURN to go back to length prompt",ANS
8130 GOSUB 1230
8999 RETURN 369
9000 REM HELP FOR SPAN LENGTH
9010 CLS
9020 PRINT "                          HELP FOR SPAN LENGTH"
9030 PRINT "                          --------------------"
9040 PRINT
9050 PRINT "     The length of the contact wire span measured in metres between consecutive"
9060 PRINT "cantilever locations is required as a fundamental quantity for all blow"
9070 PRINT "off calculations."
9080 PRINT
9090 PRINT
9100 INPUT "RETURN to go back to length prompt",ANS
9110 GOSUB 1230
9999 RETURN 400
10000 REM HELP FOR STAGGER
10010 CLS
10020 PRINT "                            HELP FOR STAGGER"
```

```
10030 PRINT "                                ----------------"
10040 PRINT
10050 PRINT "     The stagger is the alternating offset of the contact wire at each"
10060 PRINT "consecutive tower which is used to minimize local wear of the pantograph"
10070 PRINT "system. It is measured horizontally at the location of the tower between"
10080 PRINT "the contact wire and a line drawn vertically upward from the centre-line"
10090 PRINT "of the tracks."
10095 PRINT
10100 PRINT
10110 INPUT "RETURN to go back to the stagger prompt",ANS
10120 GOSUB 1230
10999 RETURN 440
11000 REM HELP FOR MECHANICAL DAMPING
11010 CLS
11020 PRINT "                          HELP FOR MECHANICAL DAMPING"
11030 PRINT "                          ---------------------------"
11040 PRINT
11050 PRINT "     The mechanical damping of the overhead conduction system is the "
11060 PRINT "inherent damping due to mechanical friction and does not include"
11070 PRINT "resistance to motion provided by the air. The aerodynamic"
11080 PRINT "damping is calculated in the program and is provided in the detailed "
11090 PRINT "output. The mechanical damping can be estimated for an exsisting OCS"
11100 PRINT "by measuring the decay rate in free oscillation and using a logarithmic"
11110 PRINT "decrement method. This method can be found in engineering handbooks."
11120 PRINT "     In the absence of more accurate information a value of between .5% and"
11130 PRINT "1% can be used.
11140 PRINT
11150 PRINT
11160 INPUT "RETURN to go back to damping prompt",ANS
11170 GOSUB 1230
11999 RETURN 520
12000 REM HELP FOR MEAN WIND SPEED
12010 CLS
12020 PRINT "                        HELP FOR MEAN WIND SPEED"
12030 PRINT "                        ------------------------"
12040 PRINT
12050 PRINT "     This value represents the time averaged mean hourly wind speed"
12060 PRINT "at the site of the OCS. The program assumes the worst case direction"
12070 PRINT "which is that at right angles to the contact wire. This value is specific"
12080 PRINT "to the site under consideration. It is extremely important to input the"
12090 PRINT "mean hourly wind speed and not a gust wind speed as the program uses"
12100 PRINT "a buffeting response analysis to determine the gust effect on blow off."
12110 PRINT "     Two potential sources for obtaining this wind speed value are suggested."
12120 PRINT "The first source is to use the 10 year return period wind obtained from"
12130 PRINT "the National Building Code of Canada which provides a detailed table of"
12131 PRINT "values for most regions in Canada. Use of these values would allow a"
12132 PRINT "conduction system design closely tailored to the specific site."
12134 PRINT "     The second source is to use the wind speed values provided in CSA"
12135 PRINT "standards. These values however have a built in factor to account for"
12136 PRINT "the gustiness of the wind. To use these values with this program they "
12137 PRINT "must first be divided by 1.4 to approximate a mean hourly wind speed."
12139 PRINT "CSA Speed          CSA Wind                Mean Hourly Speed"
12140 PRINT " (m/s)          Pressure(N/m^2)         for Program Input(m/s)"
12141 PRINT "---------       ---------------         ----------------------"
12142 PRINT "   25                385                        18"
12143 PRINT "   22                285                        16"
12160 INPUT "RETURN to go back to the wind speed prompt",ANS
12170 GOSUB 1230
12999 RETURN 560
13000 REM HELP FOR LONGITUDINAL TURBULAENCE INTENSITY
```

```
13010 CLS
13020 PRINT "                HELP FOR LONGITUDINAL TURBULENCE INTENSITY"
13030 PRINT "                ------------------------------------------"
13040 PRINT
13050 PRINT "     This is a value which relates to the strength of the turbulent gusts"
13060 PRINT "within the wind flow. It varies primarily with the roughness of the "
13070 PRINT "upwind terrain and the height above ground. For typical OCS installations"
13080 PRINT "the following values can be used."
13090 PRINT
13100 PRINT "UPWIND TERRAIN CHARACTERISTICS"
13105 PRINT "------------------------------"
13110 PRINT "Open Water, Featureless Flatland          .14"
13120 PRINT "Farmland, Small Trees, Bushes             .18"
13130 PRINT "Single Storey Structures, Wooded Areas    .27"
13140 PRINT
13150 PRINT
13160 INPUT "RETURN to go back to intensity prompt",ANS
13170 GOSUB 1230
13999 RETURN 500
14000 REM HELP FOR INTEGRAL LENGTH SCALE
14010 CLS
14020 PRINT "                      HELP FOR INTEGRAL LENGTH SCALE"
14030 PRINT "                      ------------------------------"
14040 PRINT
14050 PRINT "     The integral length scale is a value which describes the typical"
14060 PRINT "size of the turbulent eddies passing over the OCS. It is used in the program"
14070 PRINT "to estimate the correlation of wind speeds along the length of the span."
14080 PRINT "The value is calculated by the following equation:"
14090 PRINT
14100 PRINT "       L1=12*z^.5"
14110 PRINT
14120 PRINT " where z is the height above ground of the contact wire."
14125 PRINT
14130 PRINT "     Thus, a value of 30 (m) would be representative of most OCS installations."
14140 PRINT
14150 PRINT
14160 INPUT "RETURN to go back to integral length prompt",ANS
14170 GOSUB 1230
14999 RETURN 640
16000 REM HELP FOR CURVE RADIUS
16010 CLS
16020 PRINT "                        HELP FOR CURVE RADIUS"
16030 PRINT "                        ---------------------"
16040 PRINT
16050 PRINT "     The radius of the curve is input to allow calculation of the midspan"
16060 PRINT "offset of the contact wire due to the combined effect of the stagger"
16070 PRINT "(which is assumed to always be towards the outside of the curve) and the "
16080 PRINT "fact that the wire is a chord line on the curve. If it is tangent track"
16090 PRINT "simply enter T in this radius prompt. For tangent track the stagger "
16100 PRINT "effect is incorporated in the output results."
16110 PRINT
16120 PRINT
16130 INPUT "RETURN to go back to radius prompt",ANS
16140 GOSUB 1230
16999 RETURN 430
19000 REM DETAILED PRINTOUT ROUTINE
19010 LPRINT "                         OCS DEFLECTION PREDICTION"
19020 LPRINT "                          DETAILED OUTPUT SUMMARY"
19030 LPRINT "                         -------------------------"
19040 LPRINT
```

```
19050 LPRINT "*******"
19060 LPRINT "INPUTS"
19070 LPRINT "*******"
19080 LPRINT
19090 LPRINT "CONTACT WIRE"
19100 LPRINT "------------"
19110 LPRINT "DIAMETER (mm)                                          ",DC
19120 LPRINT "MASS PER UNIT LENGTH (kg/m)                            ",MC
19130 LPRINT "DRAG COEFFICIENT                                       ",CC
19140 LPRINT "TENSION (N)                                            ",TEC
19150 LPRINT
19160 LPRINT "MESSENGER WIRE"
19170 LPRINT "--------------"
19190 LPRINT "DIAMETER (mm)                                          ",DM
19200 LPRINT "MASS PER UNIT LENGTH (kg/m)                            ",MM
19210 LPRINT "DRAG COEFFICIENT                                       ",CM
19220 LPRINT "TENSION (N)                                            ",TEM
19225 LPRINT
19230 LPRINT "GENERAL"
19240 LPRINT "-------"
19250 LPRINT "NUMBER OF DROPPERS PER SPAN                            ",NDROP
19260 LPRINT "LENGTH OF MIDSPAN DROPPER (m)                          ",LDO
19270 LPRINT "SPAN LENGTH (m)                                        ",L
19280 IF RAD$<>"I" THEN LPRINT "RADIUS OF CURVE (m)                                        ",RAD
19290 LPRINT "STAGGER (m)                                            ",STAG
19300 LPRINT "MECHANICAL DAMPING OF CATENARY SYSTEM (% OF CRITICAL)  ",ZETA
19305 LPRINT
19310 LPRINT "WIND CHARACTERISTICS"
19320 LPRINT "--------------------"
19330 LPRINT "MEAN WIND SPEED (m/s)                                  ",U
19340 LPRINT "LONGITUDINAL TURBULENCE INTENSITY                      ",INTENS
19350 LPRINT "INTEGRAL TURBULENCE LENGTH SCALE (m)                   ",L1
19355 LPRINT
19360 LPRINT "*************"
19370 LPRINT "INTERMEDIATE"
19380 LPRINT "*************"
19385 LPRINT
19390 LPRINT "CONTACT WIRE CORRECTIONS TO ACCOUNT FOR DROPPERS"
19400 LPRINT "-----------------------------------------------"
19410 LPRINT "DIAMETER (mm)                                          ",DCC
19420 LPRINT "MASS PER UNINT LENGTH (kg/m)                           ",MCC
19425 LPRINT
19430 LPRINT "MESSENGER WIRE CORRECTIONS TO ACCOUNT FOR DROPPERS"
19440 LPRINT "-------------------------------------------------"
19450 LPRINT "DIAMETER (mm)                                          ",DMC
19460 LPRINT "MASS PER UNIT LENGTH (kg/m)                            ",MMC
19465 LPRINT
19470 LPRINT "*********::******"
19480 LPRINT "CALCULATED VALUES"
19490 LPRINT "*****************"
19500 LPRINT "RATIO OF AMPLITUDE OF OSCILLATION (CONTACT/MESSENGER)",R
19510 LPRINT "NATURAL FREQUENCY OF CATENARY SYSTEM (cycles per sec.) ",NO
19520 LPRINT "MEAN BLOW OFF OF CONTACT WIRE (m)                       ",BOBAR
19530 LPRINT "PEAK FACTOR                                            ",GP
19540 LPRINT "AERODYNAMIC ADMITTANCE                                 ",MJSQ
19550 LPRINT "AERODYNAMIC DAMPING (% OF CRITICAL)                    ",ZETAT-ZETA/100!
19560 LPRINT "TOTAL DAMPING (% OF CRITICAL)                          ",ZETAT
19570 LPRINT "ROOT-MEAN-SQUARE BLOW OFF (m)                          ",SIGMAX
19580 LPRINT "PEAK BLOW OFF (m)                                      ",BOMAX
19585 LPRINT
```

```
19590 IF RAD$<>"T" THEN GOSUB 19700 ELSE GOSUB 19800
19600 RETURN
19700 LPRINT "CURVED TRACK"
19710 LPRINT "------------"
19720 LPRINT "OFFSET AT MIDSPAN DUE TO CURVE RADIUS AND STAGGER (m)  ",CLOFFS
19730 LPRINT "TOTAL OFFSET INCLUDING STATIC OFFSET AND BLOW OFF (m)  ",CLOFF
19740 RETURN
19800 LPRINT "TANGENT TRACK"
19810 LPRINT "-------------"
19820 LPRINT "PEAK DEFLECTION INCLUDING BLOW OFF AND STAGGER EFFECT (m) ",PEAK
19830 LPRINT "STAGGER EFFECT (m)                                       ",STAGEFF
19840 LPRINT "LOCATION OF PEAK DEFLECTION FROM MIDSPAN (m)             ",YMAX
19850 RETURN
19999 RETURN
```